Doctoral Dissertation

Displacement Ventilation in Large Lecture Hall: Performance Assessment of an Actual Lecture Hall and Enhancement Using a Novel Portable Cooling Unit with Air Purification

Aya Mohamed Hisham Essa

June 2023
Graduate School of Engineering
Osaka University

;

Acknowledgment

First and foremost, words cannot express how deeply grateful I am to my supervisor, Prof. Toshio Yamanaka. His vast knowledge and long experience helped me develop my skills and widened my knowledge on more than one level. Being ever so caring, understanding, and motivating made my PhD studies at the Built Environment Laboratory, Osaka University an unrepeatably enjoyable and intensively educative experience. I thank him for inspiring me to passionately and determinately seek knowledge. Thank you, professor.

I am sincerely grateful to Prof. Kondo for sparing the time to review this dissertation giving valuable advice to improve this work.

I extend my thanks to associate Prof. Tomohiro Kobayashi. I am indebted to him for sharing his knowledge whenever asked for, guiding me through difficult research points. I am as equally thankful to him for his support helping me fit in and feel welcomed while studying in a foreign country.

My sincere thanks to assistant professor Dr. Narae Choi for being as supportive and encouraging all through my study years. I extend my thanks to my junior colleagues , Eng. Miharu Komori and Eng. Shinnosuke Ishikawa who not only were a great support me through tough times but also from whom I learned most of my field measurement and experiment related skills.

To Mrs. Naoko Ommae I send my warmest thanks for her care and support without which my study time would have been very hard. Also, to Dr. Noriaki Kobayashi for sharing his knowledge and supporting my work.

I am especially thankful to DAIKIN industries ltd. for funding my research and for giving me the great opportunity to work with component and highly motivated team. I extend my thanks to Japanese government MEXT for granting me the scholarship and giving me the enriching opportunity to study in Japan.

Last but not least, to family and to friends in Japan and in Egypt, thank you for your continued unconditional support.

;

Contents

;

Chapter 1 Introduction

1.1. Background

Displacement ventilation (DV) is buoyancy dependent ventilation system which relay on heat sources inside the space to heat the cool air supplied at low velocity from inlets located near the floor. As air in the occupied zone gains heat it ascends washing along the contaminants upwards and entraining cool clean air from the supply. Compared to the typical mixed ventilation system (MV), DV, not only provides a better occupied zone air quality [1,2], but also is considered a more energy efficient ventilation system. In terms of energy consumption, Lin et al. found a reduction ranging between 26%, for office spaces, up till 42%, in classrooms [3]. The energy efficiency of DV is owing to its dependency on the passive force of buoyancy to create stratified flow. The upwards flow is created by the thermal plumes. Thermal plume is defined as the convection flow rising from a hot object, occupants or equipment. High flow velocity within the occupant's boundary layer indicates comfortable temperature sensed by occupant [4].

As mentioned above, in DV system design, the target volume is the occupied zone which is defined as the volume of space between the floor surface and 1.8 m height. Therefore, the inlets are positioned near the floor and the exhaust openings near the ceiling. As cool air flows in at low velocity, it gains heat from thermal plumes, thus, decreases in density and ascends sweeping along the contaminants away from the occupied zone resulting in a good air quality [5]. However, the room size, inflow rate, heat loads, and heat source location affect the stratification height, the height above which the temperature is linear and the contaminants concentration is high [4]. Breathing zone has an especially high air quality [2]; since it falls within boundary layer surrounding the nose and mouth of the occupant where the plume pull is strongest resulting in better air quality [4,6]. Breathing zone air quality, compared to the whole occupied zone air quality, is a more accurate indication of occupants' perception [5]. However, the thickness of the boundary layer cannot be accurately estimated as it is influenced by body posture, clothing style, thermal resistance, and obstacles amongst other factors[4].

Designing an effective DV system faces some challenges that either risk the inhale air quality or the occupants' comfort. One main challenge is draft or draught. Draft is the discomfort felt due to high velocity of low-temperature air. It is measured by draft risk rating, i.e. percentage of occupants feeling discomfort [4]. Nevertheless, in Melikov's survey, 2005, the authors deemed draft discomfort not a serious problem and can be overcome through good system design. As per the draft rates calculated Kosonen et al. according to ISO-7730 indoor environment category is for 10% dissatisfaction rate, the 21℃ inflow should have a velocity of 0.12 m/s or less. The adjacent area of higher inflow velocity should be narrowed down as much as possible by increasing the inlets surface area [4,7]. Another challenge, which manifest mainly in large rooms, is the low supply flow rate. Such problem rises from reducing the inflow rate to avoid high inflow velocity or to reduce the energy consumption. Insufficient inflow rate results in lowering the stratification height which might affect the occupied zone air quality [4,8]. Hence, to assess the performance of the system, stratification height stratification height should be calculated [4].

1.2. Displacement ventilation in educational spaces

Amongst a couple of indoor spaces, educational spaces have been targeted in many studies for optimizing ventilation systems in terms of thermal comfort and air quality. Many studies strove to define comfort indications in classrooms. For example, Chen et al. concluded that if air velocity did not exceed 0.2 m/s and temperature difference between head and foot was less than 2℃, DV can achieve 85% predicted satisfaction rate [2]. The interest in optimizing DV systems in classrooms and lecture rooms is mainly because of the fact that DV possesses the advantage of low noise, due to having low speed air supply, which is optimal for classroom use [9]. The connection between indoor air quality and students' health and academic performance as proved by multiple studies factors in as well [10,11] . Wachenfeldt et al. recommended that CO_2 concentration should be kept below 1000 ppm at 1.2 m height [11]. However, it is noticed that school classrooms [8,10–13], is more widely studied than university lecture halls [14,15]. The reason is believed to be that children are more vulnerable to low indoor air quality [10].

1.3. Displacement ventilation and cross-contamination

Optimizing ventilation system has always been studied as it is critical to providing a healthy indoor environment in an energy efficient manor [16]. In the current pandemic situation, the indoor air quality should be more intensively studied. Studies such as[17], pointed out a dissatisfied-users percentage with the air quality. Chen and Glicksman warned of low efficiency in case of high cooling load, as it requires high air velocity [2]. Nevertheless, DV, particularly, can be seen as a prime alternative ventilation system that not only because it provides good air quality, but also for its potential to reduce the cross-contamination probability [18]. One main issue addressed is breathing zone air quality. Research has shown that if facing occupants are positioned closely, less than 1 m apart, exhalation flow from one occupant, through nose or mouth, can penetrate the breathing zone of the other [19,20]. Although this observation indicates low indoor air quality, the results show this problem to be minor [19]. However, especially in the present COVID-19 situation, further investigation is called for as to assess the gravity of this observation and the probability of cross-infection in consequence.

The effect of source position was studied by multiple papers [21,22] amongst other factors in (through an experimental study and CFD analysis. They found the position to have a major influence on the contaminant's dispersion pattern. Both studies investigated the effect of source height as well and concluded that the lower the source is, the more discrete the vertical stratification becomes and thus the better the occupied zone air quality is. Srebic and Xu (2005) also concluded that the exhaust positions were found to affect the general exposure level in the whole room [19].

It has become a pressing need not only to reduce cross-infection risk in indoor spaces but to reach a set of recommendations for a low risk ventilation system as well [16]. Hence, such a study is currently important, especially that most of the investigations on the efficiency of ventilation systems in controlling the infection spread are carried out in hospital patient rooms [18,23,24]. Moreover, the majority of those infection-spread-oriented experiments and simulations are carried out in a small experimental chamber with one or two human models. It has been noticed that little research work tackled contaminants spread in educational spaces with

full room conditions. Hence, this study aims at further exploring the displacement ventilation system's capability to reduce airborne contaminant's horizontal spread and thus reducing the cross-infection probability using CFD simulation.

Cross-infection due through airborne particles can occur through various respiratory activities [16]. The first type is high speed pulse emission, i.e. coughing or sneezing; in this case, the aerosols and droplets are expelled at a velocity high enough, 10~50 m/s [25], to escape from the convective boundary layer surrounding the human body and thus they are free to travel horizontally. The second type is slow emission, i.e. breathing. In case of exhaling, the buoyancy force created by the thermal plume can be the main directing force for contaminants due to the low horizontal speed. Since the latter type is used in the majority of research assessing ventilation system efficiency [18,24,26], in this study, breathing is chosen as the contaminants emitting method. It was found reasonable that speaking, only by lecturer in this case study, would be considered a low speed emission. This assumption was supported by Kwon et al. findings in which speaking flow velocity can be as low as 2.31 m/s [27].

Regarding the exhaled contaminants dispersion, researchers usually use tiny droplets, aerosols, or droplet nuclei as tracers [28,29] in addition to gases like CO_2 [23,26,28] and SF6 [30]. Although gases differ from particle in terms of size, mass, and accordingly, dispersion pattern, it has been concluded that tracer gases and 3 μm particles gave similar representation of contaminant spread at low velocities such as that of normal breathing [30,31]. In addition, a CO_2-based risk equation that was proved effective in estimating the risk of airborne infection spread [26]. In this research, both methods are used to simulate the human generated contaminants, tracer gas and actual droplets.

1.4. DV system shortcomings and improvement potential

Although DV system does not have strong mixing air flow as found in MV, yet in practice, many variables affect the efficiency of the DV system. For example, the room size, heat loads, and heat source location affect the interface level [1]. Moreover, movement, presence of obstacles, and unequal distribution of heat sources, i.e. occupants and machines, can cause an imbalance in the temperature distribution. Such imbalance weakens the stratification, causes unwanted horizontal flow, or result in pockets of unrenewed air [33,34].

Qian et al conducted a full-scale experiment to compare the effect of DV to other ventilation systems on the exhaled air flow of patients in hospital ward. The personal exposure of patients was set as the index. They used tracer gas to simulate fine droplets and droplet nuclei. They did not recommend DV based on two main findings. First, having a slower and more steady air flows, in the DV case, more exhaled droplets could escape the source boundary layer. In MV, the exhaled jet are diluted before traveling long. The second observation in the DV case was the presence of a high concentration layer [35]. Similar observations were noted in multiple studies [36,37].

The high concentration layer, also known as the lock-up phenomenon, was investigated thoroughly by Zhou et al, 2017. Low lock-up layer was concluded to be caused by two main factors. First, small Archimedes number which indicates turbulent supply flow inertia is stronger than the buoyancy force. Second factor was

found to be steep temperature gradient. They observed a power law relation between temperature gradient and lock-up height. [38]

Moreover, Brohus et al. carried out a full-scale measurement to access the efficiency of DV system. Several factors were examined through monitoring the personal exposure to contaminants for a seated and a standing breathing thermal manikin. They found that contaminant spread is highly dependent on the horizontal air flows. [39] Another cause for unwanted turbulence, besides supply inertia [38], is movement inside the DV space. Movement in DV spaces disturbs the human boundary layer in which the upward flow induced by the thermal plume exists, thus, increases the contaminant spread [39,40].

Therefore, it can be concluded from the previous literature that DV system needs enhancement techniques to improve its efficiency in cross-contamination prevention. In the following section, factors that affect the DV efficiency and can potentially be manipulated to enhance the performance are discussed.

1.4.1. Supply diffuser location

The position of diffusers affects the air quality at certain locations in the space as concluded by Xing et al. through field measurement and CFD analysis [34]. The effect of supply port position was also studied by Xin et al. where they analyzed 27 different positioning of floor standing air conditioners in a large hall. It was found that the portable air-conditioning unit have a great effect on the thermal comfort [41]. In this aspect, the personalized DV in variant forms has been examined in many papers and was proven effective at improving the air quality and thermal comfort [42,43]. Liu et al., 2022, explored another enhancement technique for large span halls. Local diffusers were proposed and simulated in this study. The CFD simulations showed a decrease of 48.5% in contaminant concentration in the occupied zone compared to the tradition DV system diffusers. [44]

1.4.2. Temperature gradient

In DV rooms, the height of heat source in a room has a major effect on the temperature profile. In rooms where the heat sources are located at a high level or where an additional heat source was added above the interface level, DV is more efficient in cooling the occupied zone, as shown in the heated roof example, Figure 1.1.

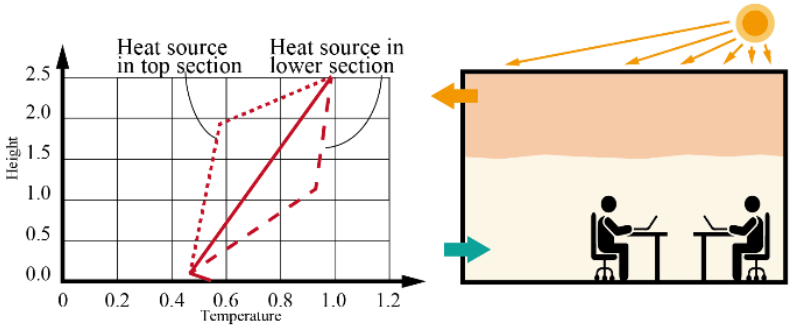

Figure 1.1 Heated roof temperature distribution [Adapted from [1]]

Kosonen et al. studied the effect of varying heat load conditions on the temperature profile of a room with DV system using experimental measurements. Amongst the factors was the roof heating. The ceiling height was 3.1 m and 5 m. Supporting the vertical distribution in Figure 1.1, it was found that in the heated ceiling case, only the air near the ceiling gains heat, leaving the lower levels at much lower temperature than other cases. However, when combined with large number of occupants, the heated ceiling had negligible effect on the stratification height [45].

Wu et al. studied the effect of ceiling heating as well as heated floor for DV systems in 2 m-high experiment room. The results showed that the heated ceiling did not only increase the temperature of the top air layer, but also lowered the temperature at 1.1 m and below [46].

On the other hand, the temperature stratification if increased beyond a certain level can cause either discomfort due to large temperature gradient, [47], or lower the occupied zone air quality if the interface level fell to a low height [38]. In their 2017 study, Zhou et al carried out a field experiment comparing temperature gradients ranging from 0.2 ℃/m to 6 ℃/m. It was found out that the steeper the gradient is the lower the interface height becomes [38,48].

Hence, with the background acquired from the aforementioned literature, this study proceeds to investigate the effectiveness of DV and explore techniques to improve its performance, widen its applicability and minimize the cross-infection risk in DV spaces.

1.5. Outline of this Study

This work is composed of five summarized by the flowchart in Figure 1.2. This section gives a brief overview of the study's flow and chapters contents.

Chapter 1. Introduction

This chapter presents basic background information about DV system, its properties, strengths, and weaknesses supported by literature and related studies findings.

Chapter 2. Double Wall Flat Diffuser with Non-Uniform Supply in Large Lecture Hall

This chapter focuses on a special DV system installed in a university lecture hall. The system performance is assessed in terms of temperature and contaminant distribution. Multiple variables are investigated exploratory CFD analyses, steady-state and transient, and field measurements including contaminant source position, seating pattern of occupants, and diffusers settings. In addition, CFD validation results are presented and analyzed.

Chapter 3. Displacement Ventilation Performance Enhancement using a Novel Portable Cooling Unit with Air Purification Function

In this chapter a novel portable DV unit is introduced. Details of the design, specifications, operation method are defined. The effectiveness of the proposed unit is evaluated using zonal model calculation, full-scale experiment, and CFD analysis in terms of temperature and PM distribution. Several parameters are explored such as the unit's COP and flowrates, DV flowrate, and the position of exhaust relative to the PDV unit.

Chapter 4. CFD Application: Operating the Portable Displacement Ventilation Unit in the Large Lecture Hall

This chapter presents the CFD application of operating the novel PDV unit in the investigated lecture hall as a representative of the unit's performance in enhancing DV system performance in large spaces. Two main sets of analyses are found in this chapter. First, operating the PDV units in the base-case as an additional system booster. The second is testing the effectiveness of the PDV units as a complementary or replacement ventilation system.

Chapter 5. Conclusion and Outlook

Summarizing the main findings, this chapter reviews the previous chapters and defines areas where further work is needed.

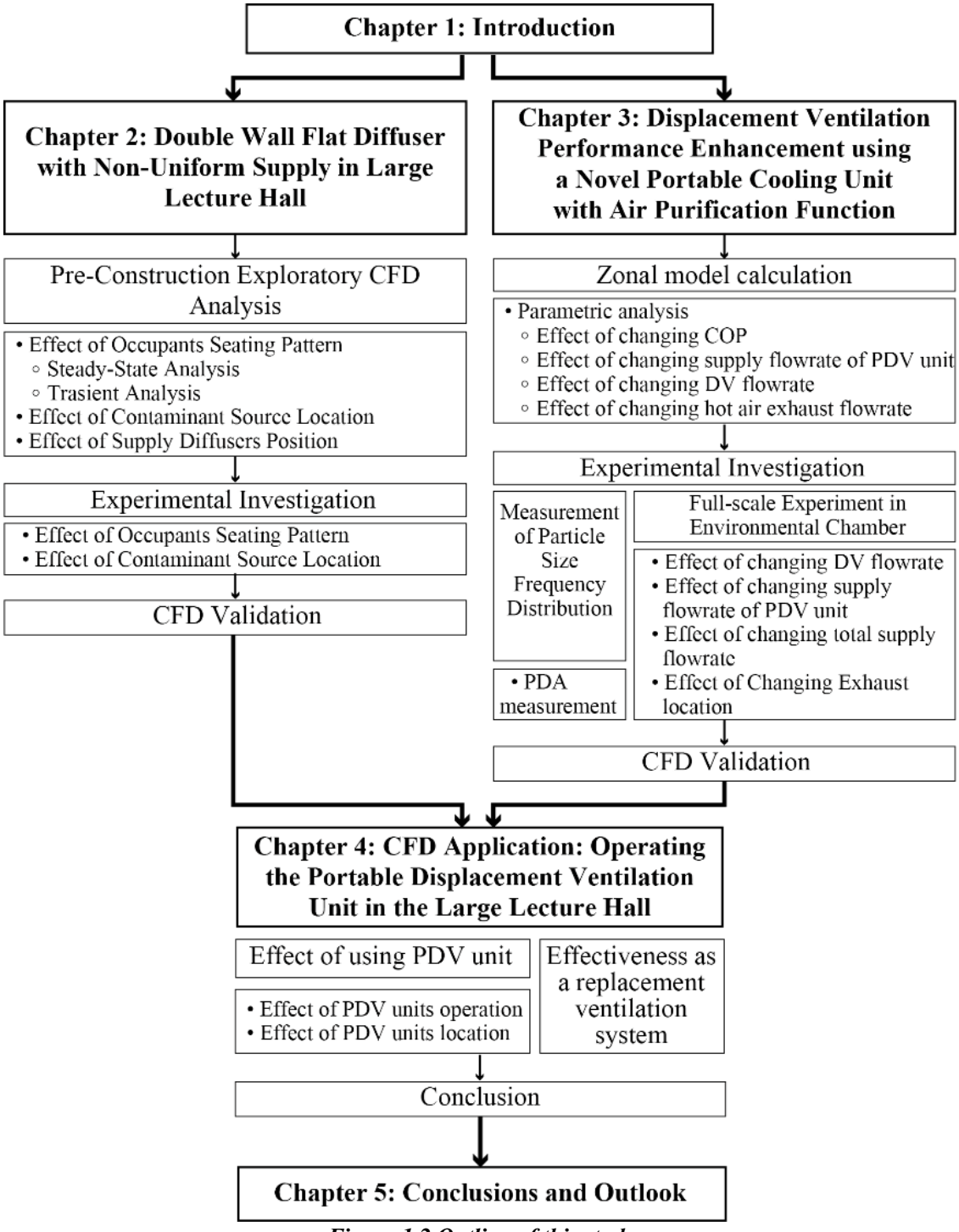

Figure 1.2 Outline of this study

1.6. Abbreviations

DV; Displacement ventilation

MV: Mixed ventilation

PDV unit: Portable displacement ventilation unit

CFD: Computational fluid dynamics

1.7. References

[1] A. Melikov, J. Kaczmarczyk, Measurement and prediction of indoor air quality using a breathing thermal manikin, Indoor Air. 17 (2007) 50–59. https://doi.org/10.1111/J.1600-0668.2006.00451.X.

[2] Q. Chen, L.R. Glicksman, System Performance Evaluation and Design Guidelines for Displacement Ventilation, n.d. https://scholar.google.com/scholar?hl=en&as_sdt=0%2C5&q=System+Performance+Evaluation+and+Design+Guideline+for+Displacement+Ventilation&btnG= (accessed August 12, 2021).

[3] Z. Lin, C.K. Lee, S. Fong, T.T. Chow, T. Yao, A.L.S. Chan, Comparison of annual energy performances with different ventilation methods for cooling, Energy Build. 43 (2011) 130–136. https://doi.org/10.1016/J.ENBUILD.2010.08.033.

[4] R. Kosonen, A. Melikov, E. Mundt, P. Mustakallio, Displacement Ventilation, 2017. https://biblioteka.ktu.edu/wp-content/uploads/sites/38/2017/06/23_Displacement_Ventilation.pdf (accessed August 19, 2021).

[5] H. Xing, A. Hatton, H.B. Awbi, A study of the air quality in the breathing zone in a room with displacement ventilation, Build Environ. 36 (2001) 809–820. https://doi.org/10.1016/S0360-1323(01)00006-3.

[6] H. Stymne, M. Sandberg, M. Mattsson, Dispersion pattern of contaminants in a displacement ventilated room-implications for demand control, in: 12th AIVC Conference, 1991: pp. 173–189.

[7] International Organisation for Standardization ISO, Ergonomics of the Thermal Environment: Analytical Determination and Interpretation of the Thermal Comfort Using Calculation of the PMV and PPD Indices and Local Thermal Comfort Criteria, ISO, 2005.

[8] B.J. Wachenfeldt, M. Mysen, P.G. Schild, Air flow rates and energy saving potential in schools with demand-controlled displacement ventilation, Energy Build. 39 (2007) 1073–1079. https://doi.org/10.1016/J.ENBUILD.2006.10.018.

[9] N.M. Mateus, G. Carrilho da Graça, Simulated and measured performance of displacement ventilation systems in large rooms, Build Environ. 114 (2017) 470–482. https://doi.org/10.1016/J.BUILDENV.2017.01.002.

[10] Z. Bakó-Biró, D.J. Clements-Croome, N. Kochhar, H.B. Awbi, M.J. Williams, Ventilation rates in schools and pupils' performance, Build Environ. 48 (2012) 215–223. https://doi.org/10.1016/J.BUILDENV.2011.08.018.

[11] G. Smedje, M. Mattsson, R. Wålinder, Comparing mixing and displacement ventilation in classrooms: pupils' perception and health, Indoor Air. 21 (2011) 454–461. https://doi.org/10.1111/J.1600-0668.2011.00725.X.

[12] R. Kosonen, Panu Mustakallio, Ventilation in Classroom: a Case-Study of the Performanceof Different Air Distribution Methods, in: 10th REHVA World Congress-Clima, 2010.

[13] M.L. Fong, Z. Lin, K.F. Fong, T.T. Chow, T. Yao, Evaluation of thermal comfort conditions in a classroom with three ventilation methods, Indoor Air. 21 (2011) 231–239. https://doi.org/10.1111/J.1600-0668.2010.00693.X.

[14] N. Lastovets, K. Sirén, R. Kosonen, J. Jokisalo, S. Kilpeläinen, Dynamic performance of displacement ventilation in a lecture hall, Https://Doi.Org/10.1080/14733315.2020.1777015. (2020). https://doi.org/10.1080/14733315.2020.1777015.

[15] Q.J. Kwong, H.F. Chen, A.A. Razak, Computational Simulation of Indoor Thermal Environment in a Tropical Educational Hall with Displacement Ventilation, Pertanika J. Sci. & Technol. 25 (2017) 77–88. http://www.pertanika.upm.edu.my/ (accessed August 12, 2021).

[16] L. Morawska, J. Allen, W. Bahnfleth, P.M. Bluyssen, A. Boerstra, G. Buonanno, J. Cao, S.J. Dancer, A. Floto, F. Franchimon, T. Greenhalgh, C. Haworth, J. Hogeling, C. Isaxon, J.L. Jimenez, J. Kurnitski, Y. Li, M. Loomans, G. Marks, L.C. Marr, L. Mazzarella, A.K. Melikov, S. Miller, D.K. Milton, W. Nazaroff, P. V. Nielsen, C. Noakes, J. Peccia, K. Prather, X. Querol, C. Sekhar, O. Seppänen, S. Tanabe, J.W. Tang, R. Tellier, K.W. Tham, P. Wargocki, A. Wierzbicka, M. Yao, A paradigm shift to combat indoor respiratory infection, Science (1979). 372 (2021) 689–691.

[17] A. Melikov, G. Pitchurov, K. Naydenov, G.L.-I. air, undefined 2005, Field study on occupant comfort and the office thermal environment in rooms with displacement ventilation,

Researchgate.Net. (n.d.). https://doi.org/10.1111/j.1600-0668.2005.00337.x.
[18] F.A. Berlanga, M.R. de Adana, I. Olmedo, J.M. Villafruela, J.F. San José, F. Castro, Experimental evaluation of thermal comfort, ventilation performance indices and exposure to airborne contaminant in an airborne infection isolation room equipped with a displacement air distribution system, Energy Build. 158 (2018) 209–221. https://doi.org/10.1016/J.ENBUILD.2017.09.100.
[19] B. E, N. PV, Dispersal of exhaled air and personal exposure in displacement ventilated rooms., Indoor Air. 12 (2002) 147–164. https://doi.org/10.1034/J.1600-0668.2002.08126.X.
[20] C. Habchi, K. Ghali, N. Ghaddar, Displacement ventilation zonal model for particle distribution resulting from high momentum respiratory activities, Build Environ. 90 (2015) 1–14. https://doi.org/10.1016/J.BUILDENV.2015.03.007.
[21] J. Srebric, W. Xu, Removal of contaminants released from room surfaces by displacement and mixing ventilation: modeling and validation, Indoor Air. (2005). https://doi.org/10.1111/j.1600-0668.2005.00383.x.
[22] K. Zhong, Y. Kang, Y. Wang, Effect of source location on particle dispersion in displacement ventilation rooms, Particuology. 6 (2008) 362–368. https://doi.org/10.1016/j.partic.2008.05.005.
[23] N. Choi, T. Yamanaka, T. Kobayashi, T. Ihama, M. Wakasa, Influence of vertical airflow along walls on temperature and contaminant concentration distributions in a displacement-ventilated four-bed hospital ward, Build Environ. 183 (2020) 107181. https://doi.org/10.1016/J.BUILDENV.2020.107181.
[24] J.M. Villafruela, I. Olmedo, F.A. Berlanga, M.R. de Adana, Assessment of displacement ventilation systems in airborne infection risk in hospital rooms, PLoS One. 14 (2019) e0211390. https://doi.org/10.1371/JOURNAL.PONE.0211390.
[25] X. Xie, Y. Li, A. Chwang, P. Ho, W. Seto, How far droplets can move in indoor environments-revisiting the Wells evaporation-falling curve, (n.d.). https://doi.org/10.1111/j.1600-0668.2006.00469.x.
[26] R. SN, M. DK, Risk of indoor airborne infection transmission estimated from carbon dioxide concentration., Indoor Air. 13 (2003) 237–245. https://doi.org/10.1034/J.1600-0668.2003.00189.X.
[27] Study on the initial velocity distribution of exhaled air from coughing and speaking | Elsevier Enhanced Reader, (n.d.). https://reader.elsevier.com/reader/sd/pii/S0045653512000987?token=BCD9F88B43D84BFC70C50F97883B88D8467CC96C6FF35BA859ED12F3C76D3F487157DF3B318ECB1C9A52C5FF8142F79A&originRegion=us-east-1&originCreation=20220124075703 (accessed January 24, 2022).
[28] R. Yang, C.S. Ng, K.L. Chong, R. Verzicco, D. Lohse, Optimal ventilation rate for effective displacement ventilation, (2021). https://arxiv.org/abs/2104.03363v1 (accessed August 12, 2021).
[29] A. Jurelionis, L. Gagyte, T. Prasauskas, D. Čiužas, E. Krugly, L. Šeduikyte, D. Martuzevičius, The impact of the air distribution method in ventilated rooms on the aerosol particle dispersion and removal: The experimental approach, Energy Build. 86 (2015) 305–313. https://doi.org/10.1016/J.ENBUILD.2014.10.014.
[30] Y. Yin, J.K. Gupta, X. Zhang, J. Liu, Q. Chen, Distributions of respiratory contaminants from a patient with different postures and exhaling modes in a single-bed inpatient room, Build Environ. 46 (2011) 75–81. https://doi.org/10.1016/J.BUILDENV.2010.07.003.
[31] Y. Yin, W. Xu, J. Gupta, A. Guity, P. Marmion, A. Manning, B. Gulick, X. Zhang, Q. Chen, Experimental study on displacement and mixing ventilation systems for a patient ward, HVAC and R Research. 15 (2009) 1175–1191. https://doi.org/10.1080/10789669.2009.10390885.
[32] Z. Lin, T.T. Chow, C.F. Tsang, K.F. Fong, L.S. Chan, CFD study on effect of the air supply location on the performance of the displacement ventilation system, Build Environ. 40 (2005) 1051–1067. https://doi.org/10.1016/J.BUILDENV.2004.09.003.
[33] Z. Lin, T.T. Chow, C.F. Tsang, Effect of door opening on the performance of displacement ventilation in a typical office building, Build Environ. 42 (2007) 1335–1347. https://doi.org/10.1016/J.BUILDENV.2005.11.005.
[34] H. Qian, Y. Li, P. V. Nielsen, C.E. Hyldgaard, Dispersion of exhalation pollutants in a two-bed hospital ward with a downward ventilation system, Build Environ. 43 (2008) 344–354. https://doi.org/10.1016/J.BUILDENV.2006.03.025.

[35] N. Gao, J. Niu, L. Morawska, Distribution of Respiratory Droplets in Enclosed Environments under Different Air Distribution Methods, (n.d.). https://doi.org/10.1007/s12273-008-8328-0.
[36] A. Naseri, O. Abouali, G. Ahmadi, Effect of turbulent thermal plume on aspiration efficiency of micro-particles, Build Environ. 118 (2017) 159–172. https://doi.org/https://doi.org/10.1016/j.buildenv.2017.03.018.
[37] Q. Zhou, H. Qian, H. Ren, Y. Li, P. V. Nielsen, The lock-up phenomenon of exhaled flow in a stable thermally-stratified indoor environment, Build Environ. 116 (2017) 246–256. https://doi.org/10.1016/J.BUILDENV.2017.02.010.
[38] H. Brohus~, ~ And, P. V Nielsen', Personal Exposure in Displacement Ventilated Rooms, Indoor Air. 6 (1996) 157–167. https://doi.org/10.1111/J.1600-0668.1996.T01-1-00003.X.
[39] J. Hang, Y. Li, R. Jin, The influence of human walking on the flow and airborne transmission in a six-bed isolation room: Tracer gas simulation, Build Environ. 77 (2014) 119–134. https://doi.org/https://doi.org/10.1016/j.buildenv.2014.03.029.
[40] S. Xin, H. Xu, S. Li, W. Wang, J. Guo, W. Yang, Efficiency evaluation of a floor standing air conditioner with different installation positions and air supply parameters applied to a large laboratory, Journal of Building Engineering. 32 (2020) 101701. https://doi.org/10.1016/J.JOBE.2020.101701.
[41] R. Cermak, A.K. Melikov, L. Forejt, O. Kovar, Performance of Personalized Ventilation in Conjunction with Mixing and Displacement Ventilation, HVAC&R Res. 12 (2006) 295–311. https://doi.org/10.1080/10789669.2006.10391180.
[42] Y. Xu, X. Yang, C. Yang, J. Srebric, Contaminant dispersion with personal displacement ventilation, Part I: Base case study, Build Environ. 44 (2009) 2121–2128. https://doi.org/https://doi.org/10.1016/j.buildenv.2009.03.006.
[43] F. Liu, T. (Tim) Zhang, L. Yang, Z. Long, An improved wall-mounted displacement ventilation system in a large-span machining workshop, Build Simul. 15 (2022) 1943–1953. https://doi.org/10.1007/s12273-022-0906-z.
[44] R. Kosonen, N. Lastovets, P. Mustakallio, G.C. da Graça, N.M. Mateus, M. Rosenqvist, The effect of typical buoyant flow elements and heat load combinations on room air temperature profile with displacement ventilation, Build Environ. 108 (2016) 207–219. https://doi.org/10.1016/J.BUILDENV.2016.08.037.
[45] X. Wu, L. Fang, B.W. Olesen, J. Zhao, F. Wang, Air distribution in a multi-occupant room with mixing or displacement ventilation with or without floor or ceiling heating Air distribution in a multi-occupant room with mixing or displacement ventilation with or without floor or ceiling heating, Sci Technol Built Environ. 21 (2015) 1109–1116. https://doi.org/10.1080/23744731.2015.1090255.
[46] X. Yuan, Q. Chen, L.G.-A.T.-A. Society, undefined 1998, A critical review of displacement ventilation, Aivc.Org. (n.d.). https://www.aivc.org/resource/critical-review-displacement-ventilation (accessed April 9, 2023).
[47] P. V Nielsen PhD, M. Buus, F. V Winther, M. Thilageswaran, Contaminant Flow in the Microenvironment Between People Under Different Ventilation Conditions, ASHRAE Trans. 114 (2008) 632–638.

Chapter 2 Double Wall Flat Diffuser with Non-Uniform Supply in Large Lecture Hall

2.1. Background and Purpose

The aim of this investigation is to assess the performance of the DV system in terms of temperature stratification, air quality of occupied zone, and more importantly, cross-infection prevention. The case-study is an uncommon system design installed in a lecture hall in Osaka University. Aiming at making DV spaces more adaptable and less restricted with diffusers, especially in large spaces, the system was designed to be flat, wall-long and embedded in double walls. In this Chapter, the process of assessing the performance of this system is reviewed, starting from the pre-construction CDF explorations, then carrying out field measurements, and ending by validating the CFD simulations. To evaluate its versatility, the system is evaluated in cases of different seating patterns, varying contaminant source position, and with different diffusers design.

2.2. Introduction of the Double Wall Flat Diffuser Displacement Ventilation System

The lecture hall

The lecture hall studied in this research is a lecture hall located in Minoh campus, Osaka University. It should be noted that the study started before construction was finalized, thus differences between the design phase plan and constructed one can be noticed, Figure 2.1. The main alteration besides slight dimensions change is the hall capacity; although it was designed to accommodate 120 students, after construction, the final seat arrangement was enough for 80 students.

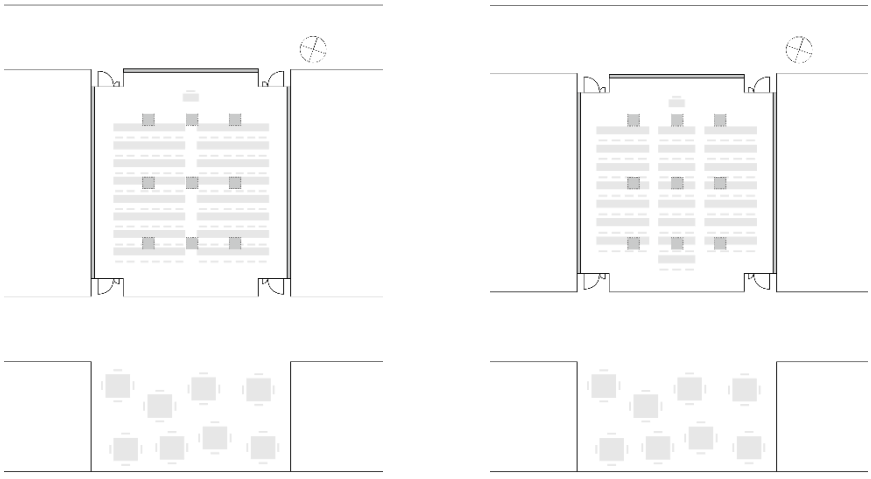

a. Design phase ***b. Construction phase***

Figure 2.1 Lecture hall plan

The displacement ventilation system

As shown in Figure 2.2, the ventilation system is composed of inlet fans, diffusers, and exhaust openings. Unlike a typical DV system, the inlet fans at ceiling level blow the cool air through 20 cm wide double walls

to flow into the space through the perforated metal flat diffusers installed along the bottom of the walls. The perforated metal panels have a percentage opening of 39.27%. Exhaust openings, on the other hand, are nine equally spaced typically installed in the ceiling. Openings dimensions, shown in Figure 2.3, are as follows; exhausts are 0.6 m×0.6 m squares, all diffusers are 0.9 m high, 10.7 m long for side diffusers and 7.7 m for the front one. The diffusers' system is installed in the front and side walls. The backside is an 8 m wide operable wall, as shown in Figure 2.1, which allows users to expand the lecture room area to include the students lounge in special events.

A comparable system was introduced in 1996 for application in cold climate [1]. The authors concluded that having air flow within double walls acted as insulation reducing the heat loss through walls and enhancing the system performance. Although, the double wall system was designed for the exhaust opening, not inlets as in the current case-study, the insulation effect should still apply. Choi et al., on the other hand, addressed the effect of wall temperature on the magnitude of the near-walls downdraft and consequently on contaminants stratification. It was concluded that cooler the wall surface is, the larger downward airflow becomes increasing heat loss in the space and lowering the contaminants interface level [2]. Nevertheless, it should be mentioned that both of the referenced studies had small number of occupants, small space volume i.e. higher surface area to volume ratio than the case-study addressed in this research. Moreover, as to counteract the estimated negative effects in this case-study, the gypsum board double walls are insulated using polyethylene foam sheets.

Another feature of the examined system is flat diffusers. Flat diffuser unit is an optimal option to provide large surface area without using any space of the DV room. Although the commonly used DV diffuser designs are free standing circular, wall-mounted semi-circular, or corner-mounted semi-circular [3], radial and flat diffusers are studied in multiple researches [3–5]. Cehlin and Moshfegh (2010) worked on validating flat diffusers simulation in terms of flow and thermal behavior [6]. Xing et al. (2001) compared the performance of the wall-mounted flat and semicircular units and floor-mounted swirl units [7]. It was noticed that the air quality in the flat diffuser case came second to the semicircular unit by 10% in terms of local air change. However, according to Kosonen et al. (2017), the major challenge in flat diffusers DV systems is draft within the adjacent zone. Instead of decreasing the inlet flow rate and affecting the air quality, the authors recommended increasing the number of diffusers for a more uniform indoor environment [3]. In this case-study the diffusers total surface area exceeds 25 m^2 for a 164 m^2 plan and are separated from occupants by 1.8 m wide aisle.

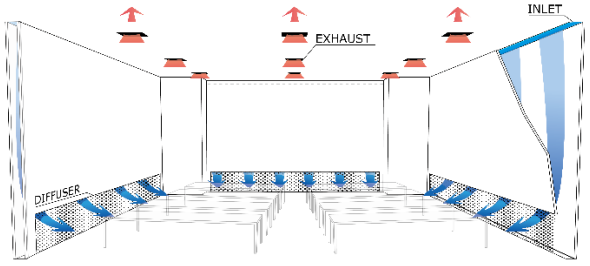

Figure 2.2 Displacement ventilation system in the lecture room

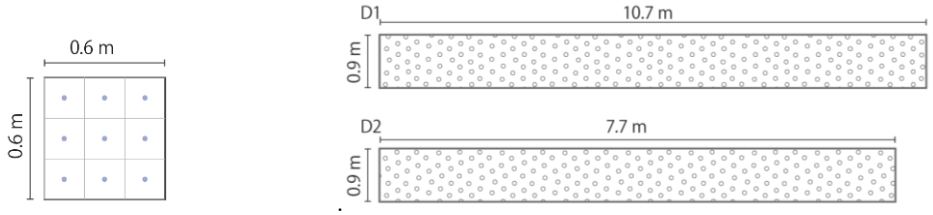

a. Exhaust opening ***b. Diffusers; D1: side diffusers, D2: Front diffuser.***

Figure 2.3 Openings dimensions

2.3. Pre-Construction Exploration using CFD Analysis

2.3.1. Effect of Occupants Seating Pattern Temperature and Contaminant Distribution in Steady State

2.3.1.1. Analysis Conditions and Cases

The ventilation system inflow rate is 11910 m^3/h in total, divided as 4830 m^3/h for side fans and 2850 m^3/h for the front ones. These values are the maximum capacity of the DV system including fresh and return air. Exhaust openings are all operating with natural outflow settings. Regarding the occupants, 120 seated students and one standing teacher are modeled as 0.2 m x0.4 m cuboids with heights of 1.2 m and 1.7 m respectively as shown in Figure 2.4c. Students are split into two 10-rows seating zones separated by a 1 m aisle. All occupants emit 60 W heat from the whole-body surface area, and CO_2 from a 0.05 m× 0.05 m mouth surface. CO_2 concentration of exhalation is set to 1000 ppm and the emission rate to 0.25 m^3/h.

Standard k-ε turbulence model was used for the CFD simulation. Heat, radiation, and diffusion calculations were carried out. Thermal boundary conditions were set to adiabatic for ceiling, floor and external walls. 3.06 of heat transfer coefficient was deducted from ASHRAE Handbook [(3)] for the duct walls, Table 2-5a. Finally, the model meshing resulted in 4,856,000 cells. The main mesh size was set to 40 mm with a geometric ratio of 1.15. However, the mesh layer adjacent to the walls was increased to 100 mm wide to include the near wall down draft based on a test with low Reynolds number simulation as shown in Figure 2.4b. Table 2-1and Table 2-2 sum up the analysis and boundary conditions discussed in this section.

To compare the effect of occupation pattern, 6 cases were simulated. Table 2-3Table 2-3 is an enlistment of the cases C1 to C6. C1 is the full room scenario with double the occupation and flow rate compared to the other cases. The arrangements of C2 to C4 are designed to test the dispersed-occupants scenarios, i.e. social distancing. Finally, C5 and C6 are the front and back half room occupation scenarios.

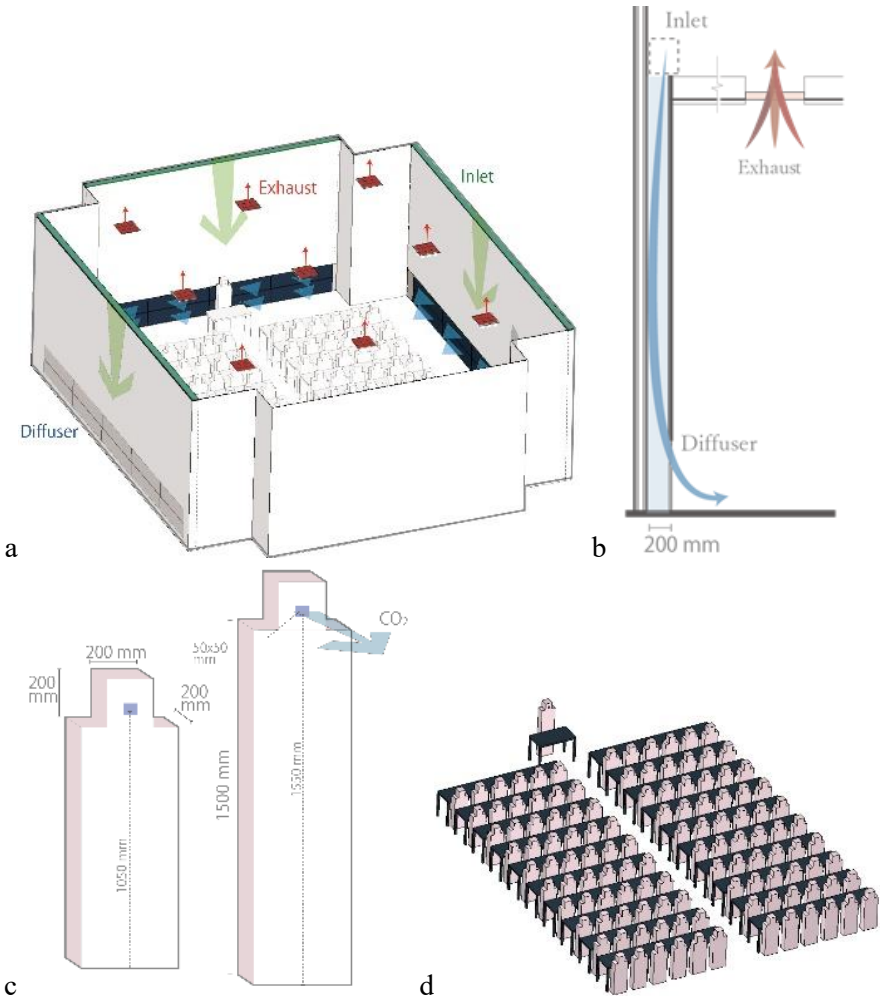

Figure 2.4 Lecture hall model attributes

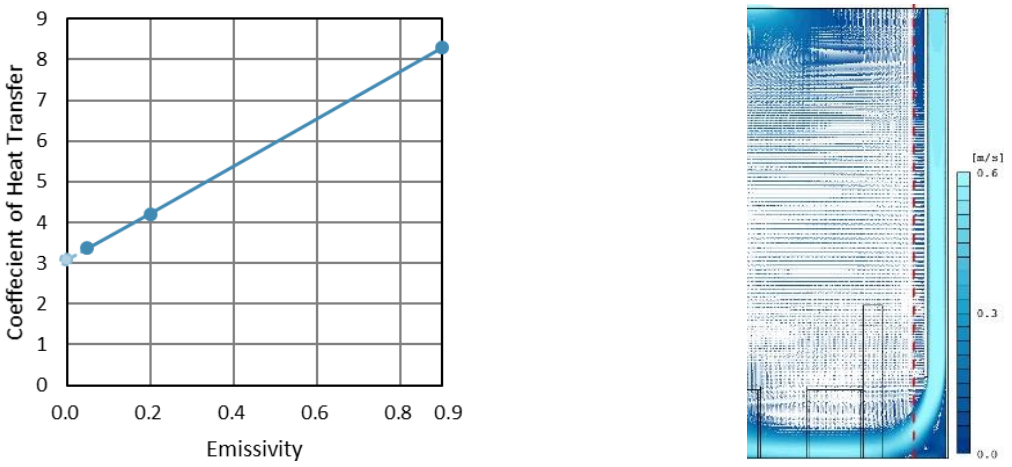

a. Coefficient of heat transfer vs emissivity b. Low Reynolds number simulation section

Figure 2.5 Analysis conditions

Table 2-1 Analysis conditions

Analysis Software	Stream 20
Turbulence model	Standard k-ε model
Calculations	Heat, Radiation, Diffusion (CO_2)
Mesh count	4,841,200

Table 2-2 Boundary conditions

Wall Boundary	Duct wall	Heat transfer coefficient, 3.06 W/m K
	Exterior	Adiabatic
Outflow Boundary	Natural outflow	
Heat generation	60 W/ person	
CO_2 generation	0.25 m^3/h . person (Concentration: 1000 ppm)	

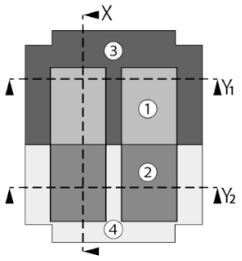

Figure 2.6 Zones division in plan view

Table 2-3 Occupants arrangements and room zoning

Cases		Case1 (C1)	Case2 (C2)	Case3 (C3)	Case4 (C4)	Case5 (C5)	Case6 (C6)
Occupants seating pattern		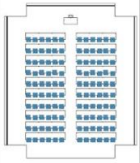		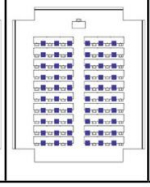	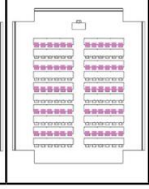	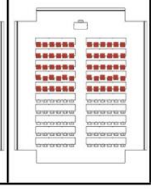	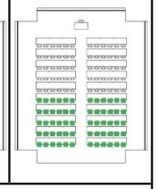
Number of students		120	60				
Inflow boundary	Diffuser 1	4530 m^3/h	2265 m^3/h				
	Diffuser 2	2850 m^3/h	1425 m^3/h				
	Total	11910 m^3/h	5955 m^3/h				

2.3.1.2. Results and Discussion

The room plan was divided into 4 zones as shown in Figure 2.6. Z1 and Z2 are the occupied areas containing 60 seats each while Z3 and Z4 are the unoccupied ones. Plottings of temperature, Figure 2.9, and CO_2 concentration, Figure 2.10, as well as contours in one longitudinal section, two cross-sections, and two plan sections at seated and standing occupants heights are analysed.

Analysing the sections, Figure 2.7 and Figure 2.8, it can be noted that C1 and C6 show plume interaction increasing the temperature around occupants especially in C1. In accordance, CO_2 concentrations in breathing level in C1 are higher compared to the widely spaced occupants' cases, C2, C3, and C4 where thermal plumes are separate. C5, as well, exhibits no plume interaction as occupants are seated nearer to the front diffuser providing cool fresh air. As for C2 and C3, only minimal differences can be noted.

Average temperature and normalized CO_2 concentration data for each zone are plotted in Figure 2.9 and Figure 2.10, respectively. To start with, the temperature plot in Z1 shows C5 to have the highest readings, even higher than C1. C1 displays lowest temperature at higher levels. In Z2 and Z4, all cases are similar, except for C5 in which the front zone is empty. As for Z3, reveals lower temperatures in C1 reaching 0.8 ℃ difference.

Secondly CO_2 concentration plots, in Z1, a surge appears at 1.1 m height in C1 alone. However, in Z2 the spike shows in C6 as well, yet milder. In addition, it is worth mentioning that C1 exhibits the highest levels in both zones at seated occupant level. Furthermore, Z3 has less CO2 concentration in C1 and C6. Finally, in Z4, all cases experience the same trend with small differences.

To get a clearer picture of the concentration of inhaled CO_2 in the different cases, Figure 2.8 sums up the average normalized CO_2 concentration at 10 cm under occupant's mouth, compared to 5 cm above. The concentrations in the inhaling level are less than the CO_2 concentration at exhaust in all cases except for C1. Despite showing similar results in the zones average plots, C2 was shown to be advantages over C3 displaying the lowest concentration, of half that of the exhaust. C3 and C5 closely followed then C4 at 0.71, and finally C6. Further inspection of the velocity contours suggests the following deduction. As shown in Figure 2.11, the occupants were modelled with no space separating them from their desks, Figure 2.12. Such an arrangement hindered the up-flow from sweeping the contaminants up. Instead, a downward swirl was produced pushing contaminants to the breathing level fighting against side flow and buoyancy forces.

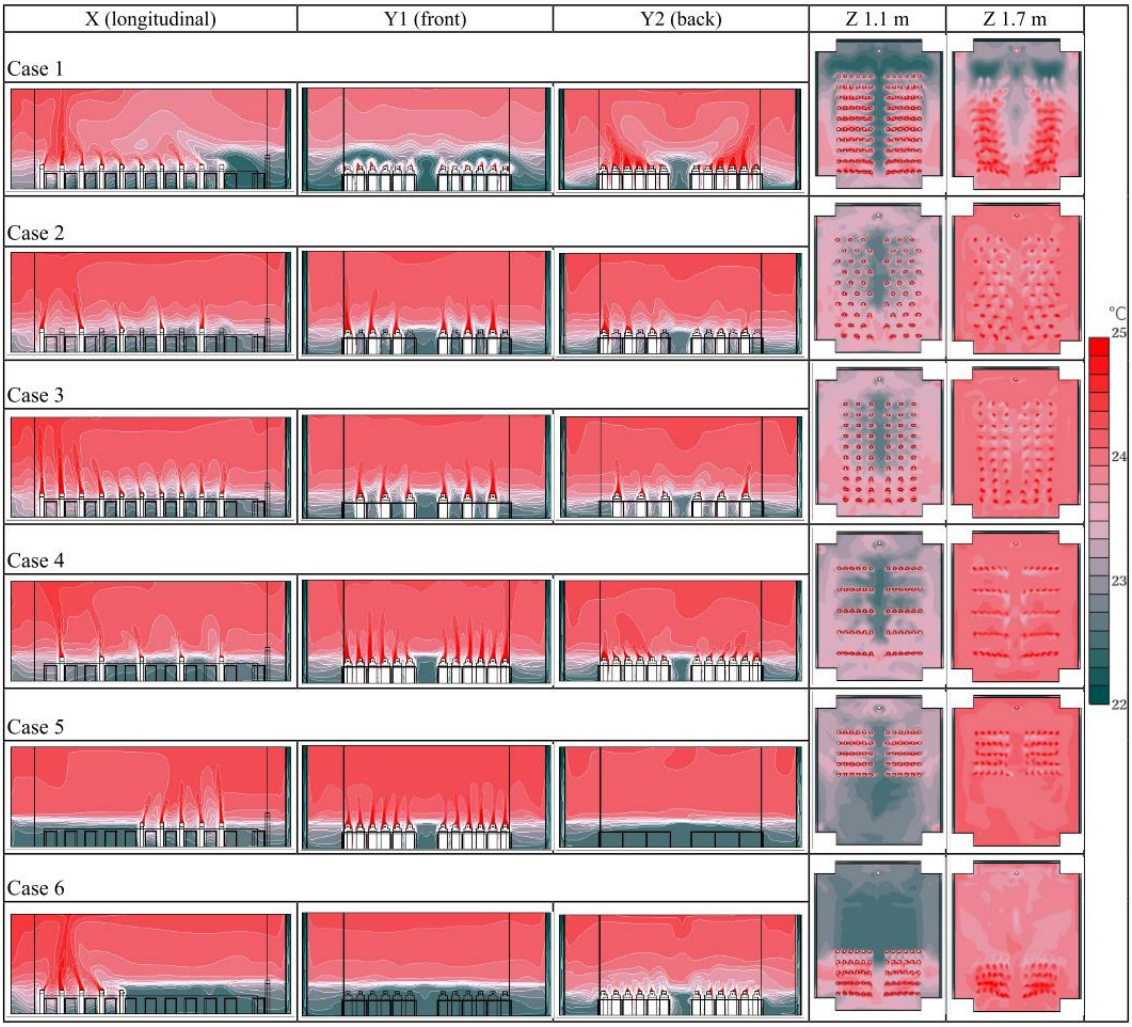

Figure 2.7 Temperature contoursf for different seating patterns cases

Table 2-4 Inhalation level average normalized CO2 concentration

	C1	C2	C3	C4	C5	C6
1.1m	4.40	2.55	2.31	3.88	2.29	4.28
0.95m	1.11	0.52	0.61	0.71	0.63	0.82

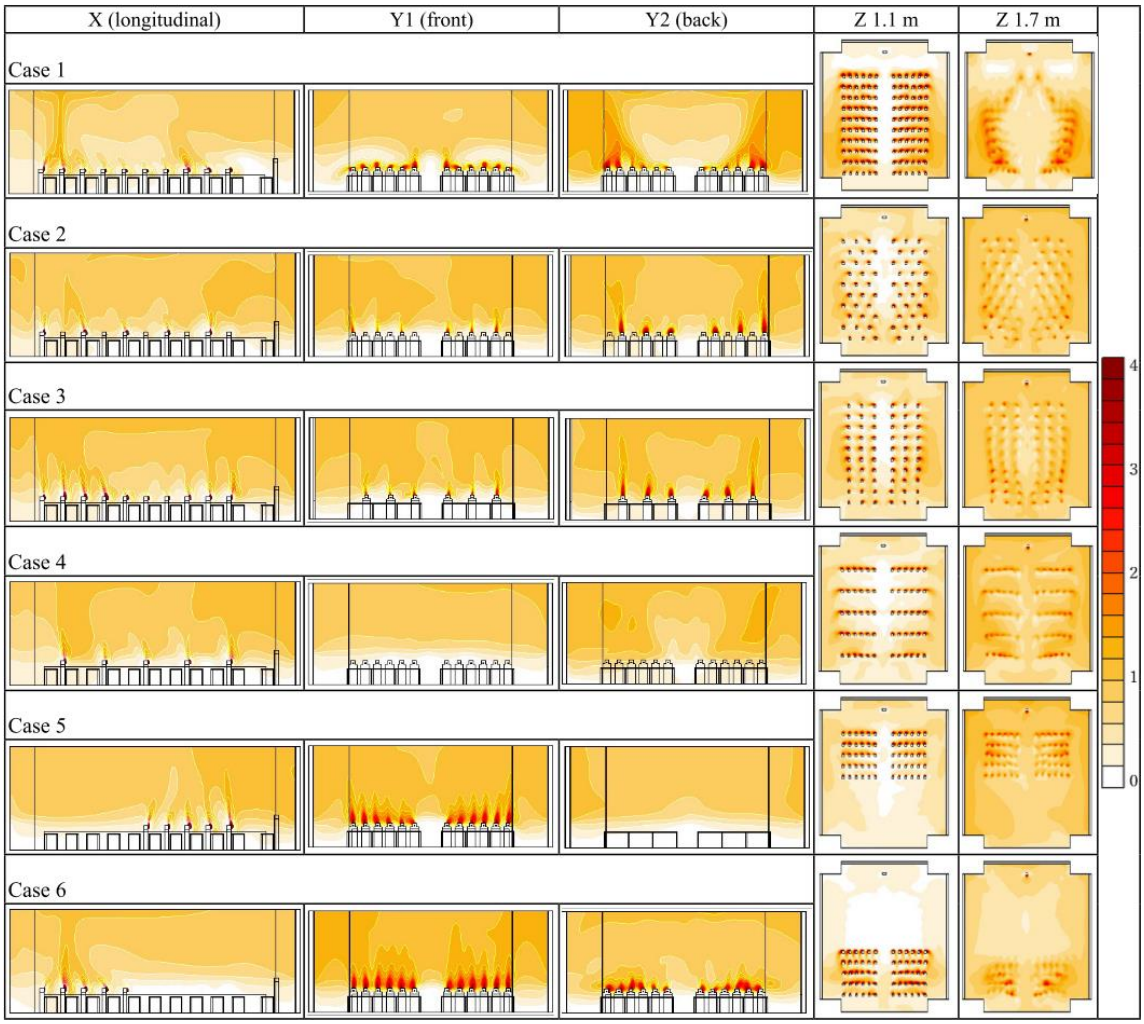

Figure 2.8 Normalized CO2 concentration contours for different seating patterns cases

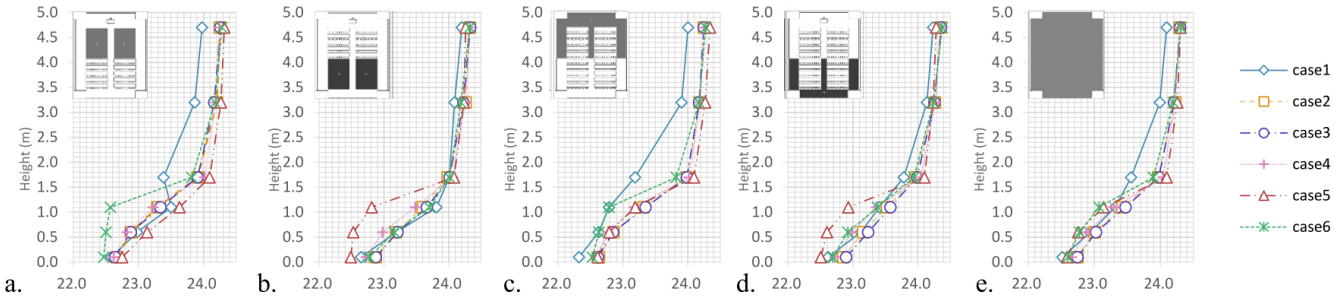

Figure 2.9 Zones' average temperature: a. Z1, b. Z2, c. Z3, d. Z4, e. Room average

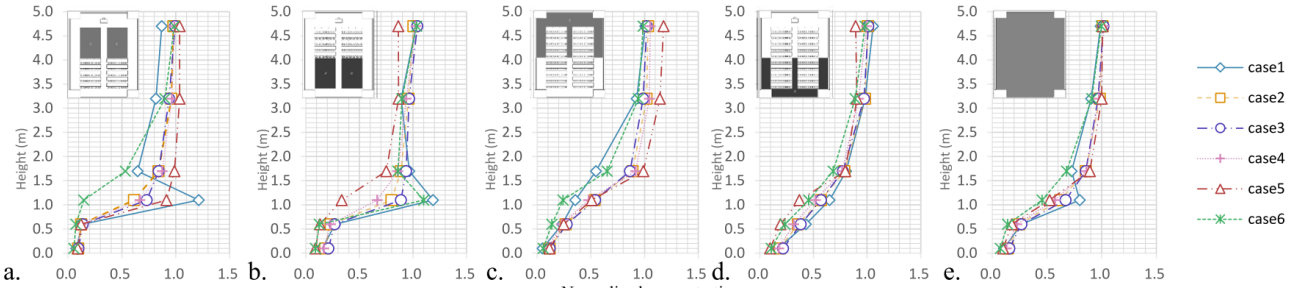

Figure 2.10 Zones' average normalized CO2 concentration: a. Z1, b. Z2, c. Z3, d. Z4, e. Room average

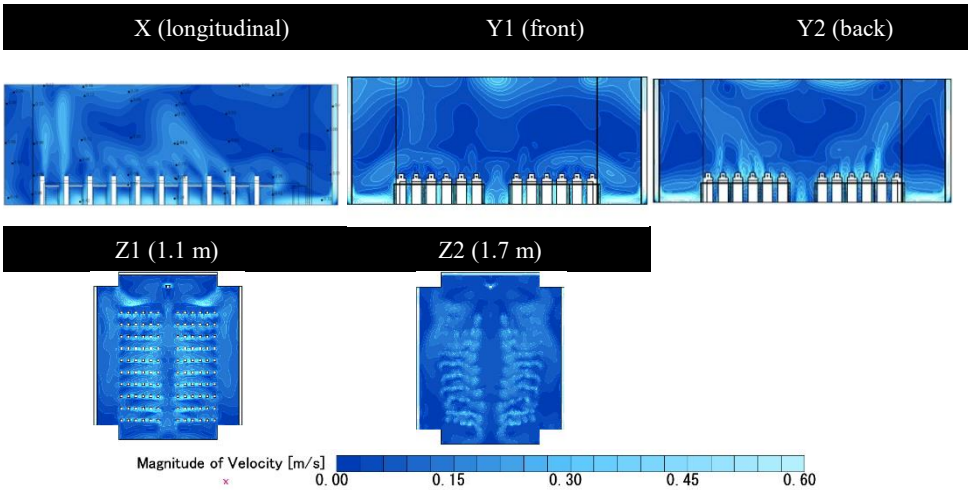

Figure 2.11 Velocity contours of C1

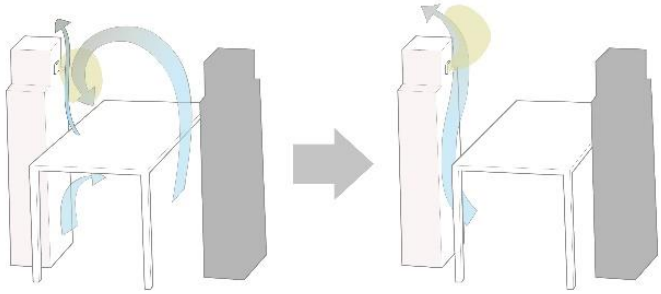

Figure 2.12 Effect of spacing between occupants and desks

2.3.2. Effect of Source Location on Temperature and Contaminant Distribution in Steady State

In this study, ten cases were simulated assuming one infected individual. As infection spread indicator, CO_2 was set as the exhaled air contaminant. The design version of the lecture room which has 120 seats for students in addition to the lecturer is used in this analysis. The students' seats are divided into two 10-rows-zones symmetric along the central aisle with six seats in each row as illustrated in Figure 2.15a.

2.3.2.1. Analysis Conditions and Cases

The analysis was carried out using the CFD software Cradle Stream v.21.1. The RNG k- ε turbulence model was chosen. Although Rohdin and Moshfegh found the calculation time of simulations carried using RNG k-ε model to take longer time than that done using the standard k-ε model [8], many studies preferred RNG k-ε model in terms of accuracy in simulating DV airflow, temperature and contaminant concentration [9–11]. Calculations of heat, radiation, and diffusion were computed. Thermal boundary for all surfaces was set to log. law calculation method. However, the outer layer of all external surfaces, i.e. ceiling, floor, and double walls' outer wall, was set to a fixed temperature of 25℃ as shown in Figure 2.13

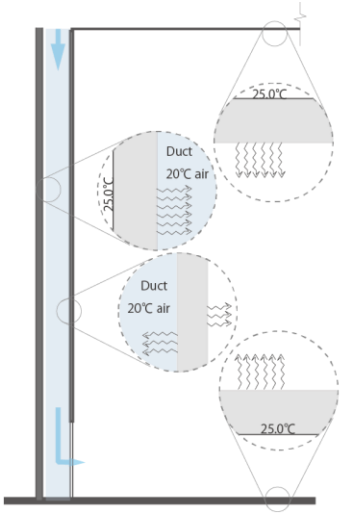

Figure 2.13 Thermal boundary settings in section

To accurately simulate heat transfer using log. law, minimizing the molecular viscous effect, an appropriate y+ should be achieved [12]. Accordingly, a test model was simulated using low Reynold's number model to deduce the proper size of the mesh layer adjacent to the inner side of double walls, room side. The test model is a 3 m × 3 m square of 5 m height. The test model consisted of 6,048,000 mesh cells of 2 mm width and sustained the same flow rate per volume as the main case-study. By inspecting air velocity vector in section, the downdraft varied in width along at different heights, nevertheless, taking in consideration the occupied zone height, 1.8 m, the downdraft thickness was presumed to be 100 mm. Based on the CFD software interpretation of the heat transfer equation [13,14], the first mesh centerline should be at least 100 mm away from the wall surface, for the calculations not to be affected by the downdraft's unrepresentative temperature. Consequently, for the main analysis, the room was divided into around 3.5 million cells of a 50 mm size except near the walls where it increases, with a growth rate of 1.15, to 200 mm for the first mesh layers. These meshing

settings resulted in an average Y+ value for the double walls inner layer of 33.2 while that of the ceiling and floor was 59.9.

Although 50 mm grid size was decided upon as it resulted in a manageable cells number, an additional check of grid dependency was necessary. In the finer-mesh model, the regular cell size was set to 30 mm with a total of 6.0 M cells compared to the 3.5 M cells in the medium-size meshing. Figure 2.14a shows the temperature distribution of vertical plane near the double wall. Comparing the two mesh sizes only a negligible difference was found and accordingly the 50 mm grid size was adopted.

Another step was to verify the set thermal boundary conditions. The log. law model results were compared to another model in which the heat transfer condition for the inner layer of the walls, floor, and ceiling were set as coefficient of heat transfer. The convective heat transfer values, where the emissivity is 0, were deducted from ASHRAE Standard 140-2017 by extrapolation to be 3.067 W/m^{2}k, 4.037 W/m^{2}k, and 0.967 W/m^{2}k for the walls, floor, and ceiling respectively [15]. The vertical distribution of average temperature, as shown in Figure 2.14b, displays minimal differences between the two conditions. Thus, the aforementioned thermal boundary conditions can be seen acceptable.

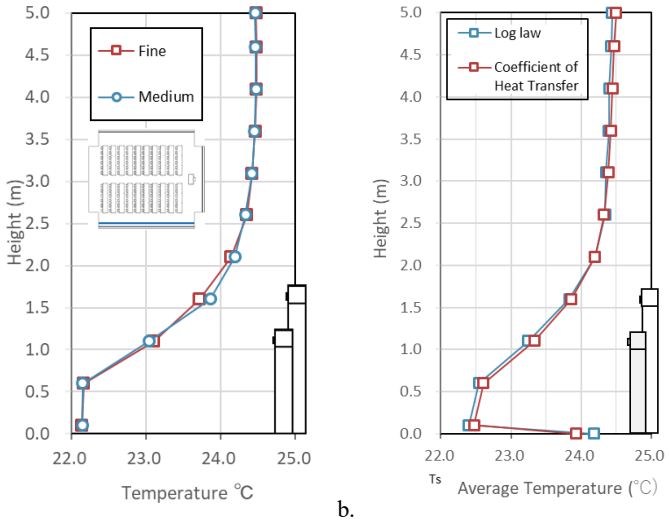

a. Fine vs Medium-size mesh b. Log. law vs Heat transfer coefficient

Figure 2.14 Temperature vertical distribution of different analysis conditions

Regarding the human model, adding more details like torso and legs would increase the calculation time considerably but have a negligible effect on results according to Bjørn and Nielsen (2002) [16]. Hence, the occupants were modelled as simple cuboids with heads as shown in Figure 2.15a. The body is 0.2 m × 0.4 m × 1.0 m with a 0.2 m × 0.2 m head for sitting students. For the standing lecturer the height was increased by 0.5 m. The CO_2 generation is through the mouth, modelled as 50 mm × 50 mm square. Heat flux generated from all occupants was set at 75 W/person. CO_2 generation, on the other hand, was limited to one occupant per case. Despite the fact that neither breathing nor speaking are of a steady flowrate, the average flow velocity is low enough to be represented as a stationary source [17]. Given that exhalation rate at rest ranges from 5-6 l/min, [16], exhalation flow rate was set to 5.21 L/min based on Zhang et al. field measurement [18]. The

source occupant's 10 positions are highlighted in Figure 2.15b. Finally, Table 2-5 summarizes the analysis conditions while the boundary conditions are listed in Table 2-6.

Table 2-5 Summary of analysis conditions

Software	Stream v.21.1	
Turbulence model	RNG k-εmodel	
	Steady state	
Calculations	Heat, Radiation, Diffusion (CO_2)	
Mesh		
Count	~ 3.5M	
Size	Default	0.05 m
	Near bounding	0.2 m
Growth rate	1.15	

Table 2-6 Summary of boundary conditions

Flow Boundary Conditions		
Inlet fans	Front	Fixed flow rate: 2850 m^3/h
	Sides	Fixed flow rate: 4530 m^3/h
Diffusers	Perforated metal panels 39.27% open	
Exhaust	Fixed velocity	
Thermal Boundary		
Heat transfer	Exterior	Outer layer fixed temp.
	Duct wall	Log law
	Floor-	
Construction	Ceiling	Rock wool λ=0.035W/(m.K)
	Floor	Concrete λ=1.2 W/(m.K)
	Walls	Hardwood λ=0.15W/(m.K)
Emissivity	0.9	
Heat Generation and Contaminant Emission Settings		
Heat	Source	120 seated occupants, 1
	Load	75 W/person
CO_2	Diffusivity	1.64×10^{-5}
	Source	1 mouth (0.05 m × 0.05 m)
	Temperature	32 ℃
	Rate	5.21 L/min.person

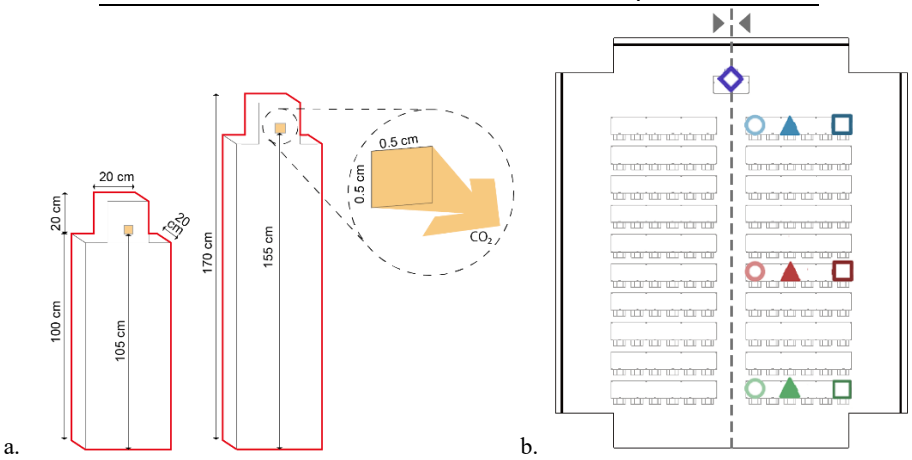

Figure 2.15 CFD model, a. Occupants model, b. Source individuals highlighted in plan

Finally, given the supply flow rate and convective heat load of occupants, theoretical calculation of the interface level of caused by the plume of one occupant can be calculated using the following equations set (2-1) and (2-2) [3]. This calculation simplifies the heat source to be cylindrical with one virtual point source as shown in Figure 2.16.

$$q_{v,z} = 0.005 \times {\phi_{cf}}^{1/3} \times z^{5/3} \quad (2\text{-}1)$$

$$z_0 = {D}/{2 \times \tan(12.5°)} \quad (2\text{-}2)$$

where $q_{v,z}$ is the thermal plumes vertical air volume flow (m³/s), set to equal supply flow rate/occupant, ϕ_{cf} is the convective heat flux (75 W), and z is the stratification height at which the plume vertical flow rate should equal the supply flow rate to attain equilibrium. z_0 is the height between virtual point source and the source top (m), and D is the heat source diameter (m) as illustrated in Figure 2.16 Through these calculations, the stratification height can be assumed to be 1.47 m. In spite of lying within the occupied zone, the stratification height is above the seated occupant head level, thus, the supply flow rate can be seen as adequate. It should be mentioned that the CFD results are expected to result in lower stratification height as the theoretical calculation did not take in consideration the plume interaction, which should slow the vertical flow rate, or the diffusers shape which ought to have an effect on the stratification height as well

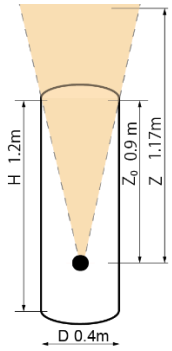

Figure 2.16 Heat source model simplification for interface level equation

2.3.2.2. Results and Discussion

The results can be divided into three main sections; DV system efficiency assessment, air quality evaluation, and exploring enhancement potential for the current DV system design. The section assessing the system efficiency addresses the analysis of temperature vertical distribution, airflow velocity vectors, and contaminant concentration distribution. Secondly, the air quality at occupant breathing zones was evaluated in addition to quantitative assessment of contaminants spread through numerical indices. Finally, the effect of altering two design aspects on the DV system performance was investigated.

2.3.2.2.1. Temperature distribution

DV system relies on controlling the desired air temperature in the occupant zone. Hence, the estimation of the vertical temperature gradient is essential for DV performance assessment [19]. From the horizontal and

longitudinal sections of temperature distribution, Figure 2.17 the relatively cool temperature surrounding all occupants can be noticed. At 1.1 m, the seated occupants head height, very gradual rise in temperature which increases going backwards, can be observed. The first and last rows of seats, however, have to some extent different temperature distribution from the other rows

Vertical temperature distribution graphs are plotted in Figure 2.18. Figure 2.18a shows the average temperature vertical distribution. It is clear that the temperature vertical distribution follows the typical profile for displacement ventilation, especially the model introduced by Mateus and da Graça [14]. Figure 2.18b compares the first, fourth, seventh and last row temperature distribution measured at 12 points centred in front of the occupants in the given row. The points are positioned midway between the rows at 0.5 m distance from occupants. The graph supports the observation noted from the temperature contours. Nevertheless, the stratification height for all points is almost the same, around the 2 m high. Special trends can be observed for the first and forth row. As seen in the contours, the first row maintains low, almost constant, temperature up till 1.7 m. As for the forth row, after the 1.1 m heat spike, the temperature decreases again at 1.7 m height, obviously due to the cool air current flowing from the front diffuser. Finally, comparing the occupied (seats) area to the unoccupied (aisles) area, the largest difference at the same height is about 0.5 K as shown in Figure 2.18c. In addition, the difference in temperature between 0.1 m and 1.7 m (occupied zone), for the front half of the room, is about 1 K, and for the rear part around 1.5 K. Which means that both fulfil ASHRAE guidelines [20] but the rear part difference falls slightly over the threshold set by Chen and Glicksman [21].

.

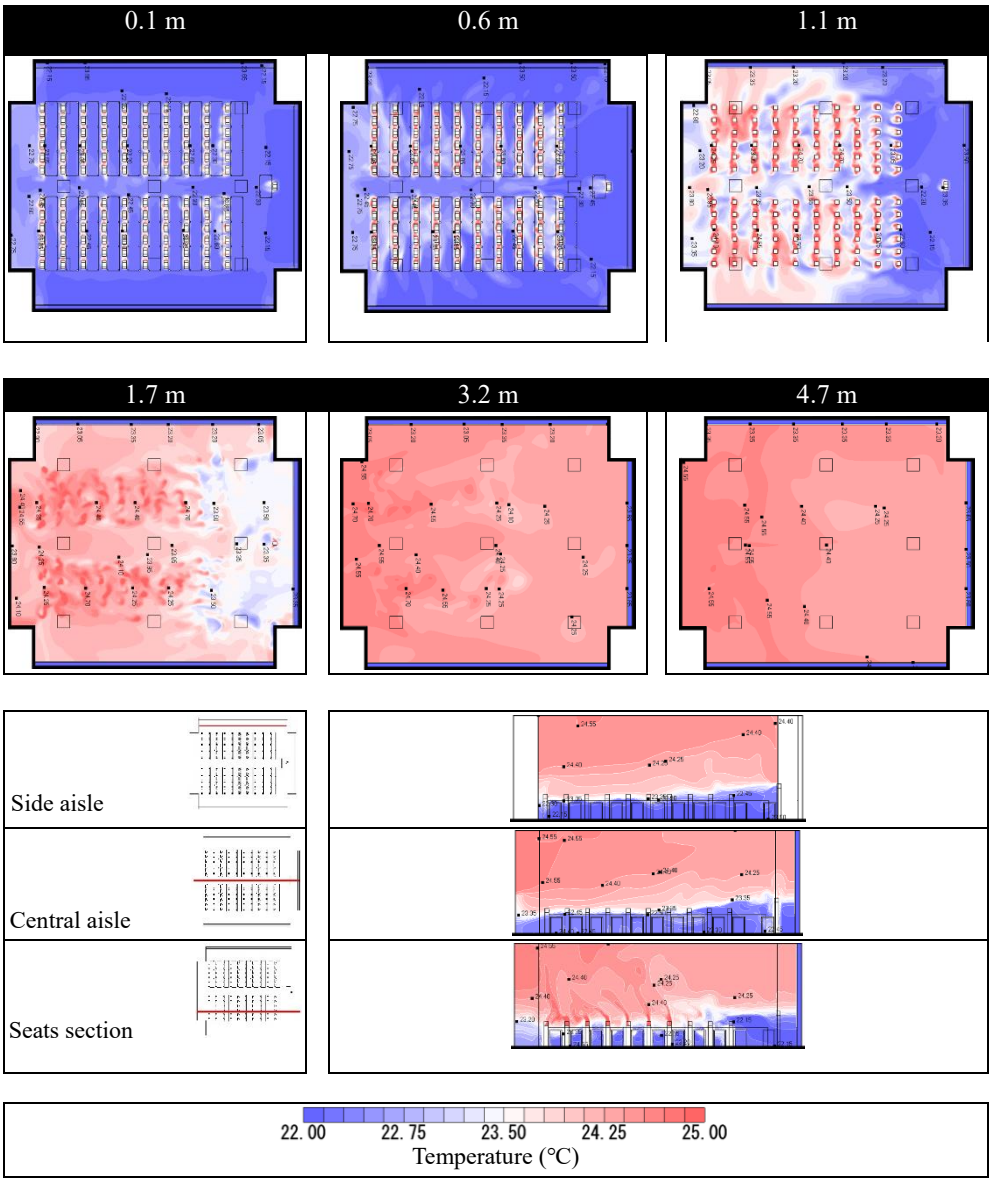

Figure 2.17 Temperature contours in plan and section views of a sample case from the different source position cases

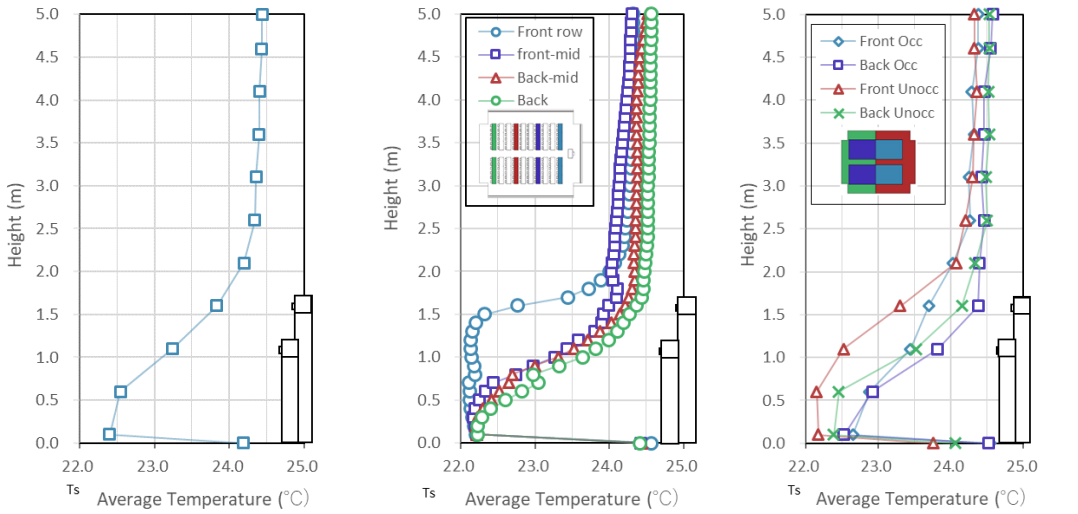

a. First vs Last row point temperature distribution, ***b. average temperature distribution with standard deviation,*** ***c. temperature distribution of occupied area vs unoccupied area***

Figure 2.18 Temperature vertical profile of a sample case from the different source position cases

Airflow velocity contours and vectors at horizontal and vertical planes are shown in Figure 2.19. The main significance of velocity contours is assisting in the estimation of discomfort due to draft. Since the highest velocity in DV is expected at 0.1 m and lower levels [22], 0.1 mm contour should be thoroughly inspected. Reviewing the velocity contour with that of temperature in Figure 2.19, the following is observed. At ankle level, the air of a temperature just above 22°C is flowing with velocity about 0.2 m/s. According to surveys carried out by Melikov et al, 2005, a typical DV air distribution discomfort due to draft is a serious issue [20]. Secondly, from the vertical section through the seats, the plume can be seen to have a relatively high vertical velocity which is a good indication of occupants experiencing comfortable temperature range [3]. Finally, horizontal planes are at 1.1 m, 1.7 m, 3.2 m, and 4.7 m while the vertical sections are cut through the central aisle and a side aisle. Air currents are generally of low speed, less than 0.1 m/s. Within the occupied zone, 1.1m and 1.7m plans, air flows backwards in the aisles and outwards between the rows. At higher levels, the aisles currents flip to be forward directed with a general trend of flowing towards the exhaust openings. In addition, above the occupied zone, at 3.2 m, asymmetric currents are noted flowing towards the right side. These currents are expected to have an effect on horizontal contaminants dispersion pattern as discussed in Srebic and Xu's publication [19] in which they concluded that the distribution of contaminants is strongly affected by the air currents. Another trend that should affect the diffusion pattern is the turbulent observed near the back wall at different levels and in section.

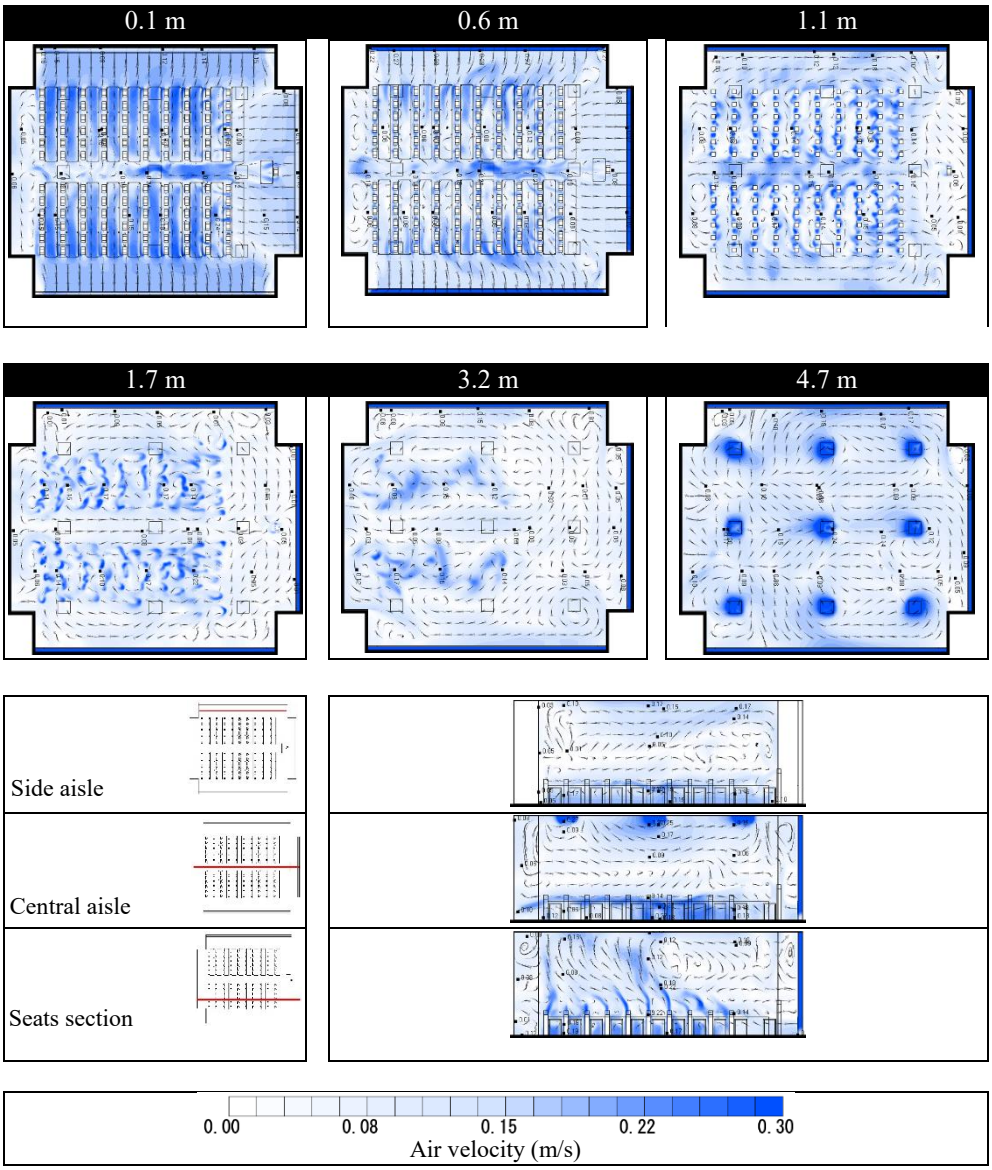

Figure 2.19 Airflow velocity vectors and contours of a sample case from the different source position cases

2.3.2.2.2. Contaminant concentration distribution

Inspecting the output results, the 10 cases were named as follows; lecturer case and nine student cases in a 3×3 matrix: 'front, middle, back' × 'left, center, right'. It should be stated that since the room is symmetrical along the Y-axis, as previously shown in Figure 2.15b, the 'left' cases represent the seats near the central aisle on both sides, and "right" ones stand for the seats on both outer aisles. Contaminant concentration contour plans at 1.1 m from floor level, seated occupant inhalation height, are displayed in Figure 2.20 along with the contours in longitudinal sections passing through infected individual. All contaminant values are normalized by division by the exhaust concentration.

Comparing front, middle, and back cases, back cases generally, have smaller, more concise, and more vertical contaminant cloud. Middle cases come in second place wider spread yet the occupied zone was hardly affected especially in the mid-center case. The front cases, on the other hand, demonstrate the widest horizontal

spread at lowest levels and highest contaminants concentration in the room volume. In the lecturer case, asymmetric spread can be noted as the main contaminant cloud flows to the right side. It is safe to say that this diffusion pattern is caused by the asymmetric currents noticed in the air velocity contours earlier. Two general observations were found in almost all cases except the back ones. One is that the contaminant concentration increases near walls, particularly the side ones, which can be the effect of the cool double walls' downdraft as concluded by Causone at al. [33]. The second is the clear area secured by the front diffuser as all contaminant diffusion is found to be shifted backwards in low levels regardless of the source position.

In Figure 2.21, vertical distribution of normalized concentration for the 10 cases is plotted using the plan average at each height except for the 5m height where it was replaced by the exhaust concentration. Following the temperature vertical distribution trends, the concentration curves fit that of a typical DV system. Interface level, however, varied from one case to the other. For middle and back cases, the concentration increased gradually remaining relatively low in all levels. On the contrary, lecturer and front cases spiked around 1.7 m, bulging to more than twice the exhaust concentration with an exception of the front-center case.

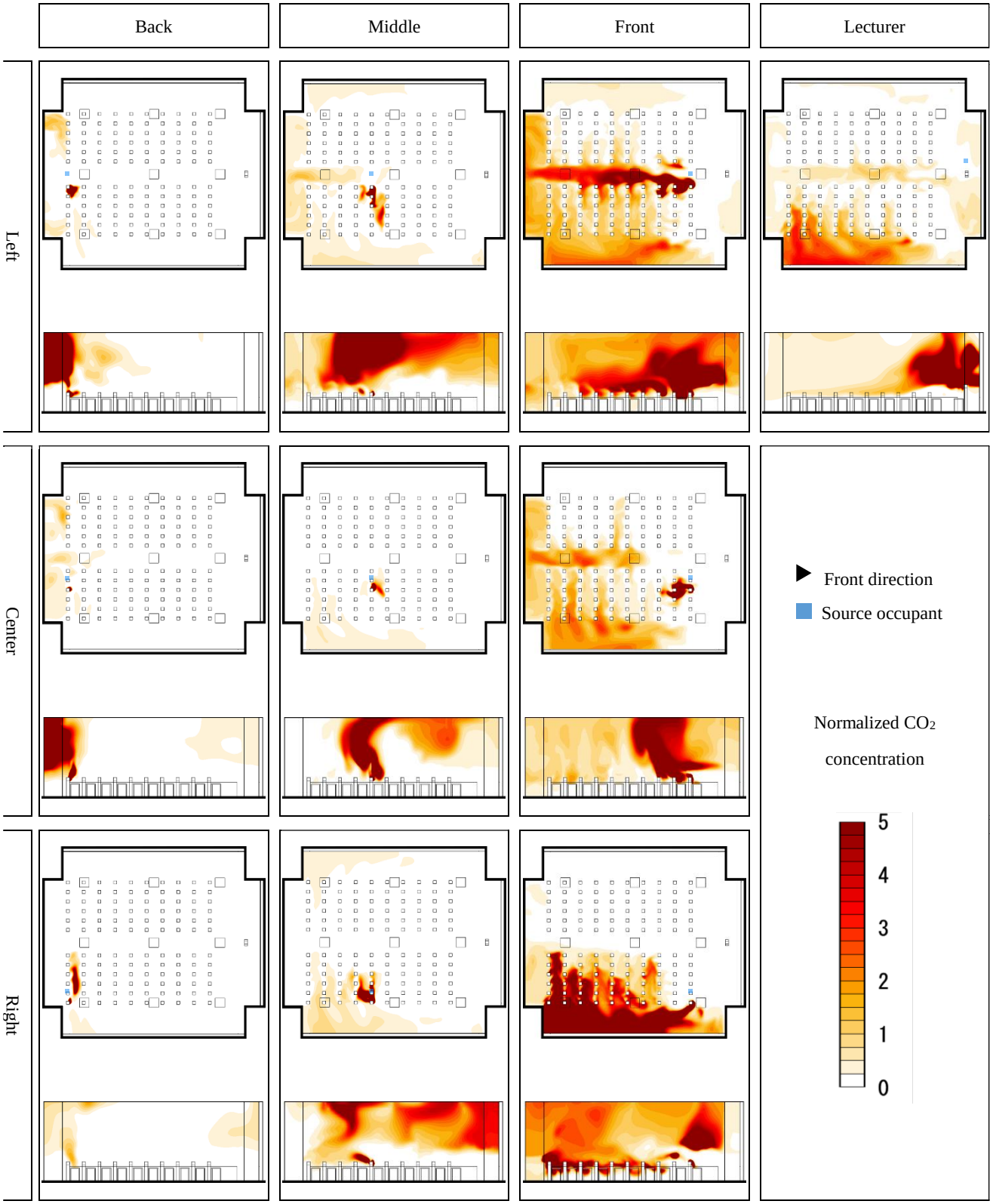

Figure 2.20 Contaminant distribution in plan at 1.1 m and longitudinal section passing through infected individual

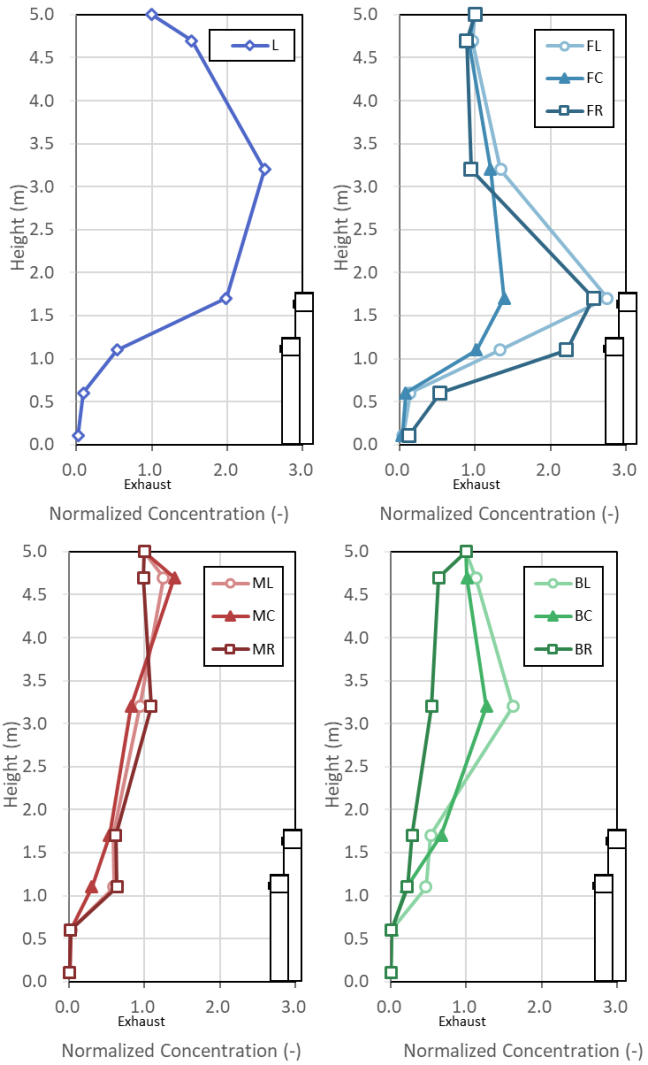

Figure 2.21 Normalized concentration vertical distribution

2.3.2.2.3. Breathing zone air quality

Although the concentration vertical distribution is indicative of air quality in the occupied zone, to assess the effect on occupants, more specific concentration values were examined. Contaminant concentration in the occupants' breathing zones was measured at the center point of the first mesh in front of the mouth, 2.5 cm away. The data was then normalized by division by exhaust concentration and finally, occupants were classified into 5 classes of concentrations starting with 0.01 with logarithmic increments as shown in Figure 2.22. This frequency curve is intended to estimate the probability of contaminants inhalation by non-source occupants.

From Figure 2.22 plotting, the following trends are observed. Firstly, lecturer case renders the largest number of occupants at 0.1 with negligible variation, a relatively high concentration compared to the other 9 cases. Secondly, front cases have the most distributed populations with multiple crests, ranging from 0.01 to 1. The highest concentration inhaled by a considerable number of occupants is in the front-right case, 1. Thirdly, all three middle cases display the general pattern of peaking at the 0.01 concentration. The largest portion of

population does not exceed 0.1. Finally, the back cases show a similar trend, however, the peak is distributed on 0.001 and 0.1 with a small percentage of the occupants exceeding the peak.

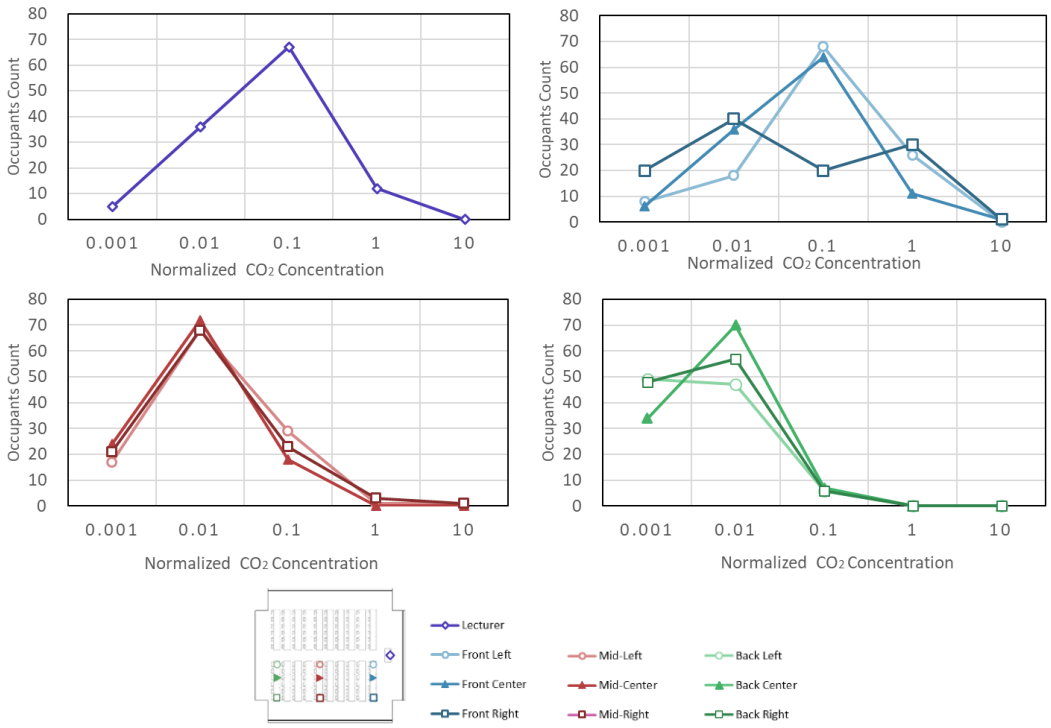

Figure 2.22 Distribution of occupants on normalized concentrations classes

2.3.2.2.4. Numerical indices (Local air quality index and Contaminants diffusion radius)

Supporting air quality assessment, two numerical indices were calculated. One method for the breathing zone air quality evaluation is local air quality index [78] calculated as per equation (2-3).

$$\langle \varepsilon_{\mathrm{p}}^{c} \rangle_{in} = C_e / \langle C_p \rangle_{in} \qquad (2\text{-}3)$$

where C_e is the average concentration at the exhaust openings and $\langle C_p \rangle_{in}$ is the average inhaled concentration measured by a sensor point in the breathing zone of each occupant. The second index is SVE2. Scale of ventilation efficiency (SVE), the set of indices (1~6) introduced by Murakami and Kato (1992), was considered as well [79]. SVE indices, especially SVE3 and SVE6 have been used in multiple studies to assess ventilation systems [80–82], or as a performance evaluation method base [83]. Nevertheless, SVE2 has also been used to estimate the contaminant diffusion radius [84] although not as widely. SVE2 was calculated as per equations (2-4 to 2~6).

$$C_0 = \int C.dv \qquad (2\text{-}4)$$

$$X_G = \int \frac{x.C.dv}{C_0} \qquad Y_G = \int \frac{y.C.dv}{C_0} \qquad Z_G = \int \frac{z.C.dv}{C_0} \qquad (2\text{-}5)$$

$$\mathrm{SVE2} = \sqrt{\int \frac{((x-X_G)^2+(y-Y_G)^2+(z-Z_G)^2)C.dv}{C_0}} \qquad (2\text{-}6)$$

where C_0 is the contaminants concentration integral, C is contaminants concentration at a given point in the room, 'v' is the room volume, (X_G, Y_G, Z_G) are contaminants concentration center of gravity, coordinates, and (x, y, z) are given point coordinates in the room. In order to carry out these calculations for all 3.5 million mesh cells, a Fortran script was written to extract and process the data automatically.

Table 2-7 shows the two indices calculated, $\langle \varepsilon_p^c \rangle_{in}$ and SVE2, in addition to the concentration integral, C_0. To start with, $\langle \varepsilon_p^c \rangle_{in}$, the lower values indicate higher relative inhaled concentrations, the front cases land lowest followed by the Mid-left and Lecturer cases. The back cases show much higher values comparable only to mid-center case. Regarding SVE2, the index display small differences as the diffusion radius for all cases ranges from 3.77 m to 4.66 m. Back-left, mid-center, and lecturer cases are found to have the smallest radius while back-right and mid-right cases show the largest radii. Although these findings oppose those of the concentration contours and local air quality index, two factors can explain this contradiction. The first is the fact that diffusion radius equation merges the three directions, specifically vertical and horizontal directions, causing cases with different diffusion direction such as back-center and mid-left, Figure 2.19, to have close spread radii. The second, and more impactive, factor is normalization by C_0 which in its turn varies greatly. The concentration integral, displayed similar pattern to that of local air quality index, considering that for C_0, a higher index indicates higher contaminant concentration since the volume is constant for all cases. In that sense, the lecturer case has 4 times the contaminants of the back-right case.

Table 2-7 Numerical indices evaluating breathing zone air quality

Index [unit]	Lecturer	Front-Left	Front-Center	Front-Right	Mid-Left	Mid-Center	Mid-Right	Back-Left	Back-Center	Back-Right
Local air quality index $\langle \varepsilon_p^c \rangle_{in}$ [-]	2.94	1.45	2.23	1.00	1.90	19.99	3.01	36.39	32.50	39.00
SVE2 [m]	4.04	4.33	4.16	4.35	4.45	3.77	4.55	3.86	4.32	4.66
Concentration integral C_0 [ppm m^3]	30.37	27.94	20	23.71	16.21	11.74	16.59	18.92	16.43	7.61

2.3.2.2.5. Investigating the cause of horizontal currents (Diffusers setting and seats arrangement)

In order to address the shortcomings of the current DV system, a further investigation was carried out to discover the factors that brought about the horizontal currents affecting the contaminants diffusion pattern and consequently the room air quality. Srebic and Xu listed several factors affecting the global air currents, such as: supply and exhaust openings types and locations, heat source intensity and location, human activity, partitioning, and vertical airflow along windows or external walls due to temperature difference [19]. However, for the specific case-study at hand, comparing the contours in Figure 2.19 with those from literature [2], two main reasons can be observed. The three-sided diffusers and the last row of seats may be blocking air flow from the back-wall forwards through the side aisles. Therefore, further simulations were carried out to investigate both factors' effect through three additional cases; 1. Last row removed with 3-sided diffusers. 2.

Base-case seats arrangement with 4-sided diffusers, and 3. Last row removed with 4-sided diffusers. The front-right case was chosen for this deeper investigation as it is the case where the current effect was most obviously manifested. Supply rate was altered so as to keep the flow rate per person constant and the diffusers' flow rate proportional.

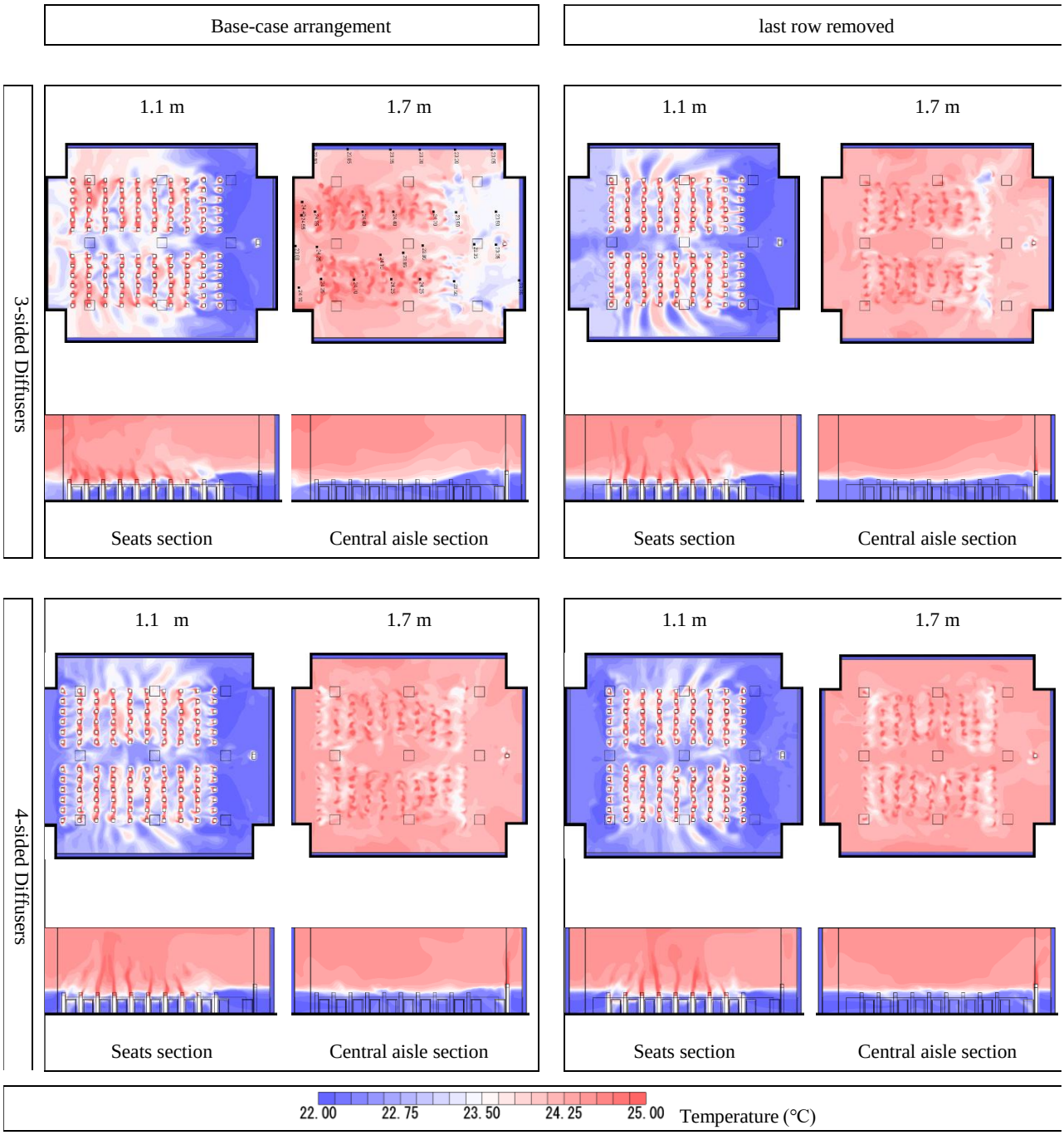

Figure 2.23 Temperature contours in plan view, 1.1 m and 1.7 m, and seats section and central aisle section

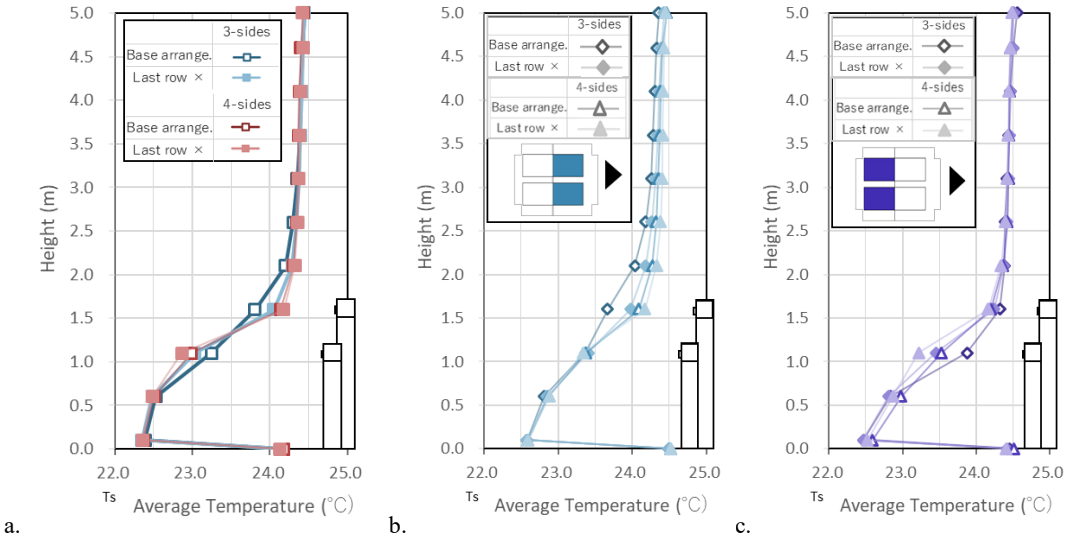

Figure 2.24 Temperature vertical distribution, a. plan average, b. front occupied zone, c. back occupied zone

To start with, the effect on temperature is evaluated using contours and vertical distribution profiles. Regarding temperature contours, Figure 2.23, stratification height is generally more uniform compared the base-case especially the 4-sides case with the last row removed. At 1.1 m level, another main change is the lower temperature at the last row, although it applies for all three cases, the decrease is more prominent in the 4-sides cases. The two observations made from the contours can also be seen in the temperature curves of the front and back occupied area, Figure 2.24. The increase in the front occupied area temperature at 1.7 m reached up to 0.8 K and the decrease in that of the back area at 1.1 m and lower is slightly smaller. These two changes were reflected in the average temperature profile of the total floor area, Figure 2.24a.

Since concentration diffusion was found to be highly impacted by the flow direction even at low velocities, the contaminant concentration contours of the enhanced cases in Figure 2.25 are overlaid by air velocity vectors. Changing either factor minimized the horizontal contaminants dispersion, nevertheless, the impact varied from one case to the other. In all cases the forward currents were allowed to flow opposing the main backward current observed in the base-case. Changing both factors, same as in temperature distribution, resulted in the largest impact. Comparing the two parameters, it can be observed form the interface height and horizontal spread area that removing the last row caused the smaller spread constriction compared to changing the diffusers settings. In opposition, the concentration vertical profiles in Figure 2.26 show that removing the last row had much lower concentrations at 1.7 m and at lower heights only negligible differences were spotted.

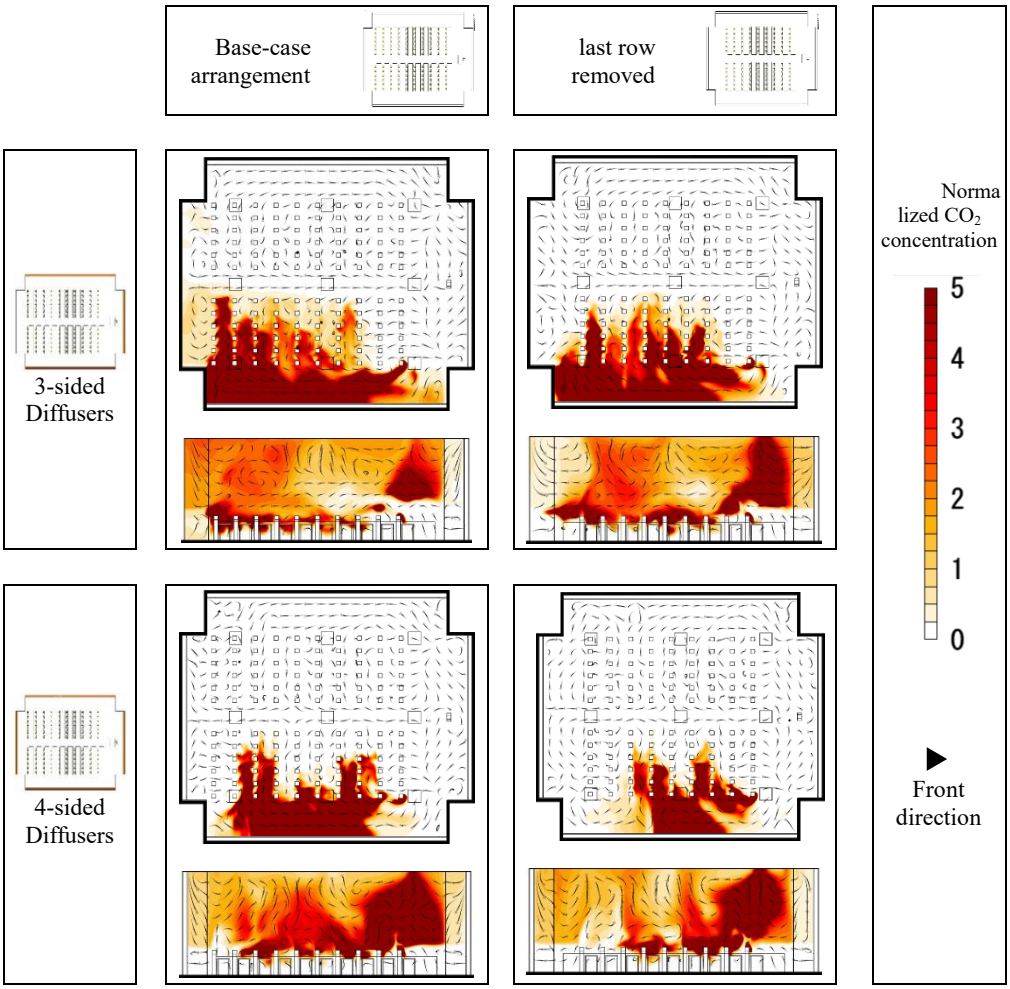

Figure 2.25 Contaminant concentration contours for enhanced cases in plan at 1.1 m and longitudinal section through contaminant source individual

Finally, air quality was reassessed using breathing zone concentration frequency distribution curves and numerical indices. Analyzing Figure 2.26, the major trend change found in all altered cases, is the depression of the original case's second peak at concentration 1 and the increase in 0.001. The local air quality, diffusion radius, and concentration integral are displayed in Table 2-8. The two single-parameter cases are found to be very similar in all indices while the both-parameter case reduced the concentration by 30% and shorten the diffusion radius by 0.76 m.

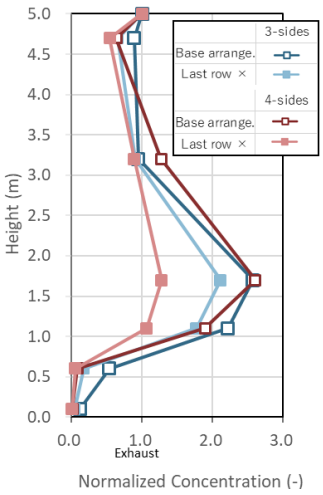

Figure 2.26 Normalized concentration vertical distribution for enhanced cases

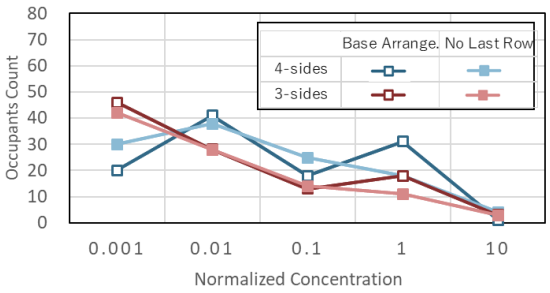

Figure 2.27 Occupants distribution on normalized concentration classes for enhanced cases

Table 2-8 Numerical indices in enhanced cases

Index	Symbol [unit]	Base-arrange. / 3-sides	No last row / 3-sides	Base-arrange. / 4-sides	No last row / 4-sides
Local air quality index	$\langle \varepsilon_p^c \rangle_{in}$ [-]	**1.00**	0.87	0.94	1.26
2nd moment for scale of ventilation efficiency,	SVE2 [m]	**4.35**	3.86	3.58	3.59
Concentration integral	C_0 [ppm m^3]	**23.71**	22.08	22.05	16.51

2.3.3. Effect of contaminant source position on transient spread of contaminant

2.3.3.1. Analysis Conditions and Cases

Continuing the investigation on source position significance in contaminant spread pattern and cross-infection probability, this transient analysis was carried out for the same cases with the same settings as the previous steady state analysis. The standard k-ɛmodel analysis was carried out using STREAM v.20 software using the conditions listed in Table 2-9 and the boundary conditions summarized in Table 2-10. CO_2 concentration was set to 1000 assuming the units to be quanta/m^3. For all cases, steady- state analysis with no emission were run until the temperature was stable, then, transient analysis was carried out for 50s, 2s to simulate one exhale then the emission was stopped to monitor contaminant diffusion.

Table 2-9 Analysis Conditions

Analysis Software	Stream v.20
Turbulence model	Standard k-ε model
Calculations	Heat, Radiation, Diffusion (CO_2)
Mesh count	~ 4M
Mesh size	0.04 m (1.1 growth rate)

Table 2-10 Boundary Conditions

Wall	Inner wall	Heat transfer coefficient, 3.06 W/m^2		
	Exterior	Adiabatic		
Inflow	Front	2850m^3/h	Sides	4530m^3/h
Outflow	Fixed flow velocity 0.98 m/s			
Heat	60 W/ person			
CO_2 emission	Emission velocity	1 m/s		
	Concentration:	1000 quanta/m^3		
	Mouth surface area	0.0025 m^2 (0.05×0.05 m)		
	Duration	2 s		

2.3.3.1. Results and Discussion

In this section covers two main points: 1) Inspecting the temperature vertical distribution for DV stratification after reaching the steady state, and 2) Assessing the inhale air quality for the source, the uninfected occupants especially the source surrounding ones. For all uninfected occupants average inhaled air concentration is calculated. For contaminant source occupant, the inhale air quality is assessed in terms of stagnant time, i.e. how long high contaminant concentration is sustained. For source surrounding occupants, the number of affected occupants and effect severity by time are two factors chosen for evaluation.

To start with, the temperature vertical distribution shows typical stratification with interface height of above 1.7 m in most of the space volume. Figure 2.28 shows 2 graphs of the temperature vertical distribution; a. whole space average with variance bars, and graph b has the temperature at 4 sample rows plotted to represent the variation in the temperature distribution in the seating zone of the hall. Figure 2.30 shows the temperature distribution at 4 horizontal sections, 3 sections within the occupied zone; at ankle level, seated and standing occupants head level, and one above the occupied zone at 3.2 m. Three vertical sections are presented as well in side and middle aisle, and through the seating zone. As can be observed from Figure 2.28b, the front row is affected by the front diffuser which can be the cause of the asymmetric air flow. This observation, as mentioned in the previous section can affect the contaminant distribution as well.

Regarding the contaminant diffusion assessment, the concentration in the source breathing zone was calculated using the average of 0.2 m cube in front of the occupant's face. For other occupants, a single measuring point in the center of the first mesh next to the mouth was used to derive the concentration as shown in Figure 2.29.

Average contaminant concentration in inhaled air of all uninfected occupants for the ten cases are plotted in Figure 2.31. It can be observed that 4 cases reached relatively high concentrations: ML, MC, BL, and FC. Although, the middle cases had the highest concentrations (> 0.1 quanta/m^3), case-FC sustained 0.01 quanta/m^3 for 40 s. Other cases showed negligible concentrations. Case-L, however, showed a delayed increase in concentration that had not reached a peak until the end of the simulation time.

Figure 2.32 shows the inhaled contaminant concentration the source and surrounding occupants for all ten cases vs. time. First, regarding the stagnant time at the source, it can be noticed that cases L, FL, and FC had slow dispersion rate as it takes around 40 s for the concentration to reach 1 quanta/m^3 while its takes under 10 s in case-BC, for example. Another point worth noting is the trend of re-peaking after steep decrease shown in cases ML and MC which is not restricted to the source but also the surrounding occupants. Assessing the effect on surrounding occupants, front cases have almost all surrounding occupants above 0.1 quanta/m3 in varying timing. ML and MC cases subjected their adjacent occupant to the right to the highest concentration of more than 10 quanta/m3. Followed by case-BL, ML and MC are the fastest cases to affect the surrounding occupants as the adjacent occupant reached the maximum concentration within 5 s. BC had no concentration exceeding 0.01 quanta/m3 which is unlike other back cases as both subjected an adjacent occupant to concentration higher than 1 quanta/m^3. Similar to Figure 2.30, the concentrations in case-L are increasing and had not reached its peak.

Finally, to visualize the diffusion direction, horizontal and vertical sections of sample cases are shown in Figure 2.33 and Figure 2.34 respectively. The difference in diffusion pattern can be seen in terms of speed, direction, and dispersion rate. Back cases show fast vertical diffusion with minimal dispersion. In contrast, in middle cases the contaminant diffused horizontally. Front cases, on the other hand, show slow horizontal diffusion with high dispersion rate, thus, affecting larger number of occupants.

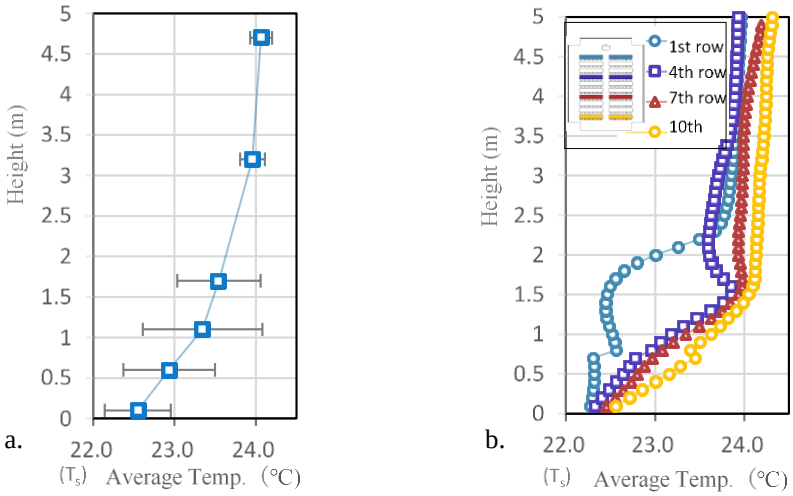

a. Plane average with variance *b. Breathing zone average of 4 sample rows*

Figure 2.28 Temperature vertical distribution

a. Sample volume at source *b. Measuring point at all non-source occupants*

Figure 2.29 Contaminant measuring points

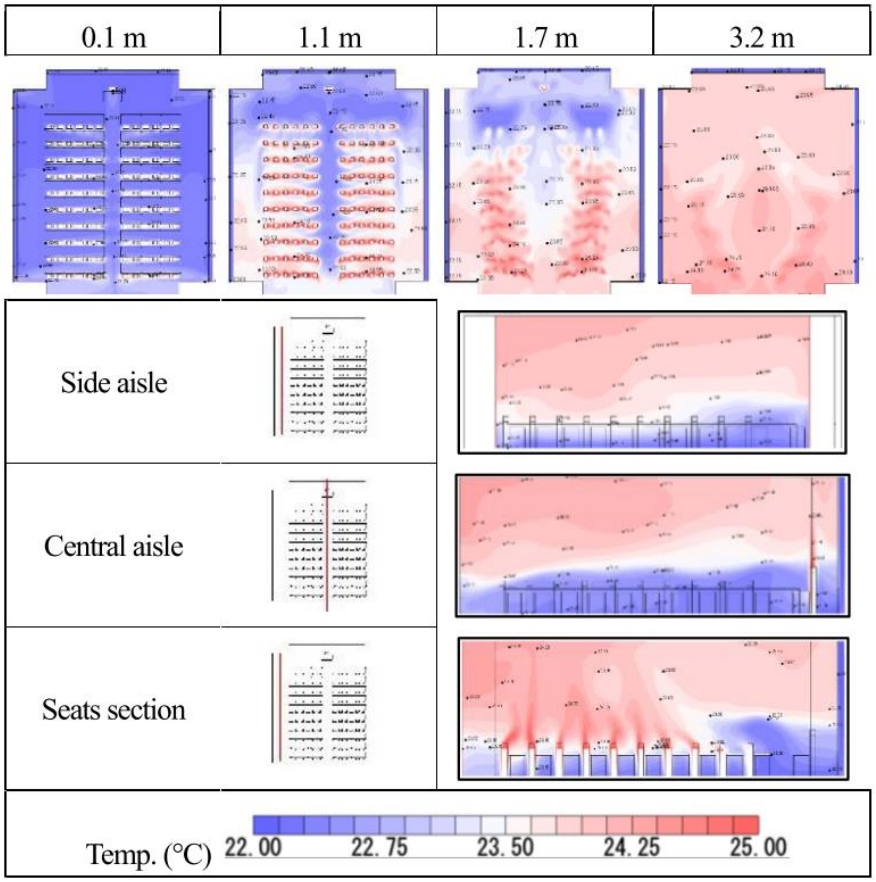

Figure 2.30 Temperature horizontal and vertical contours

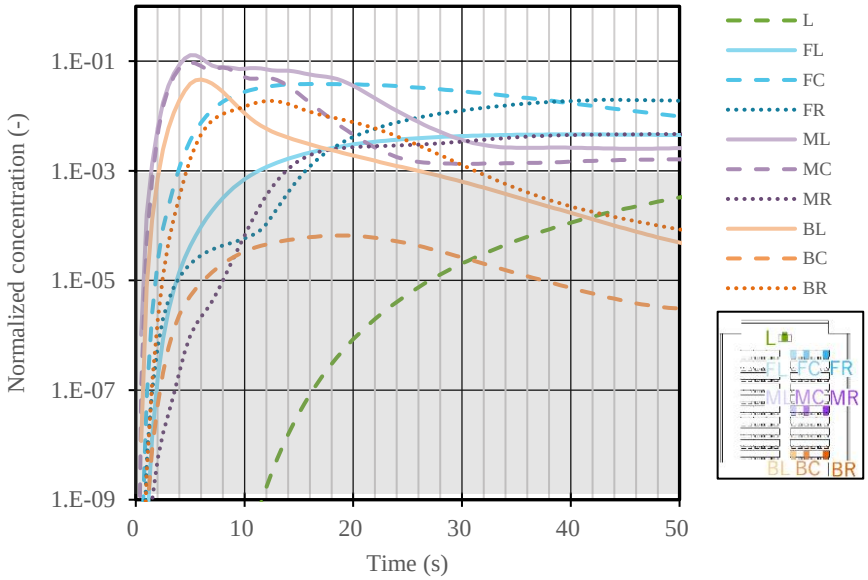

Figure 2.31 Contaminant concentration at source breathing zone vs time

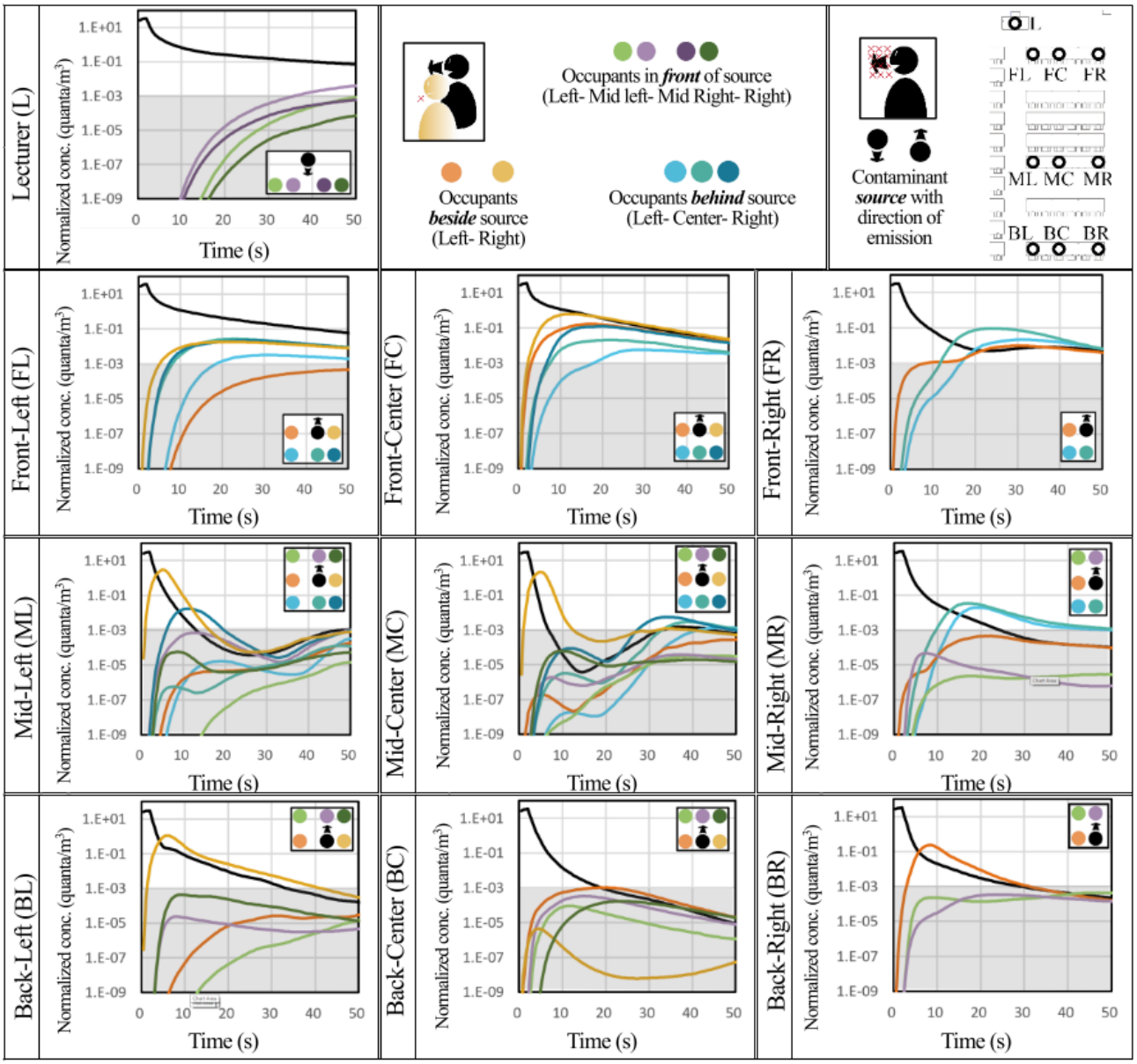

Figure 2.32 Breathing zone concentration vs time for adjacent seats

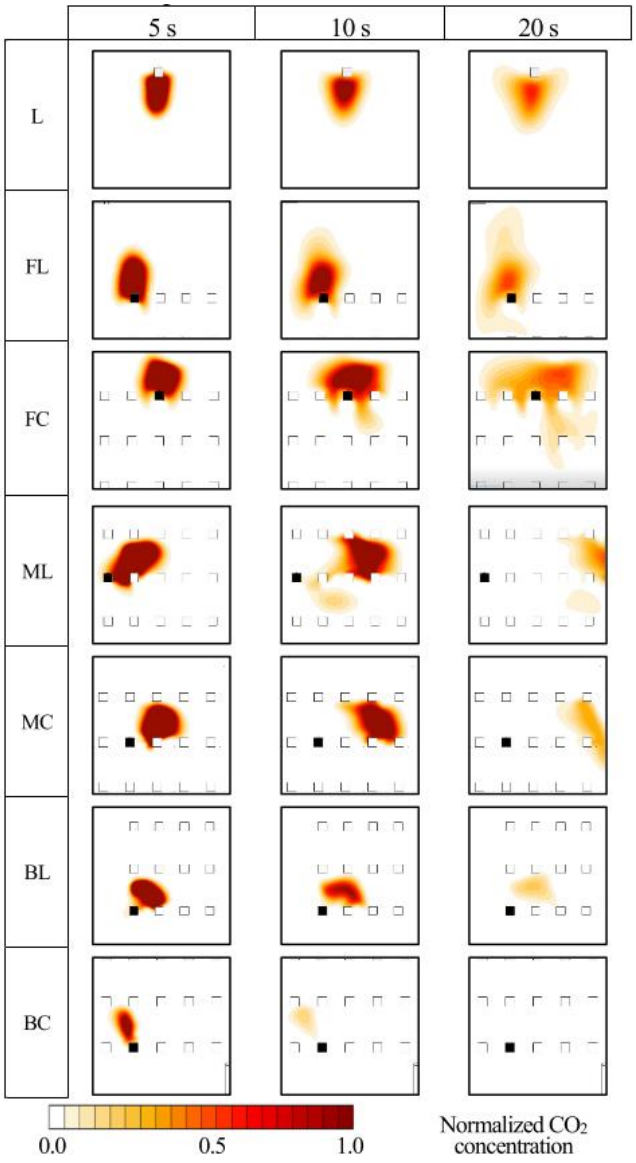

Figure 2.33 Contaminant concentration at horizontal plane

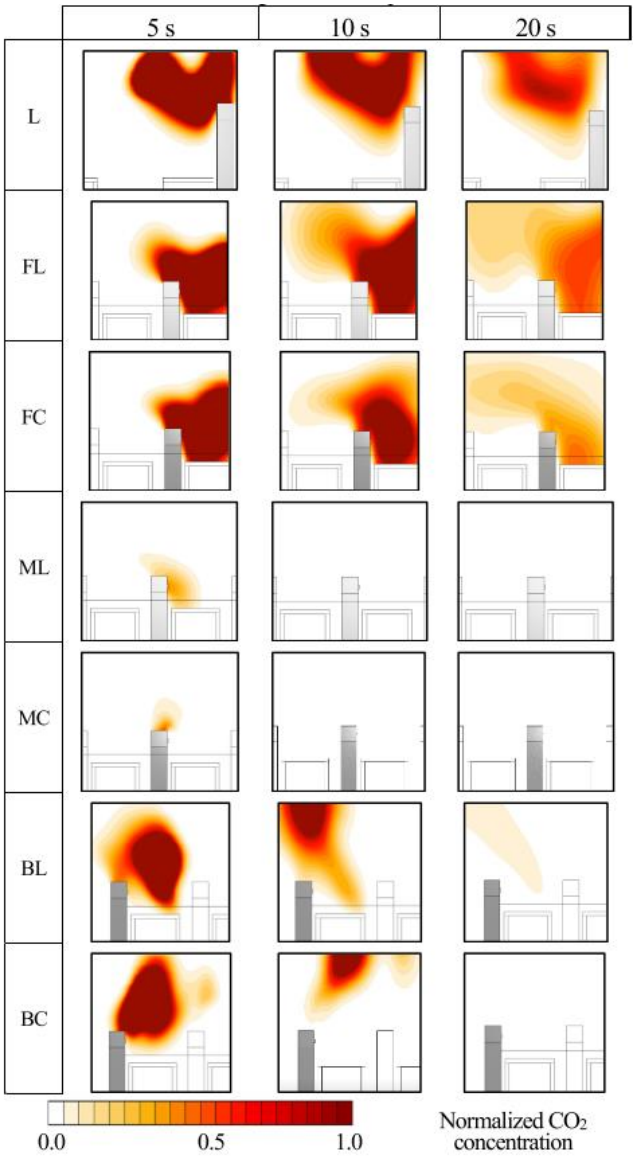

Figure 2.34 Contaminant concentration at vertical plane

2.3.4. Effect of Supply Diffusers Position and Occupants Seating Pattern on Temperature and Contaminant Concentration Distribution

The DV system where air is supplied from ceiling level inlet fans through double wall to flow in the room through wall-long flat diffusers as shown in Figure 2.2. In order to ensure uniform surface velocity at the diffusers and simplify the system for simulation, flow was set directly from the diffuser surfaces. However, the double wall surface temperature should mimic the real case scenario of having air flowing at supply temperature. To simulate this condition, a solid layer with fixed temperature precondition was attached to the external surface of the double walls. Occupant models, seated and standing, are shown in Figure 2.35. It should be mentioned that the mouth level of the seated and standing occupants is 1.2m and 1.7 m respectively. In addition, as shown in Figure-3c, the seated occupant is positioned 50 mm away from the desk.

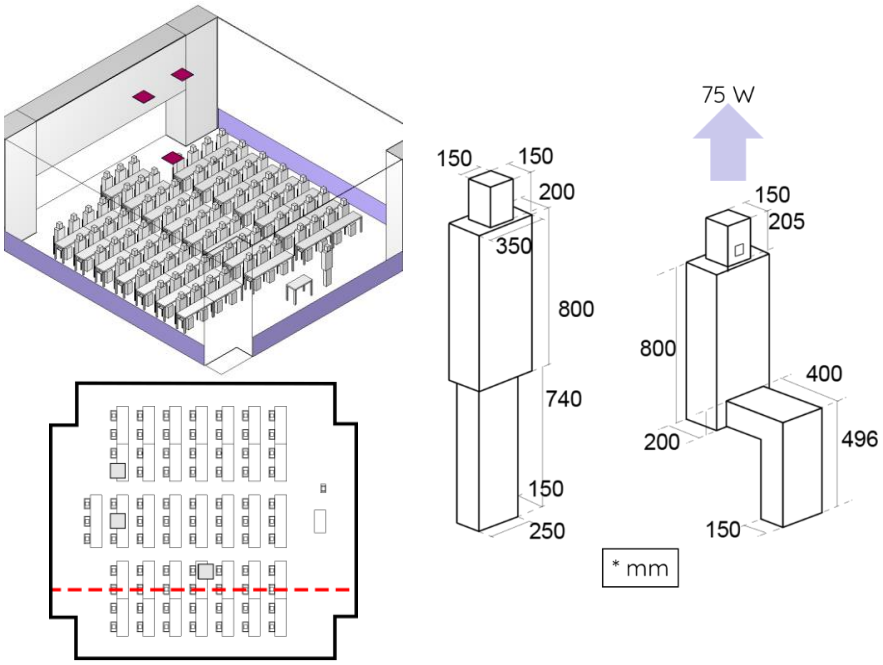

Figure 2.35 Room model in 3D and plan views, and occupant sitting and standing model

2.3.4.1. Analysis Conditions and Cases

The analysis was carried out by Stream v.21.1 using a standard k- ε model. Heat transfer was calculated using logarithmic law and was set to adiabatic between room external surfaces and the exterior. The room was divided into 50-mm size mesh except near the room envelope where the size increases to 200 mm to sustain a Y+ value of more than 30. Table 2-11 sums up the analysis conditions while the boundary conditions are listed in Table 2-12. 12 cases were simulated for three diffusers settings; 2-sides, 3-sides, and 4-sides. Each setting was analyzed for four seating patterns. Four contaminant sources positioned in accordance to the field measurement are indicated in the cases flow boundary conditions table, Table 2-13.

Table 2-11 Analysis conditions

Analysis Software	Stream v.21	
Turbulence Model	Standard k-εmodel	
Analysis Type	Steady-state	
Calculations	Heat, Radiation, Diffusion	
Mesh		
Default Size		50 mm
Wall/ Ceiling/ Floor Adjacent Mesh		200 mm
Growth Rate		1.15
Mesh Count		~ 4M

Table 2-12 Boundary conditions

Thermal Boundaries		
Solid- Fluid	log law	
External surfaces	Adiabatic	
Materials Conductivity		
Ceiling	Rock wool	λ = 0.035 W/(m.K)
Floor	Concerte	λ = 1.2 W/(m.K)
Walls	Hardwood	λ = 0.15 W/(m.K)
Heat Generation		
Source	Occupants	1 Standing/ 80 Seated
Surface Area	Standing/ Seated	1.745 m2
Heat load	75 W	
Contaminant Settings		
Contaminant	CO_2	1.64×10-5 Diffusivity
Emission rate	5.21 L/min	
Emission Temperature	32 ℃	
Emission Surface	Mouths (4)	0.025 m^2

Table 2-13 Cases flow boundary conditions

		Fully-Occupied	Alternate Seats	Front Half	Back Half
Seating Pattern.		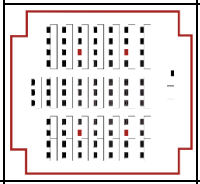	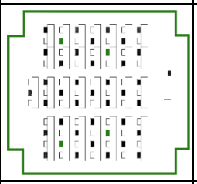	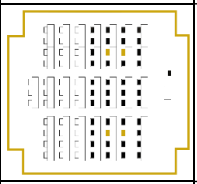	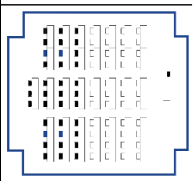
Diffusers Setting	Occupancy	81	41	45	39
	Supply Volume	8400 m3/h	4200 m3/h		
	Exhaust Flow Ex-1,3	6720 m3/h	3360 m3/h		
	Exhaust Flow Ex-2	1680 m3/h	840 m3/h		
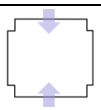	Supply Flow Velocity	0.12706 m/s	0.0636 m/s		
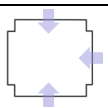	Supply Flow Velocity	0.09255 m/s	0.0463 m/s		
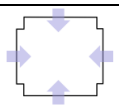	Supply Flow Velocity	0.07278 m/s	0.0364 m/s		

2.3.4.2. Results and Discussion

2.3.4.2.1. Temperature distribution

To start with, the temperature distribution was plotted for the seats area, front and back halves separately. Different diffuser settings are shown in different graphs in Figure 2.36. It can be observed that diffusers settings do not have much effect in the average temperature distribution. Front and Back Halves cases showed the most varying trend in the empty half of the room where the supply air temperature was sustained till 0.8 m height. Fully-occupied cases and alternating-seats cases have similar trends except for the higher stratification level in the alternating-seats cases. Also observed from temperature contours in Table-4.

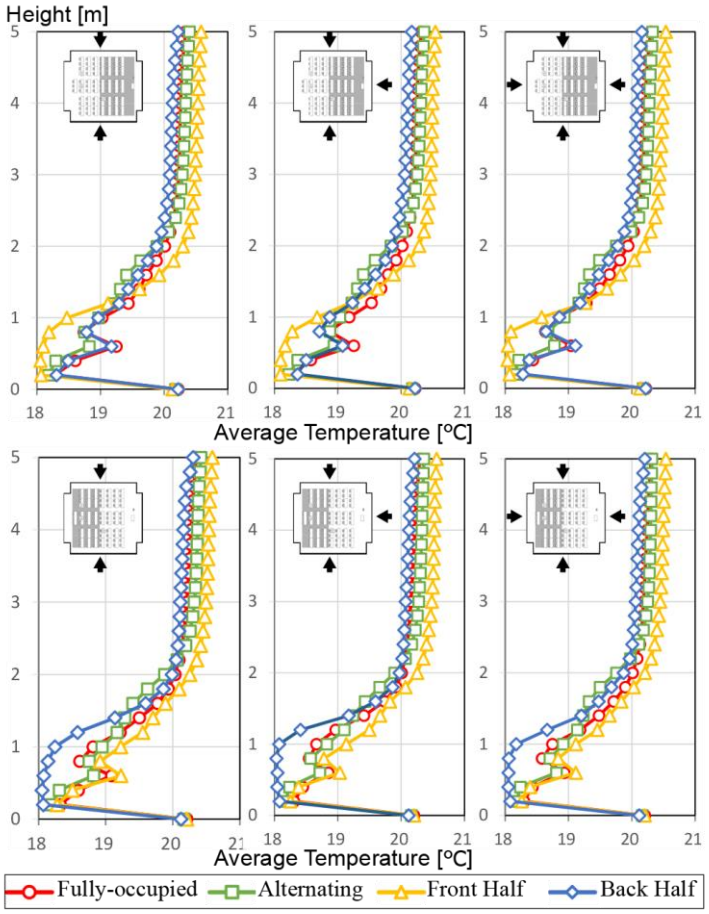

Figure 2.36 Temperature vertical distribution

2.3.4.2.2. Air Flow

As cold air flow of high velocity caused discomfort, a combination of horizontal velocity and temperature contours are compared in Figure 2.37. Full-occupancy and alternating seat cases where chosen as samples. It can be noticed that in the highest supply velocity case, fully-occupied with 2-sides diffuser, the side-aisles seats are affected by 0.2 m/s flow. The effect extends to the front and back seats in the 3 and 4-sides settings respectively but with lower velocity. The alternating case shows minimal flow in the 2-sides setting solely. Given that the temperature at the side seats are 18℃, around 1℃ below occupied zone average (18.8~19.3℃), air velocity under 0.35 m/s is within comfort range (4).

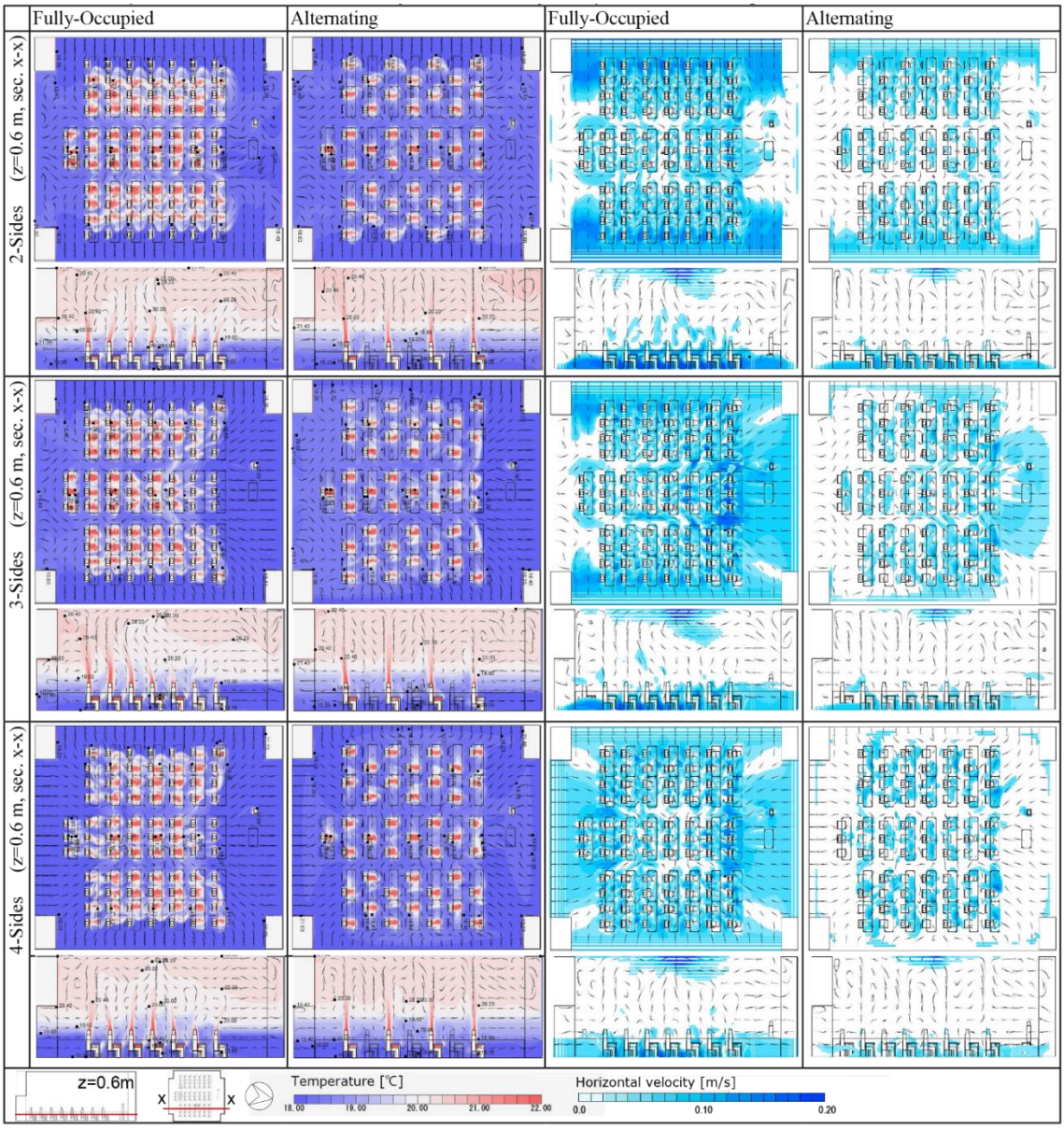

Figure 2.37 Temperature and horizaontal velocity contours in fully-occupied and alternaing cases

2.3.4.2.3. Contaminant Concentration

Comparing the 12 cases, Figure 2.38 shows concentration contours at 1.2 m plan and at section x-x passing through two of the contaminant sources as highlighted in Figure 2.35b. Comparing seating patterns, Back-Half case shows the highest concentration especially in the 3-sides settings. For the Front-Half cases, in 3 and 4-sides settings mixing down flow seen the sections caused the concentration to be relatively high at low levels. The high stratification level of the alternating case displays the clearest occupied zone for all diffuser's settings. Finally, for the Fully-occupied case, 3-sides setting displays horizontal spread of contaminants. Although 2-sides has less horizontal spread, 4-sides diffusers case shows the lowest contaminants accumulation.

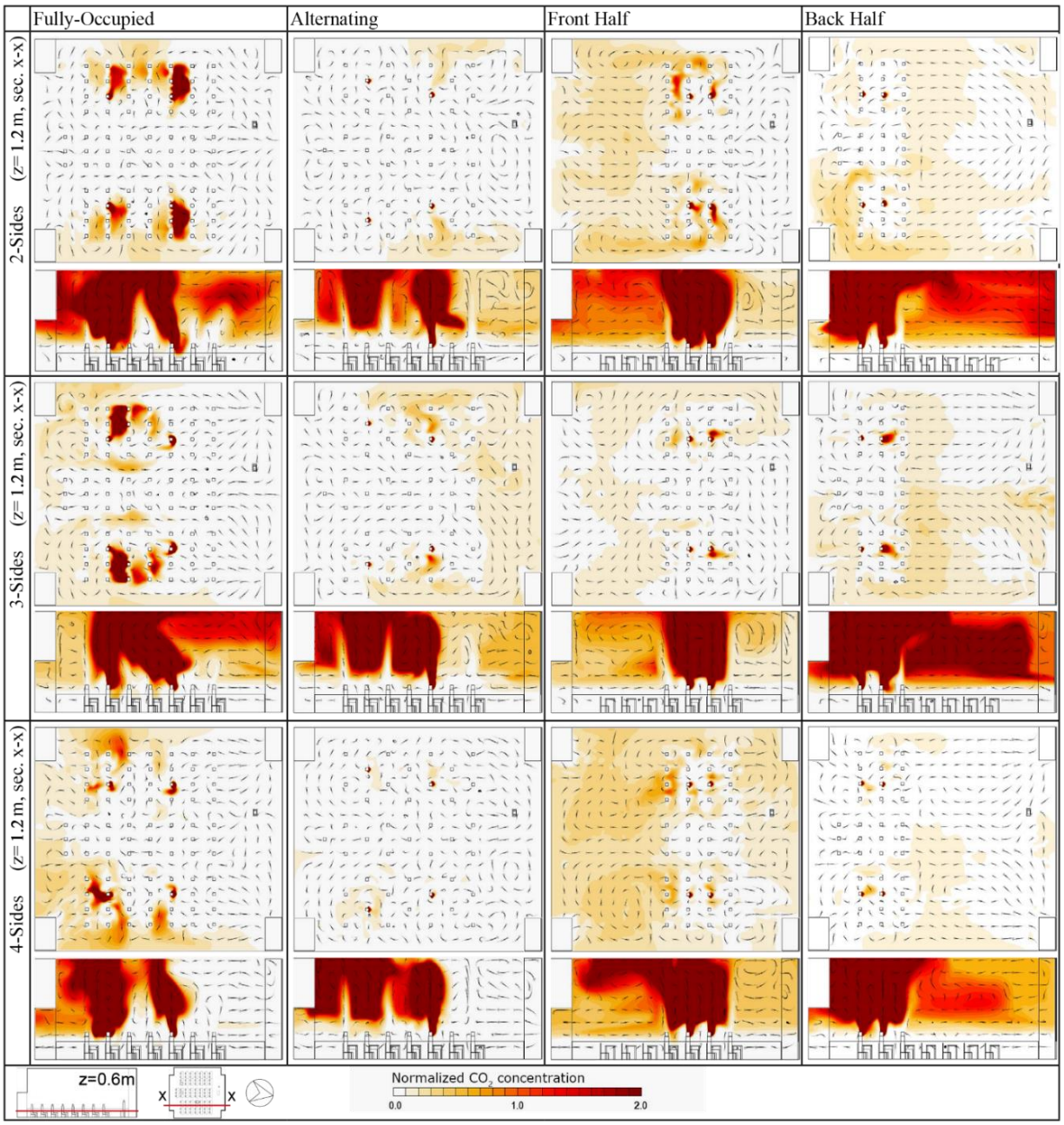

Figure 2.38 Contaminant concentration countours at 1.2 m and at section x-x

2.4. Experimental Investigations

This field study was carried on two steps; between January 9th and 31st , 2022 then between March 13th and 17th 2022. The case-study is the actual lecture hall in Minoh campus, Osaka University. The DV system in both investigations operated in all-fresh mode. The first investigation the effect of changing the location of the one contaminant source on the temperature and contaminant distribution was studied. The second investigation assessed the DV system performance in terms of temperature and contaminants distribution with four contaminant sources under different seating patterns conditions.

2.4.1. Method and Equipment

The timeline of all cases, as shown in Figure 2.39 starts with turning the DV system on and when steady state is reached, CO_2 emission is initiated. After CO_2 readings reaches a plateau, the emission is continued for a 30 minutes-long sample time. Finally, the DV and CO_2 emission is stopped.

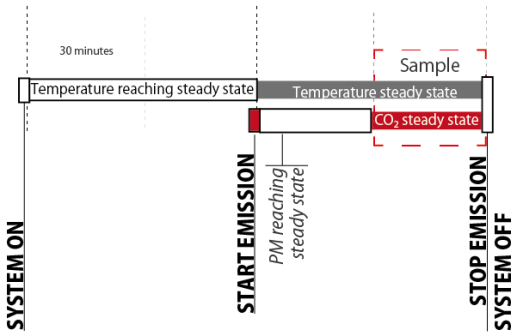

Figure 2.39 Experiment timeline

Air and surface temperatures were monitored through the experiment time as well as CO_2 concentration. Figure 2.40 shows the measurement points in plan and section views. Figure 2.41 is a 3D view of the measurement points in the lecture hall and Figure 2.42 shows a picture of the lecture hall with the measurement settings. In the following section, the measurement equipment and procedure are overviewed.

Temperature measurement

Surface temperature was measured for walls at the points Wa~j, Figure 2.40a, at heights indicated in Figure 2.40d and Figure 2.40e. Floor surface temperature was measured at poles a~j. Graphtec GL10-TK data-logger with K-type thermocouple probe was used and the fixing methods is shown in Figure 2.43 and Figure 2.43b. Ceiling temperature, on the other hand, was measured using Horiba infrared thermometer IT-480Fat the one point indicated in Figure 2.40a. Air temperature vertical distribution was measured at pols a~j at heights indicated in Figure 2.40b. T&D RTR-576 temperature/CO_2 data logger was used, Figure 2.43c. For higher points, two loggers were suspended from the ceiling at the heights indicated in Figure 2.40c at points Hn and Hs. Supply air temperature was measured using Graphtec GL10-TK data-logger as shown in Figure 2.43d. Exhaust air temperature was measured using the same method.

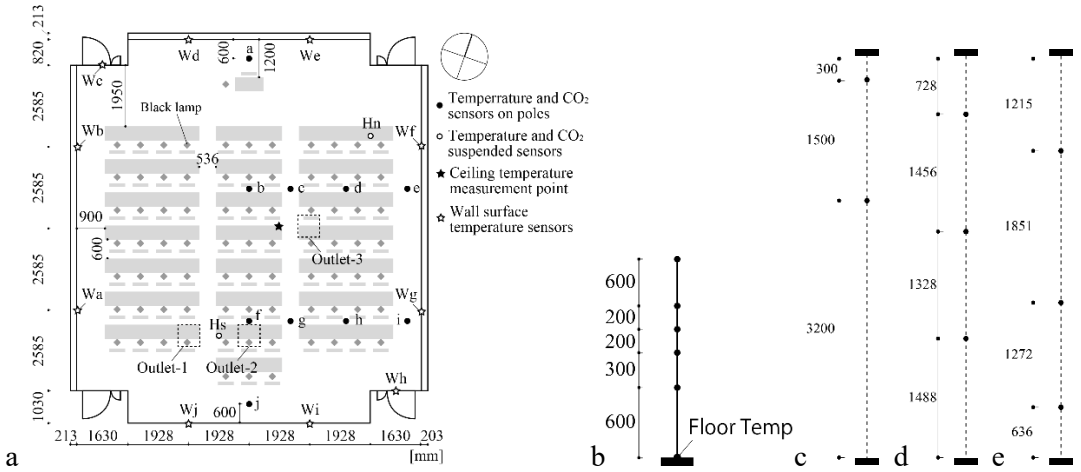

Figure 2.40 Sensor locations and measurement points, a. On room plan, b. Poles a~j vertical dimensions, c. Suspended sensors at Hn & Hs, d. Wall sensors Wa~Wf, e. Wall surface sensors Wg & Wh

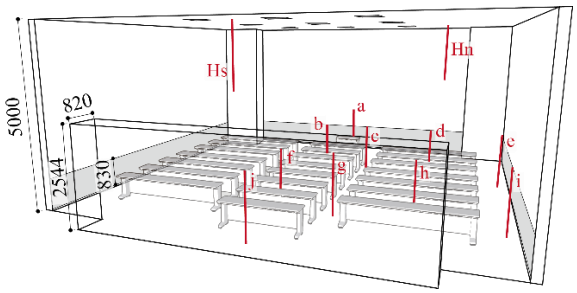

Figure 2.41 3D perspective of sensor's poles and suspension cords locations

Figure 2.42 Picture of overall measurement settings

CO2 measurement

Exhaust 1~3 and room CO2 concentration, poles a~j as well as points Hn and Hs, was monitored using T&D RTR-576 loggers. For the exhaust measurements, air pump was connected to the loggers. Supply concentration at each diffuser was measured using Vaisala GM70 pump, Figure 2.43e..

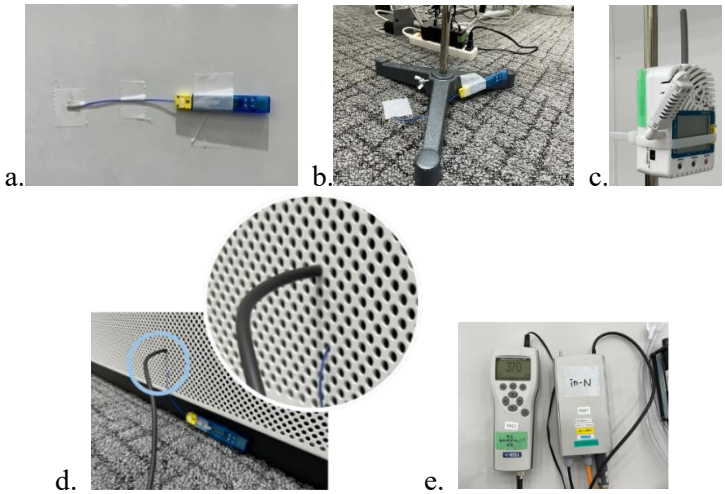

Figure 2.43 Equipment used in field measurement

Flowrate and velocity measurement

Flow rates of North, East, West walls are shown in Table 2-14 along with the exhaust flow rates at the three active outlets. The air velocity at each diffuser panel was measured on a grid of points as indicated in Figure 2.44a using anemometer 6543-21 (Kanomax Co., Ltd.), Figure 2.44b. Measurements were taken at the center point of one opening of the perforated panel as shown in Figure 2.44c. Velocity distribution of the three diffusers are shown in Figure 2.45. Vertical distribution has the same trend in all diffuser; increases moving downwards. Horizontally, it can be noticed that there is a significant variation which might affect the air flow in the room.

Table 2-14 DV system flowrate of diffusres and exhausts

		Flow rate [m^3/h]
Supply	North	1653
	East	3170
	West	3307
Exhaust	Outlet-1	3067
	Outlet-2	1566
	Outlet-3	3402

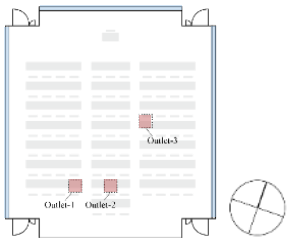

Occupants simulator

To simulate occupants' both heat generation and CO_2 emission were simulated. For heat generations, 60 W black lamps were clipped to the desks suspended above the seats mimicking seated student, Figure 2.46a. For the standing lecturer, a tripod was used to fix the black lamp, Figure 2.46b. As contaminant, CO_2 was heated then emitted through plastic tubes. To sustain the heat and to avoid a linear flow, the emission tube was split into 4 lines and wrapped around the black lamp as shown in Figure 2.46c.

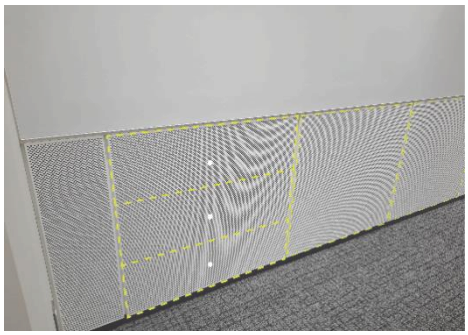

a. panel grid

b. measurement technique

c. anemometer

Figure 2.44 Air velocity measurment

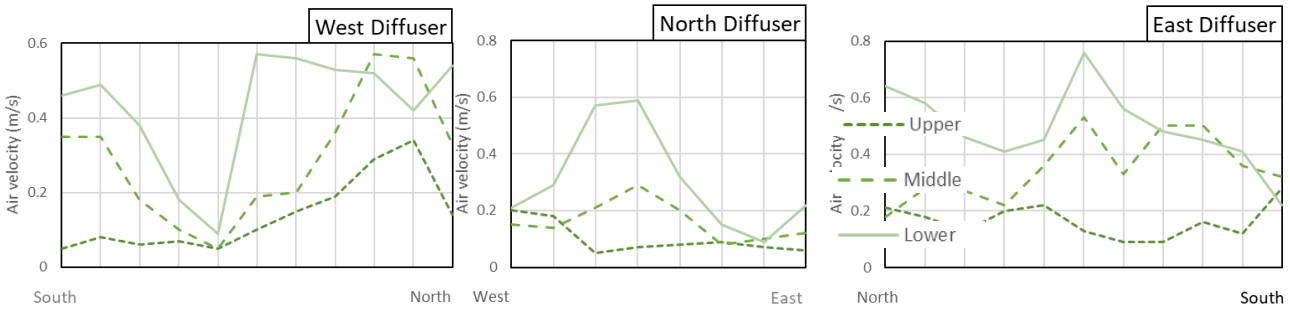

Figure 2.45 Velocity distribution in the diffusers

a. 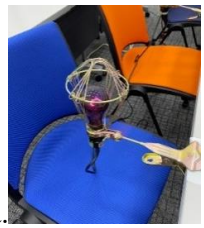 b. 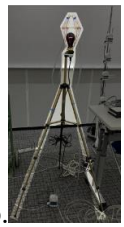 c. 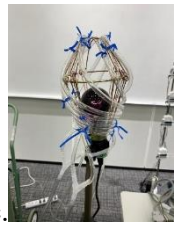

Figure 2.46 Occupant simulator equipment

2.4.2. Effect of Source Location on Temperature and Contaminant Distribution

2.4.2.1. Cases and conditions

Carried out in January 2022, this field measurement investigated the effect source positions of 6 cases with one contaminant source were carried out. The source positioned at the front, back, and middle row in the far right and a central seat as shown in Figure 2.47. CO_2 was emitted at temperature ranging from 25 ℃ to 27 ℃ with a rate of 10 NL/min.

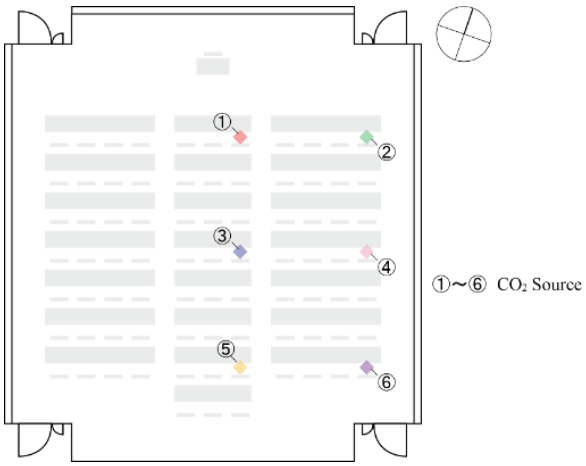

Figure 2.47 *Source position casess*

2.4.2.2. Results and Discussion

2.4.2.2.1. Temperature distribution

In this section, temperature and concentration results are presented and analyzed. All results are acquired by calculating the average of 30 minutes steady state data. Suspended sensors readings were plotted with the closest set of poles; Hn in poles a~e graphs, and Hs in poles f~j graphs. Regarding temperature distribution, in different cases, minimal variation in readings was found with negligible change in the air vertical distribution. Accordingly, only temperature results of case ① for poles a~j are shown in Fig.6. Wall surface temperature are plotted with the adjacent poles e and i. Temperature distribution shows a stratification height varying between 1.7 m in the south located poles and 3.2 m at the ones closer to the North wall. At all poles, the lowest temperature measured is at 0.6 m followed by a significant increase at 0.9 m , this can be thought of as the effect of black lamps as 0.9 m is the closest height above the black lamps. Poles a is the only pole that shows a gradual increase in temperature until interface level. Poles b~e shows the same trend but with much smaller temperature difference. On the other hand, poles f~j have insignificant temperature stratification. Ceiling temperature is around 5 ℃ higher than temperature measures at 3.2 m and 4.7 m.

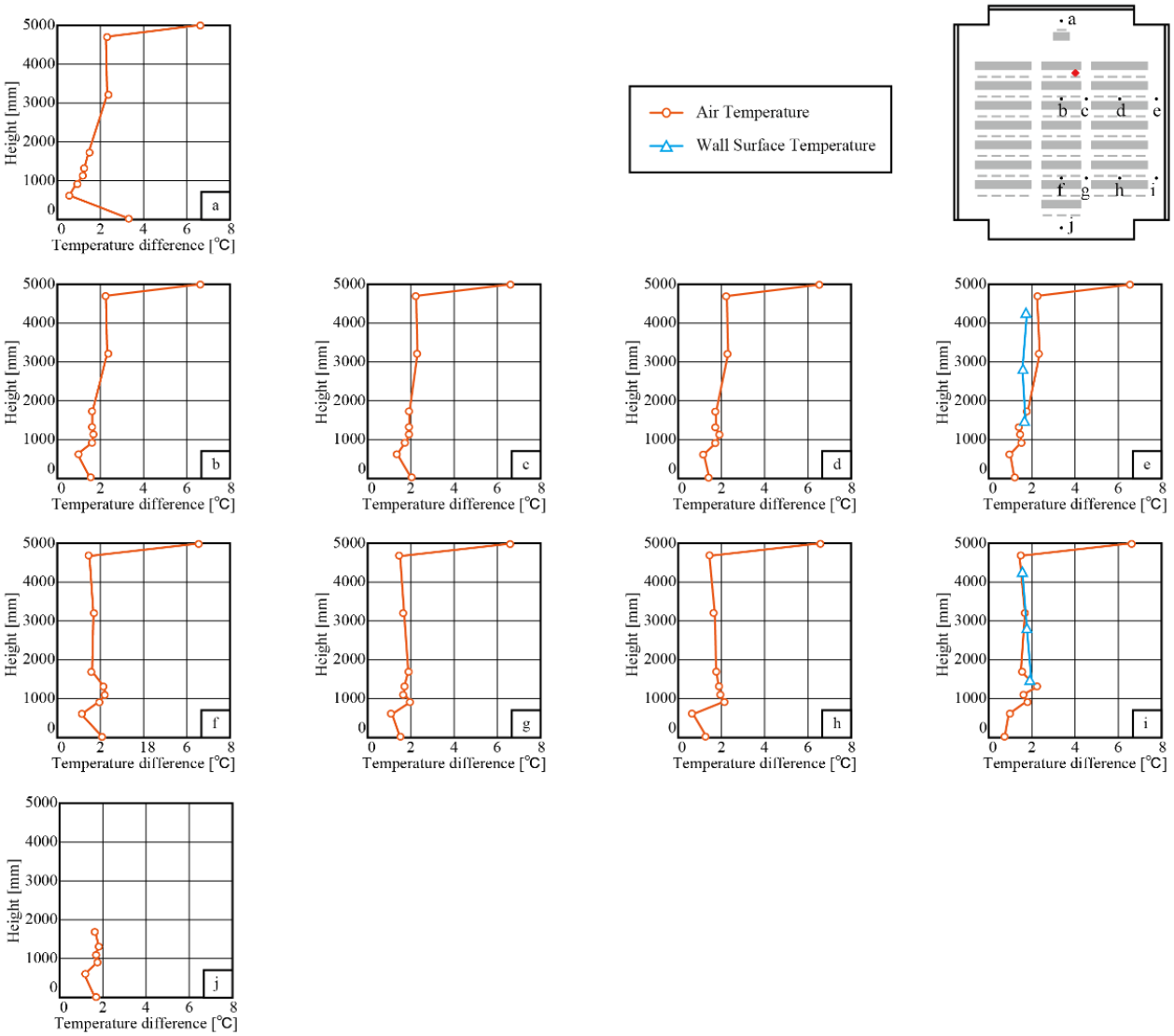

Figure 2.48 *Temperature vertical distribution of the Front-Center case*

2.4.2.2.2. Contaminant concentration distribution

The contaminant distribution graph comparing multiple cases are analyzed in this section. The two middle row cases, 3 and 4 are shown in Figure 2.49. Figure 2.50 and Figure 2.51 are comparisons between central seat cases (1,3, and 5) and right-side seats cases (2, 4, and 6) respectively. To star with, Figure 2.49 shows that, in both cases, the pole adjacent to the source displays high concentration at lower levels, 1100 mm and lower. This indicates that the main volume of the gas did not get entrained in the thermal plume of the black lamp. In case 4, a slight stratification can be seen in some poles but the main observation remains that the gas falls to the floor even at the poles near the diffusers, Pe and Pi. Similar observation can be found in all cases. For the central seats, Figure 2.50, the front seat to have the widest spread range while the middle one has the most sever effect especially in closest pole g, located behind the source point. Similarly, the side cases, show the front seat, case 2, to have spread widely and in addition have the highest concentration recorded at 1100 mm. Viewing the illustrations showing the spread direction and severity in the three figures, it can be noticed that

there is a horizontal flow driving the contaminant backwards. This observation confirms the findings of the exploratory CFD analyses on the effect of non-uniform supply on the contaminant spread.

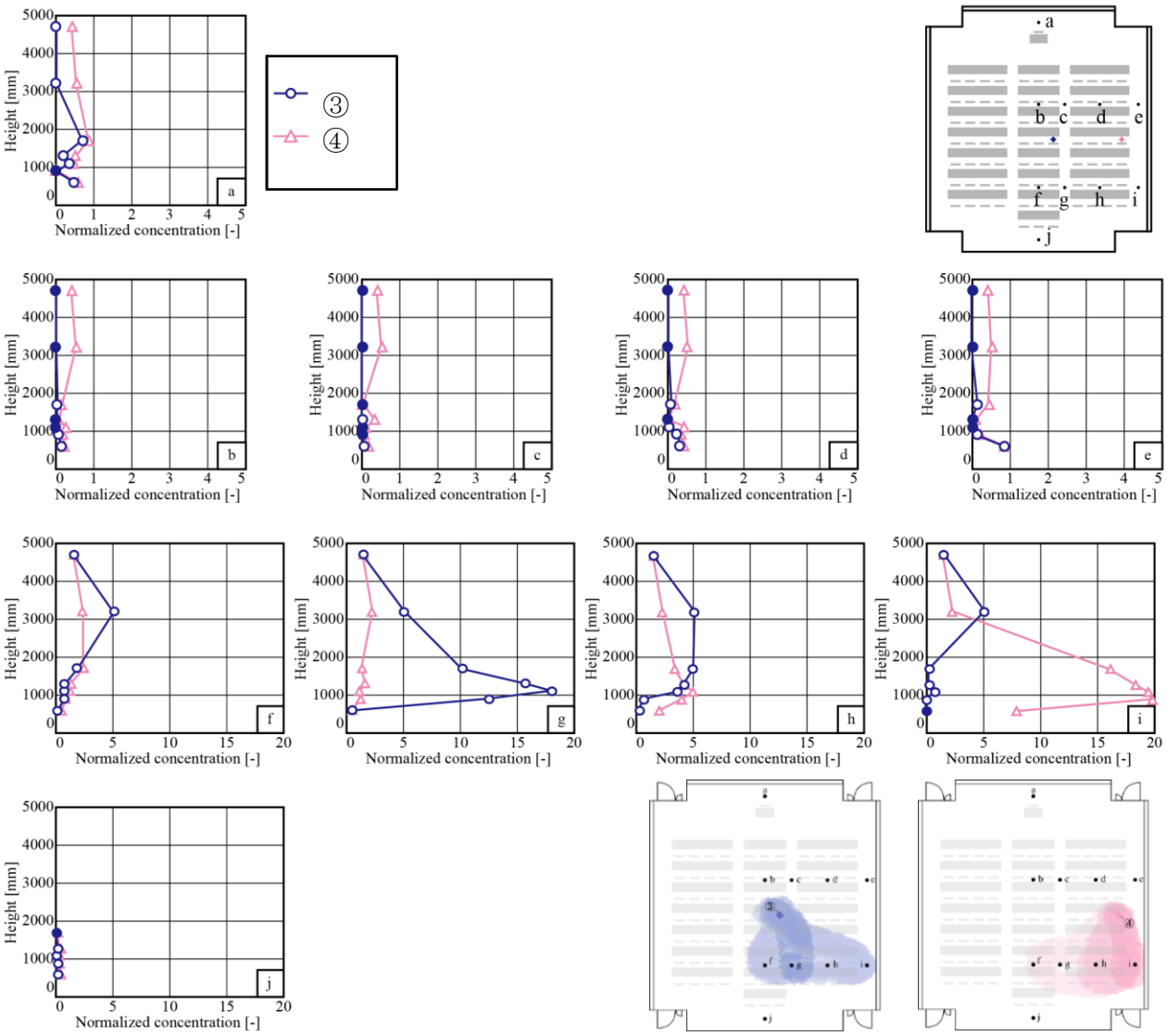

Figure 2.49 Vertical distribution of Normalized concentration for middle cases

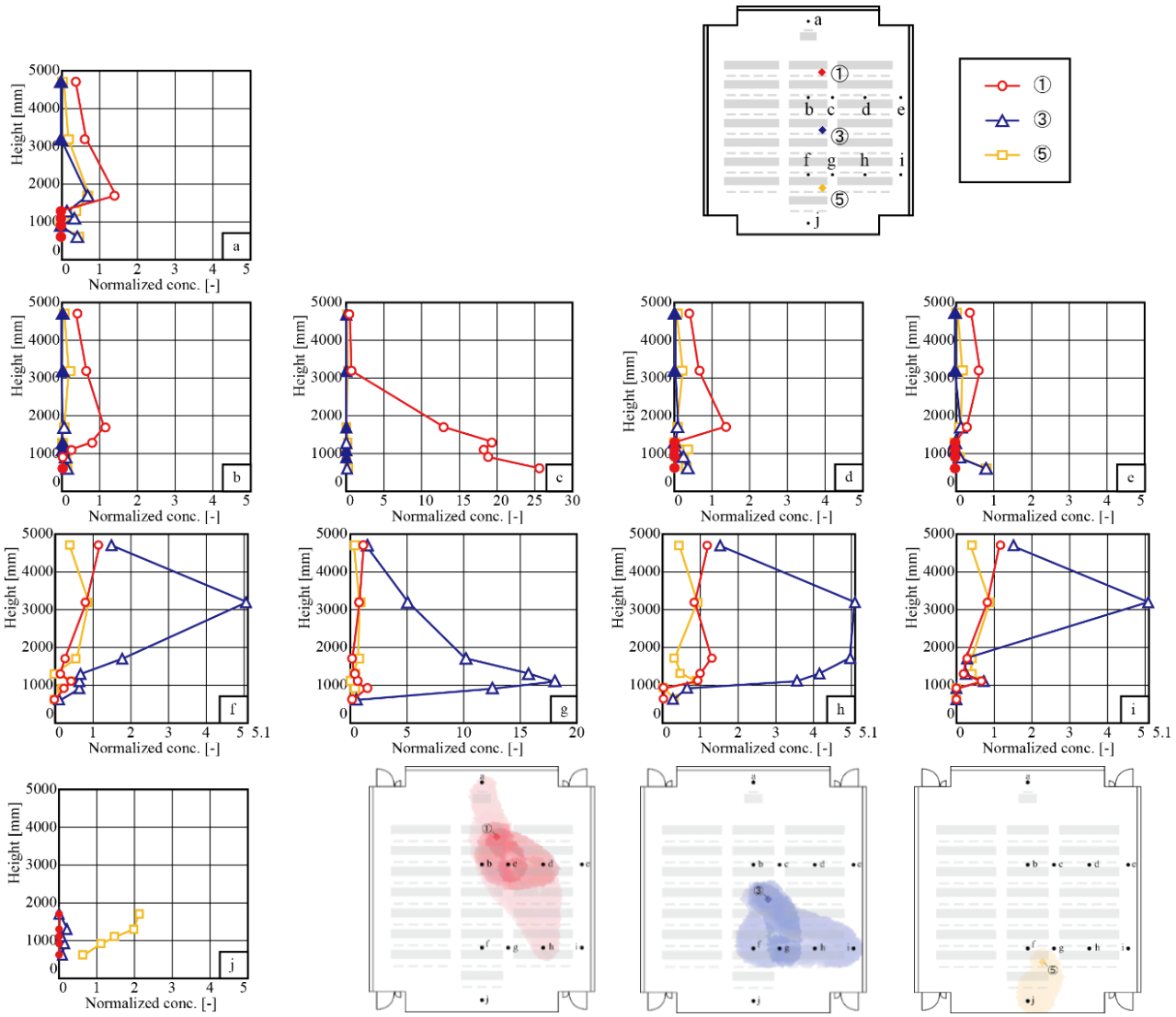

Figure 2.50 Vertical distribution of Normalized concentration for center cases

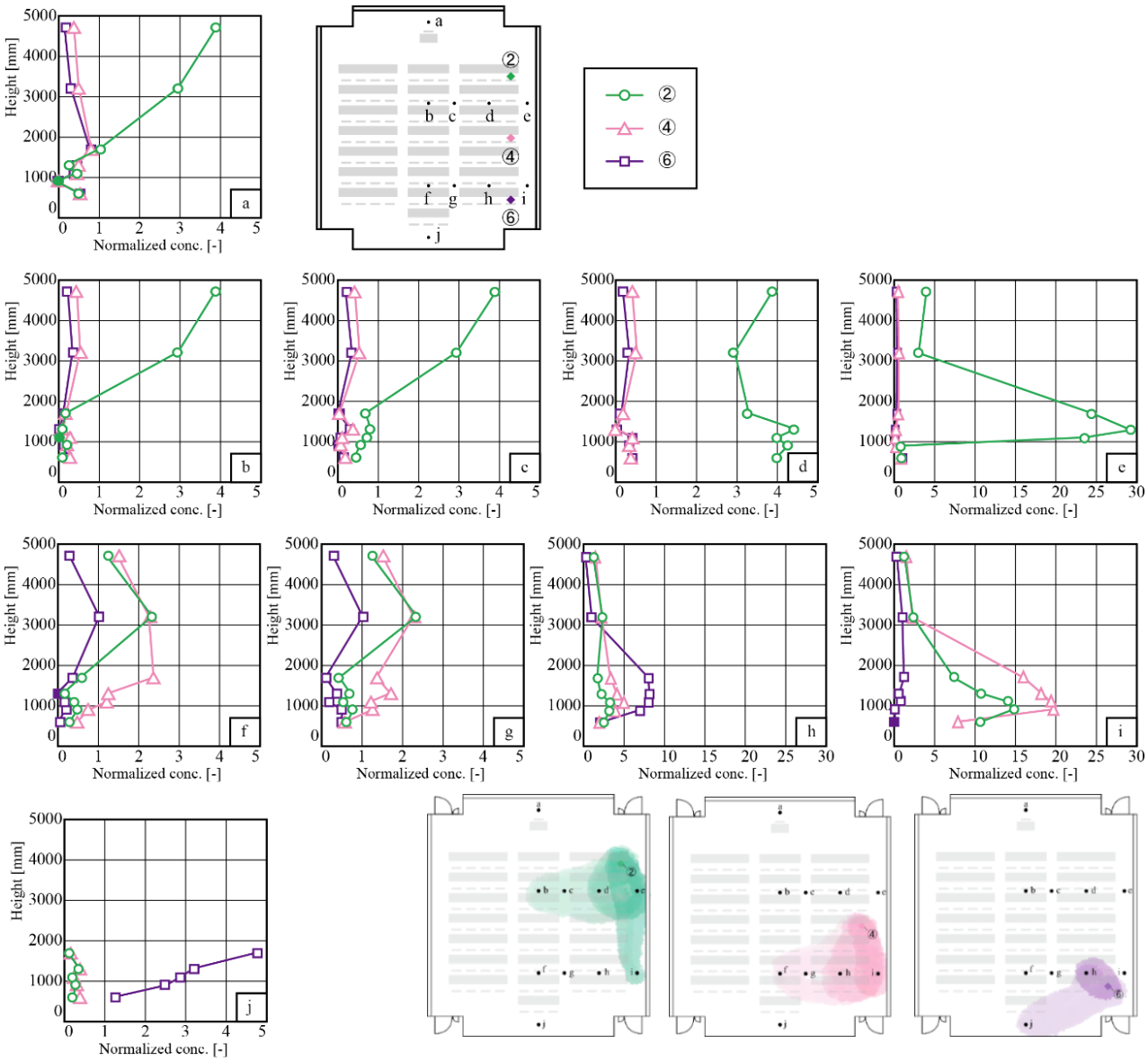

Figure 2.51 Vertical distribution of Normalized concentration for right side cases

2.4.3. Investigation of Temperature and Contaminant Distribution with Different Occupants Seating Patterns

2.4.3.1. Cases and conditions

The second field measurement was carried out in March, 2022, following the same procedure as the previous measurements. The effect of changing the occupants seating pattern on temperature and contaminant distribution was investigated. Four seating patterns were analyzed; full-occupancy, alternating seats, front-half, and back-half cases. CO_2 was emitted from four points, one from each quarter of the space as shown in Figure 2.52. The gas temperature ranged from 25 to 35 ℃. The flowrate per point was set to 10 NL/min, 40 NL/min in total per case.

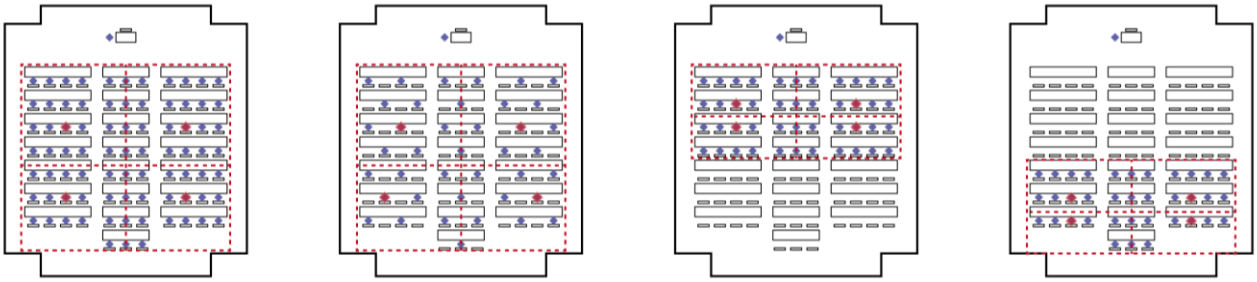

a. Fully-occupied *b. alternating-seats* *c. Front-half* *d. Back-half*

Figure 2.52 Cases of varient occupants Seating Patterns

2.4.3.2. Results and Discussion

2.4.3.2.1. Temperature distribution

Temperature vertical distribution for all cases at the 10 poles is plotted in Figure 2.53. The temperature difference between cases was small, with a maximum of 2 ℃. The full-occupancy case showed the highest temperature at all poles followed by the alternating-seats case. The back-half case demonstrated the lowest temperature in all poles except the rear pole j. Overall, the temperature gradient is small similar to the previous field measurement.

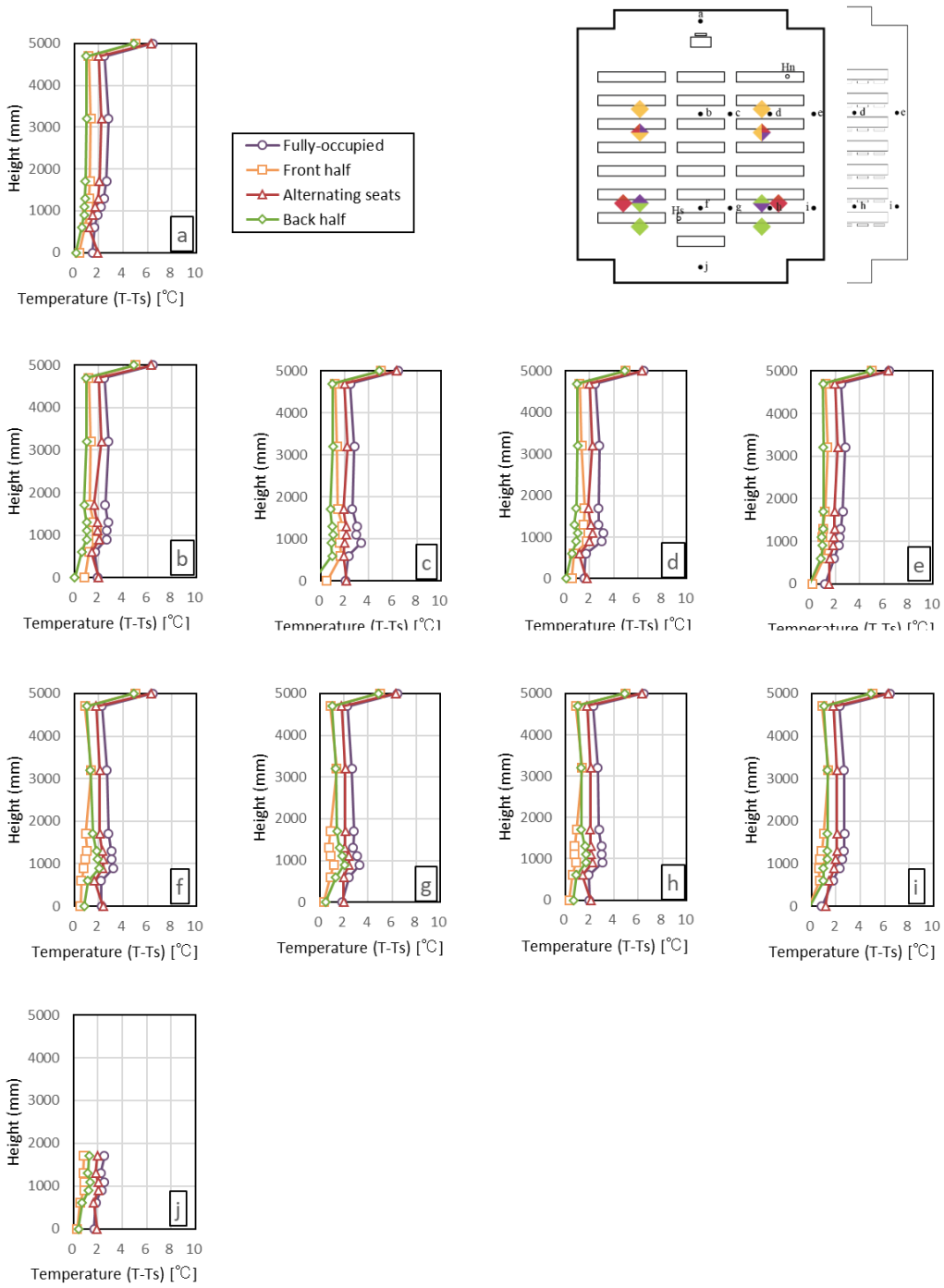

Figure 2.53 Temperature vertical distribution for the four seating pattern cases

2.4.3.2.2. Contaminant concentration distribution

Viewing the graphs in Figure 2.54, it can be observed that the front-half case showed the least spread area as high concentration was only detected in one pole, c. Full-occupancy case and alternating-seats case showed very close results. On the other hand, back-half case caused the widest spread and the highest concentration in the occupied zone, pole g. In all poles adjacent or near the source, the same observation as in the previous experiment was noticed as the CO2 tends to drop to the floor. In other poles, the stratification is minimal or non-existent.

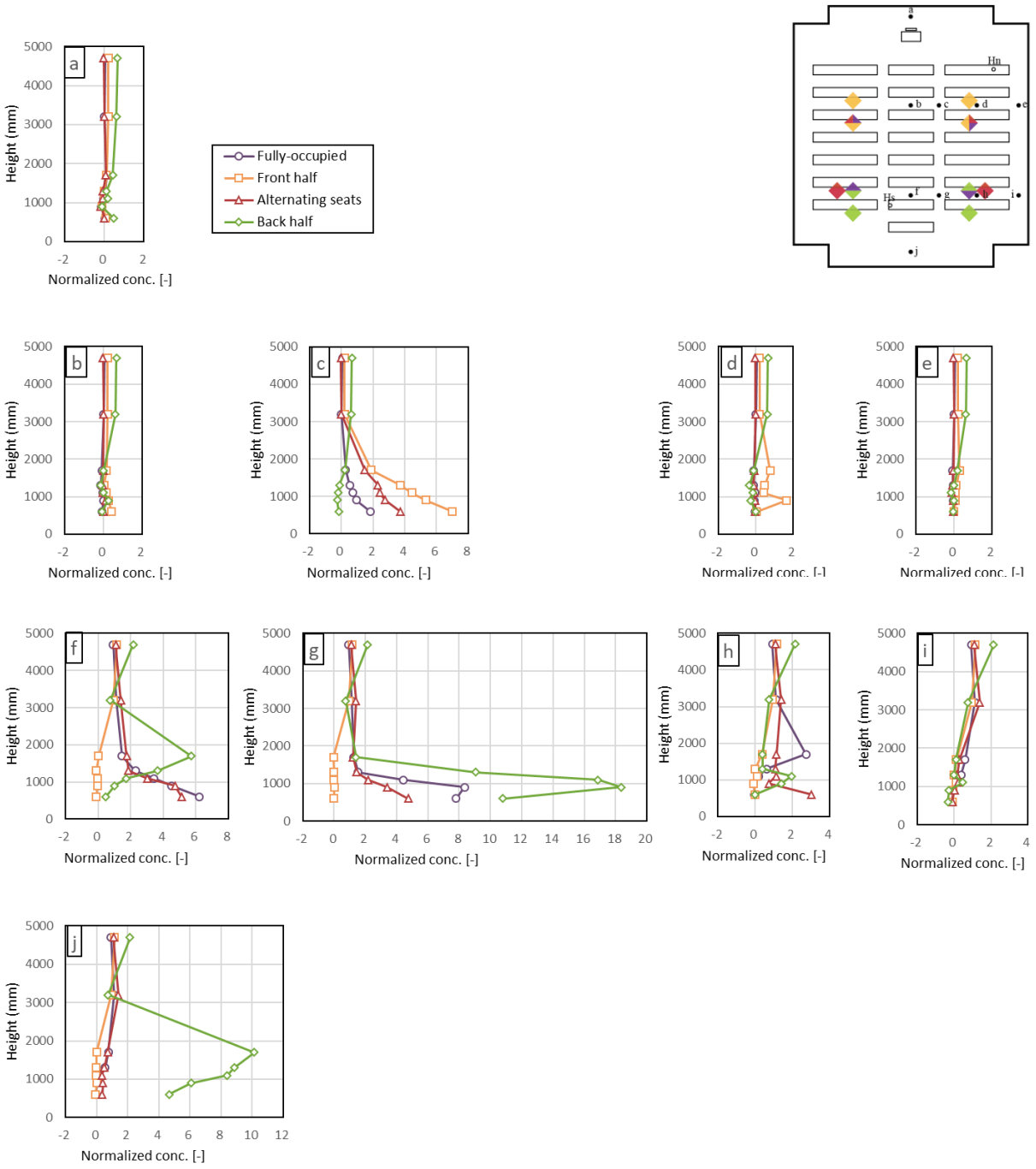

Figure 2.54 CO_2 vertical distribution for the four seating pattern cases

2.5. CFD Validation and Result Analysis

To validate the CFD simulation, one case, one source: front right case, was chosen. The case was analyzed by Stream, v.22, using the readings from the field measurements as fixed inputs. The temperature and CO_2 at all poles are then compared to the field measurements to assess the accuracy of the CFD model used. In addition, distribution contours for both temperature and contaminant were derived to visualize the results.

2.5.1. Analysis Conditions

With an RNG k-ε model, the heat calculations was carried out, radiation considered. The temperature of all inner surfaces was input to the analysis as a fixed condition. Supply flowrate and temperature were input as well as the CO_2 emission details. Analysis and boundary conditions are summarized by

Table 2-15 and Table 2-16 respectively. To reduce the calculation time, the black lamp geometry was simplified into a cube with the same surface area as the actual bulb As shown in Table 2-16, the first attempt of the CFD simulation was done using logarithmic law for heat transfer from the inner surfaces in the room. However, to improve the temperature readings to be closer to the filed measurements, other heat transfer options were tested. Coefficient of heat transfer was tested. A range of values guided by literature recommendations were tried out. The higher the coefficient is the closer the results come to match the experiment readings. Therefore. Experiment readings, and readings of log. law simulation and high coefficient of heat transfer cases are plotted and discussed in the following section.

Table 2-15 Analysis conditions

Analysis	Stream v.22
Turbulence	RNG k-ε model
Analysis	Steady state
Calculations	Heat, radiation, and diffusion
Mesh settings	
Default size	50 mm
Growth rate	1.15
Cells count	~ 4M

Table 2-16 Boundary conditions

Thermal Boundaries	
Heat transfer condition	
External surfaces	Adiabatic
Floor and ceiling	Case-1: Logarithmic law
	Case-2: Coefficient of heat transfer 20 | 30 | 50 | 100 W/m^{2}K
Other internal surfaces	Fixed temperature field measurement)
Emissivity	0.9
Heat Generation	
Heat load	60 W /lamp
CO_2 Generation	
Source	Front right seat
Emission rate	10 L/min
Emission Temperature	32.38 ℃

2.5.2. Results and Discussion

2.5.2.1. Temperature distribution

The temperature vertical distribution of the experiment readings and CFD outputs are plotted in Figure 2.55. The initial case, log.law, showed lower temperature with slightly different graph trend especially at lowers levels. It was found that increasing the coefficient of heat transfer, the gap between the readings and simulation results narrows down. Therefore, cases with coefficient 20, 30, 50 and 100 $W/m^2.K$ were simulated. These cases were found to have a closer vertical distribution to the readings than that of the log. law case. Increasing the coefficient from 20 to 30 slightly improved the results, however, further increase raises temperature more than that measured. Temperature contours at different heights are shown in Figure 2.56 and in sections in Figure 2.57.

The major difference between the log. law case and the other cases can be seen. One important observation about the nature of thermal plumes from black lamps can be seen in both plan and sections. Compared to the human model as a heat source, the black lamp plume has smaller surface area, hotter and faster air flow.

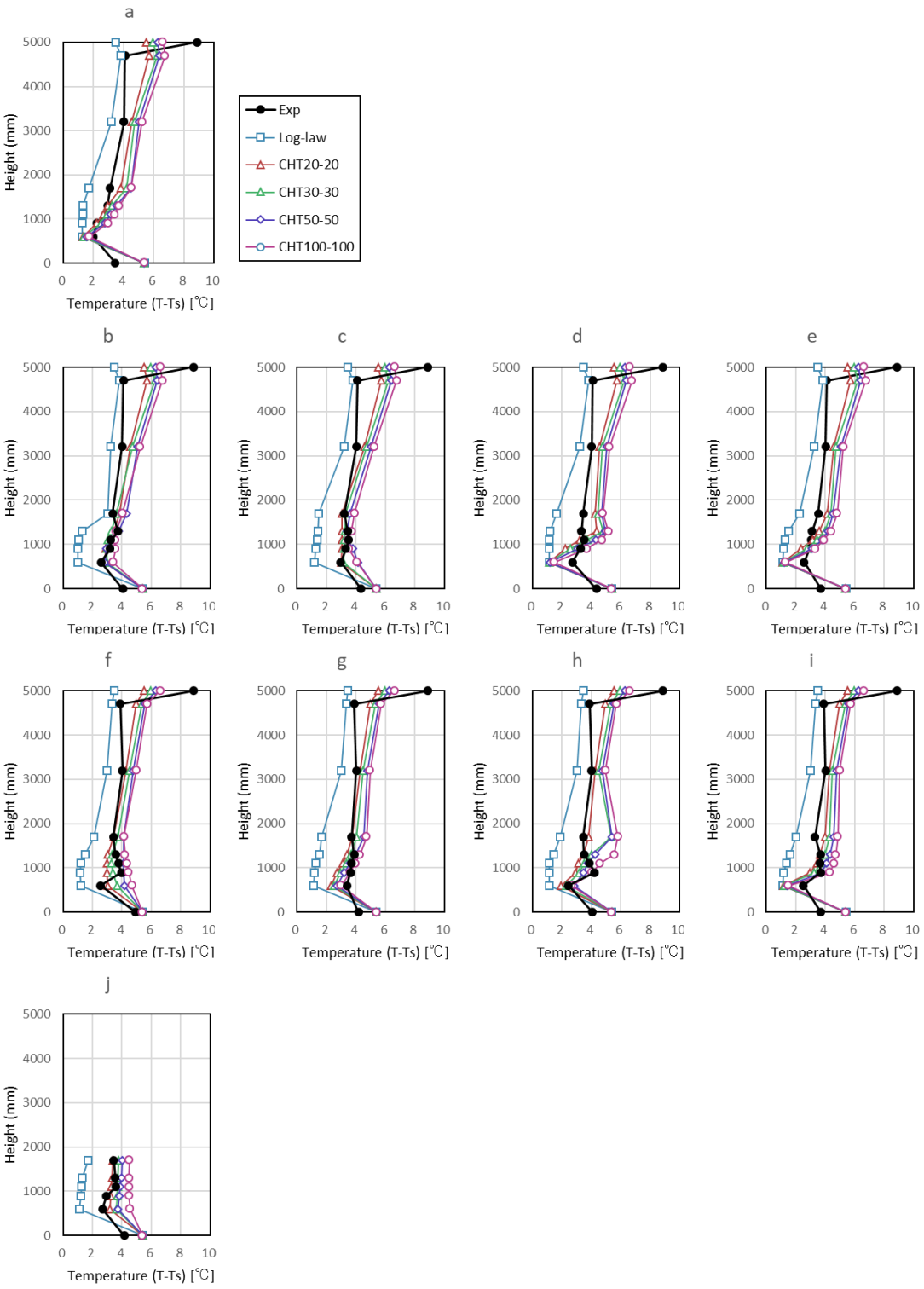

Figure 2.55 Temperature vertical distribution, experiment measurements vs CFD

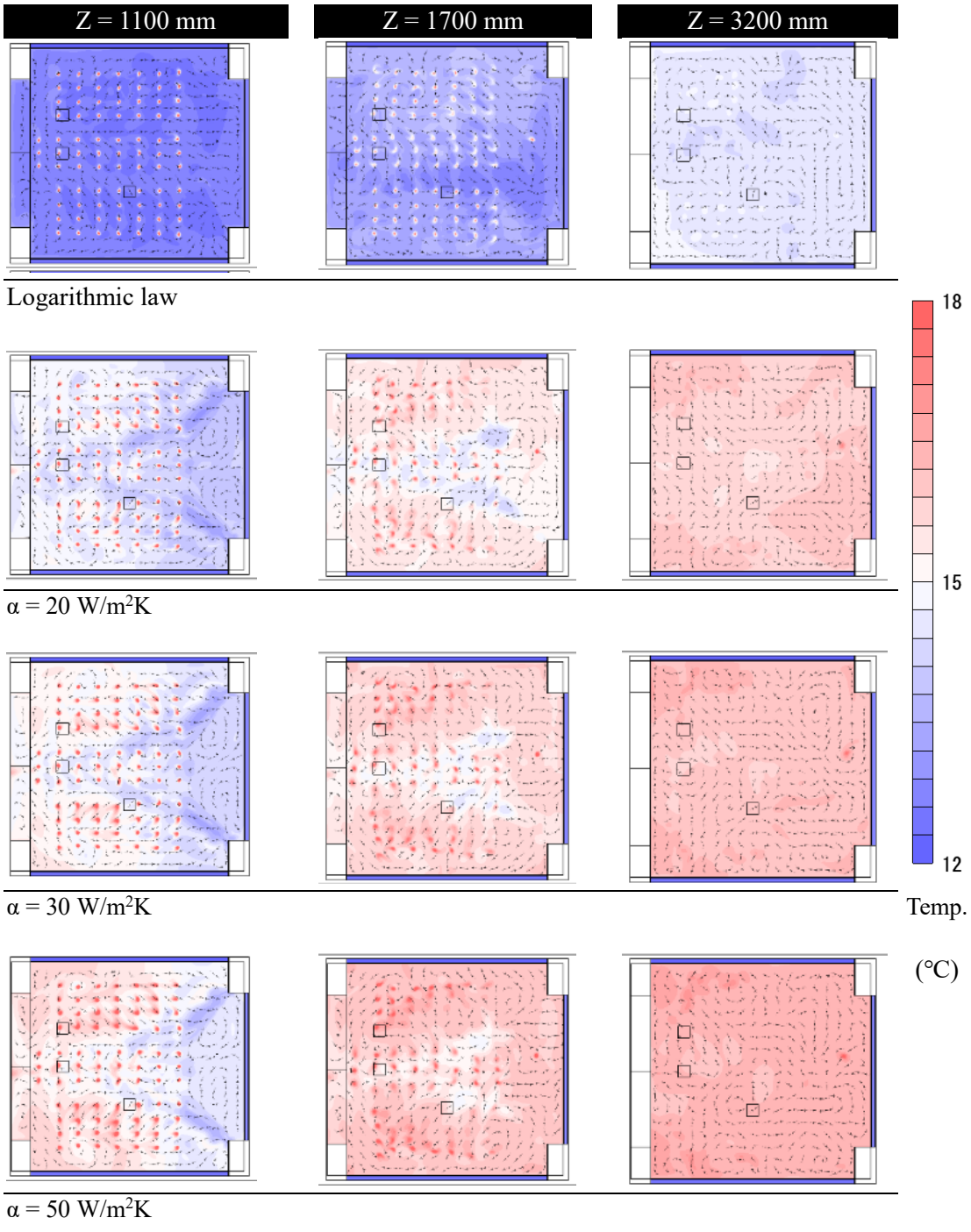

Figure 2.56 Tempearture contours for CFD cases, Plan view

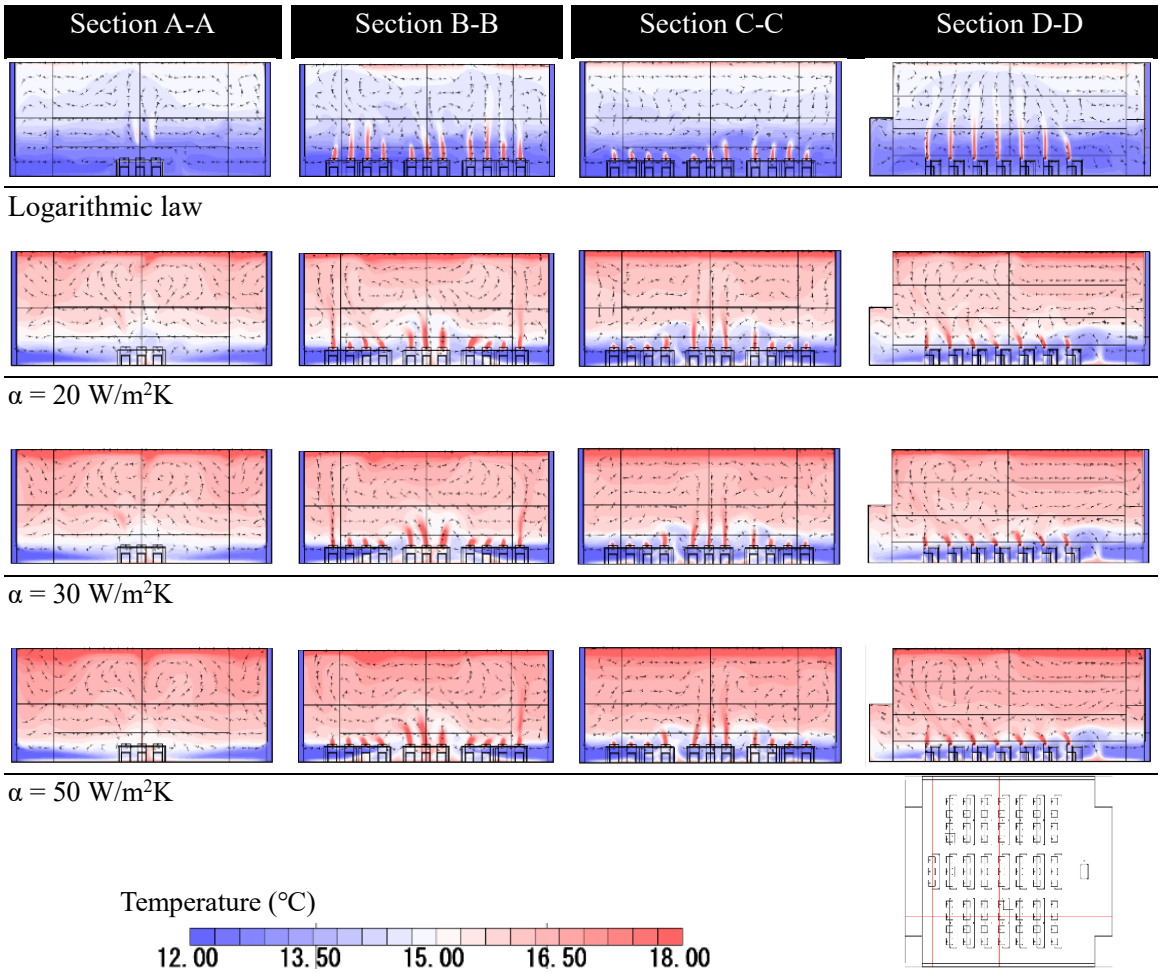

Figure 2.57 Tempearture contours for CFD cases, Longitudinal and cross-sections

2.5.2.2. Contaminant concentration distribution

Simulating CO_2 gas in Stream, diffusivity and concentration are input, however, density is automatically assumed to be equal to the air density. With air density, being significantly lighter than CO_2, the contaminant dispersion could not reach an acceptable matching percentage as shown in Figure 2.58. All CFD cases show similar trend which assumes stratification; low concentrations near the floor, an interface level at 1700 mm in most poles and a peak at a height above the occupied zone. The phenomenon of CO_2 falling to low heights that was observed in the experiment readings was found in the CFD results as well but only at Pe. In the experiment, there was an accumulation at the rear section, Pj, however, it was not reflected in the CFD. Comparing the different CFD cases, the log. law case displayed the maximum concentration height to be at 4700 mm while in the other cases it was at 3200 mm. Increasing the coefficient of heat transfer from 20 to 100 $W/m^2.K$ caused the highest concentration, at 3200 mm, to increase. From the contours in Figure 2.59 and Figure 2.60, the following points can be observed:1- log. law case shows an idealistic stratification as the concentration accumulates at the top leaving the occupied zone clear. 2- The horizontal flows in all cases carry the contaminant backwards at lower heights. 3- Especially in the $\alpha = 50$ W/m^2K case, the effect of downward draft at the side wall can be seen in Figure 2.60 section A-A.

Regarding the contours in Figure 2.59 and Figure 2.60, the effect of temperature gradient can be seen. For the higher the coefficient of heat transfer is, the steeper the temperature gradient is and the cleaner the occupied zone becomes. Although the vertical distribution particularly is not similar to the field measurements, the horizontal flows noticed from the diffusion direction in the measurements can be seen in the contours as well. This supports the findings from the pre-construction investigation and emphasizes on the importance of uniformity in supply diffusers placement.

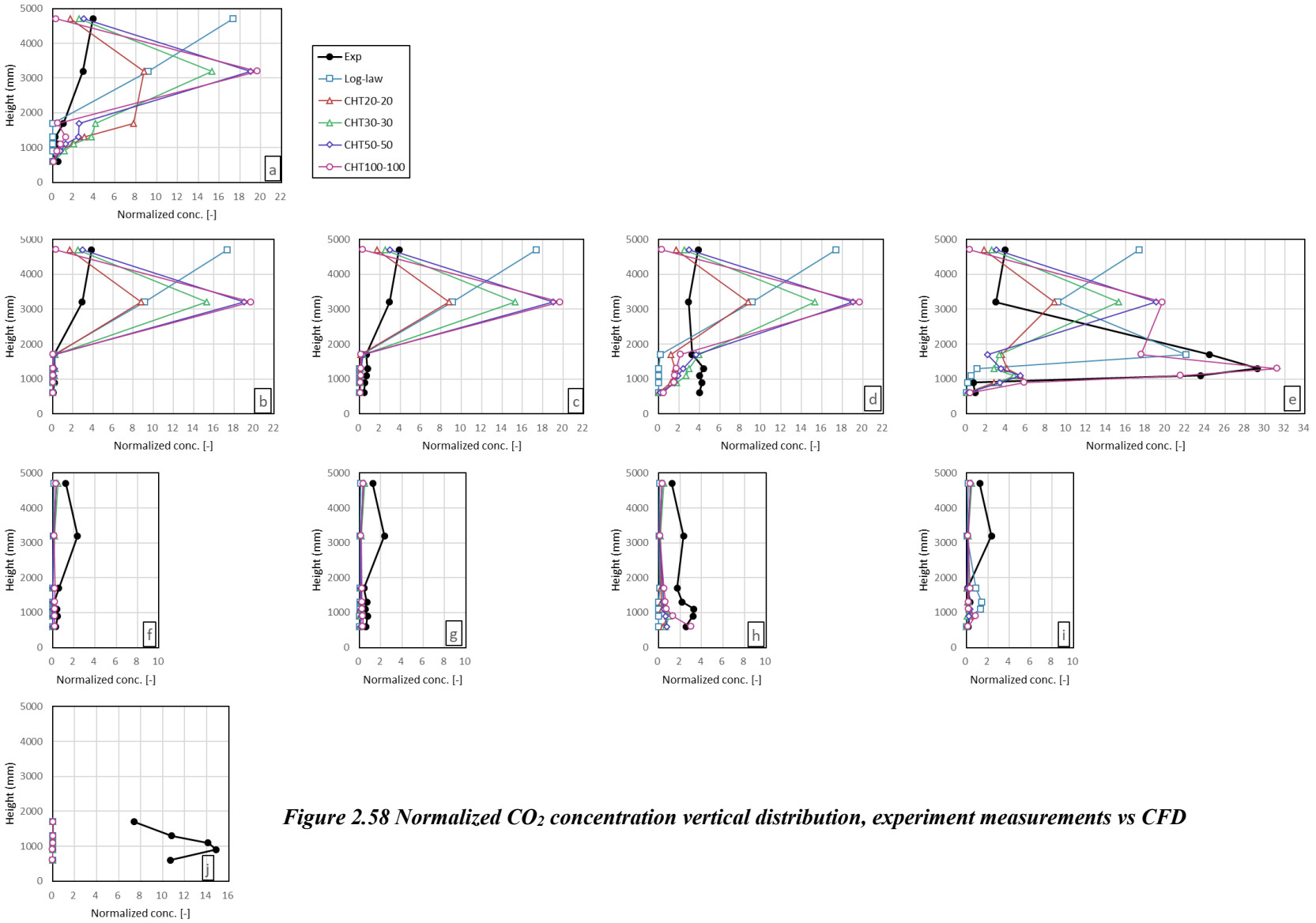

Figure 2.58 Normalized CO_2 concentration vertical distribution, experiment measurements vs CFD

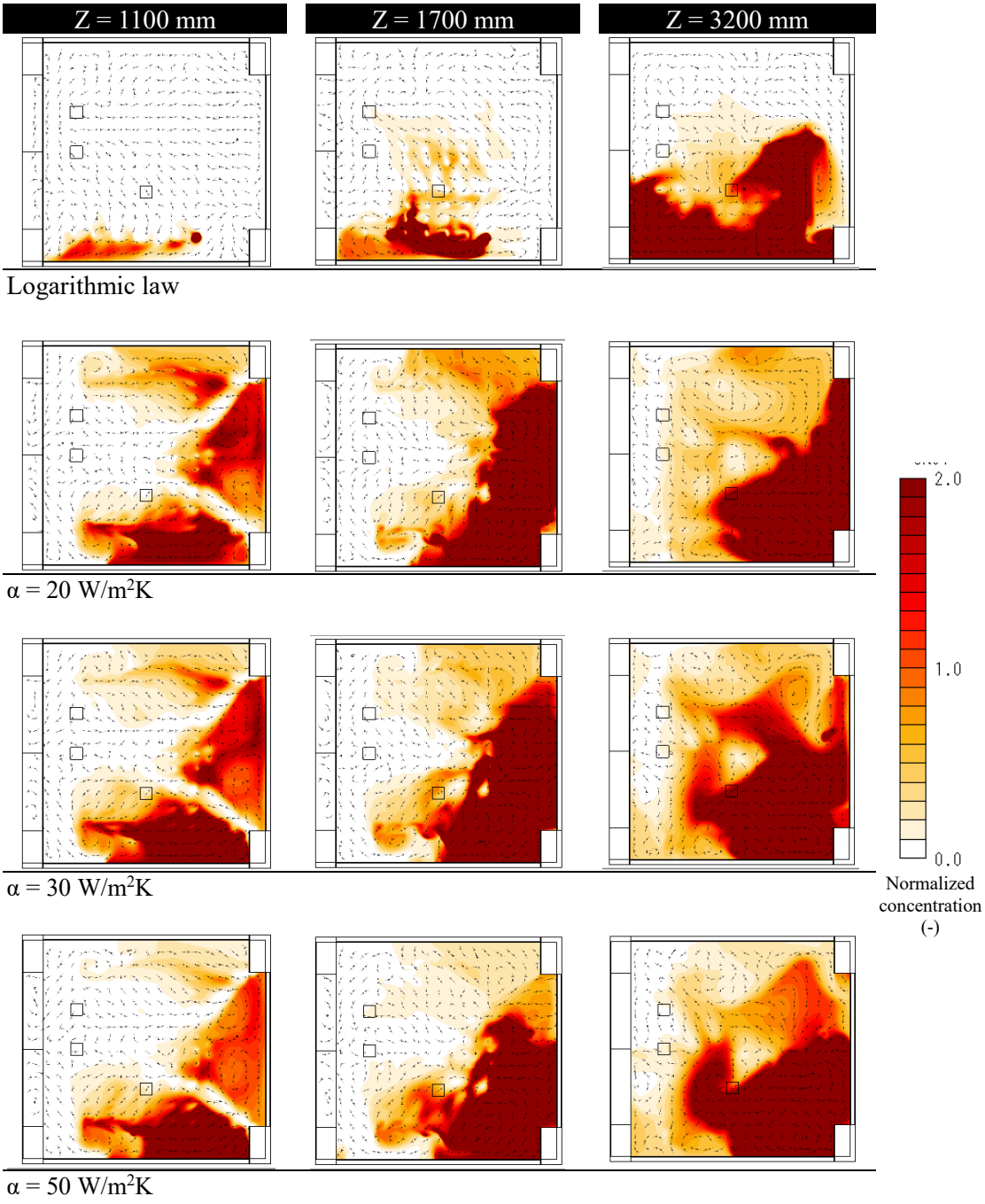

Figure 2.59 Normalized CO_2 concentration contours for CFD cases, Plan view

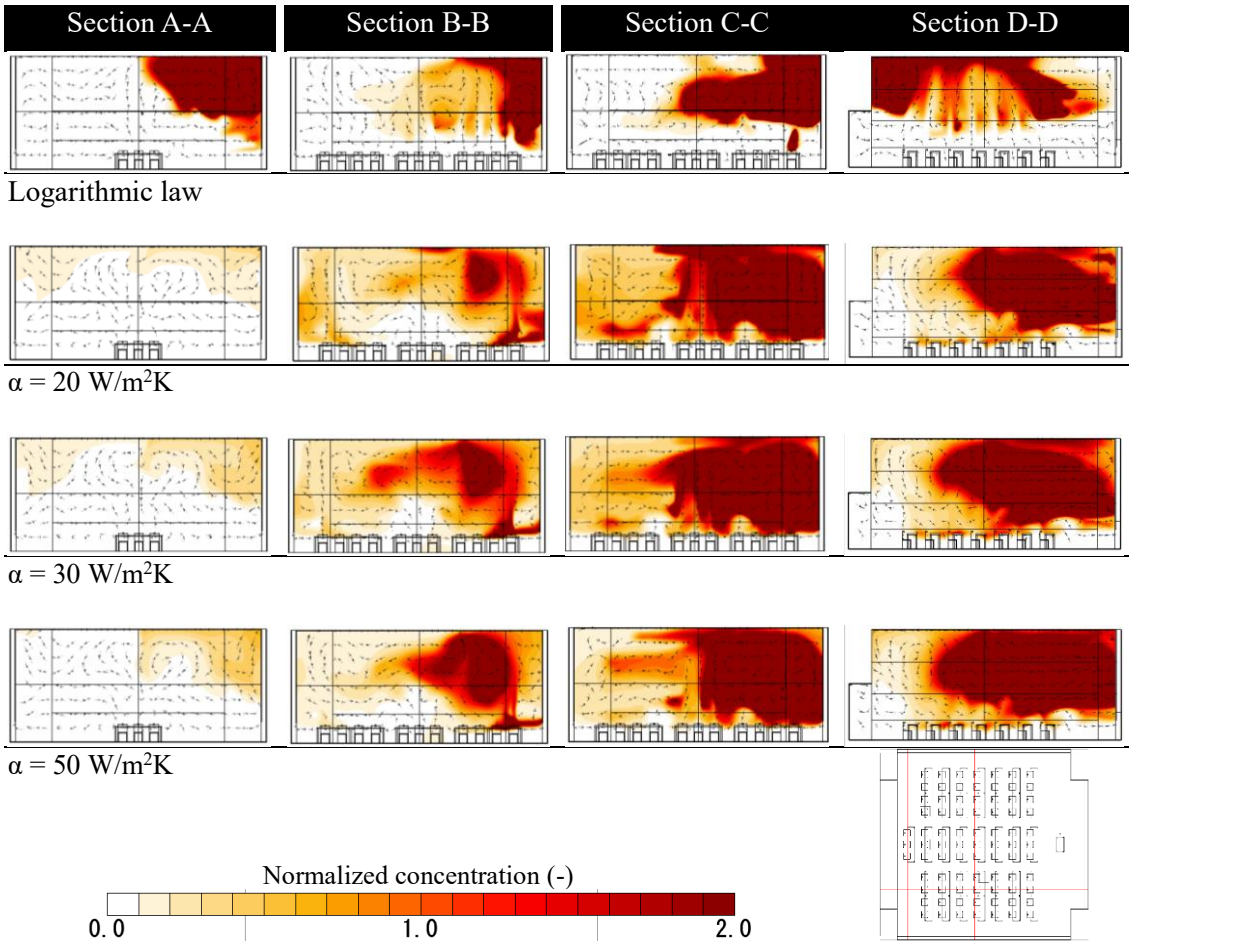

Figure 2.60 Normalized CO_2 concentration contours for CFD cases, Longitudinal and cross-sections

2.6. Chapter Discussion and Conclusion

Source position steady and transient

This investigation aimed at assessing the system's capability to prevent cross-infection. The system was evaluated in terms of temperature stratification, contaminant distribution, breathing zone air quality, local air quality index, and contaminant diffusion radius. Features that were found to have affected the system negatively were separately investigated, namely seats arrangement and asymmetric diffusers setting.

The studied system had special features which posed a challenge to the system's efficiency. One of which was flat diffusers. Typically, a system with flat diffusers face the challenge of balancing the flow velocity and flow rate, the system analyzed in this study seemed to successfully achieve sufficient flow volume/occupant and in the same time cause no draft effect for adjacent occupants as the flow velocity was kept adequately low.

Regarding temperature distribution, it was observed that the stratification was optimal all over the room plan although lower than the numeric calculations. The plume interaction, not considered in the calculations, is thought to be the main cause of reducing the upwards flow rate in the CFD analysis. Stratification height difference was found in the front section as it had a level higher than average which was thought to be the effect of the airflow from the front diffuser. This correlation was proved by further investigation as the variation in stratification level was found to disappear when a back diffuser was added balancing the supply.

In addition, removing the last row of occupants, which acted as an obstacle to air flow, balanced the stratification height as well.

Assessing the system's capability to prevent cross-infection; the contaminants stratification level was not sufficiently high in some cases in spite of the acceptable temperature gradient. As for the effect of changing the contaminant source position, it had a significant effect on the contaminant distribution pattern. Subsequently, the inhaled air quality for non-source occupants varied highly. It was observed that the reason why the impact of source position was significant is the slow horizontal air currents guiding the contaminants spread and causing great differences between the 10 cases simulated. These air currents were found to be the combined effect of the 3-sided-diffusers design and seats arrangements hindering air flow at the posterior section of the room. In spite of being of low velocity, they were found to disrupt the DV system and thus reducing its efficiency in clearing the occupied zone of contaminants. The magnitude of the horizontal flow impact on contaminant distribution was more obvious when comparing the base case to the altered cases. The effect of equalizing the backward and forward air flows reduced the horizontal distribution and consequently reduced the number of affected occupants.

Although horizontal currents were found to be the major factor causing this contaminant distribution its effect was combined with the downward drafts which aggravated its effect on occupants. Resulting from the flow of supply air through double wall, the downdraft was noticed near side walls specially. In spite of having no negative effect on temperature distribution, it caused the contaminant to mix back in the occupied zone in the majority of the simulated cases.

Assessing the air quality using the diffusion radius index, SVE2, along with concentration contours showed that depending solely on the radius value to compare different cases can be misleading. As the radius is normalized by concentration integral, having varying concentration integral values causes the radius to be insignificant. Hence, in this study, SVE2 and contaminant integral values were put side-by-side when evaluating the results. In a sense, rather than judging cases on how far the concentration spread, judgment on how much contaminants spread this far is more accurate.

From the transient simulations, it can be concluded the contaminant source occupant has varying effect severity according to his location in the room. Thus, it was observed that changing the source location has a significant effect on the adjacent occupants' air quality through the quantity of contaminants inhaled, the delay time until the contaminants reaches their breathing zone and the duration the contaminants stay within its range. In addition, the analysis results showed a clear relation between the source occupant location and his own inhaled air quality as well. This study supports the findings of the previous steady state simulation published in (Part 2), however, one significant addition of the transient results is that it highlighted the effect of buoyancy, despite the low speed horizontal air flows, in clearing the occupants' breathing zone by time.

Similar findings were observed from the filed measurements. In addition, due to the fact that supply air flows through double walls wall surface temperature were relatively low. Low wall surface temperature causes down drafts that result in mixing hot air from the top part of the room with the occupied zone air.

Seating Pattern

This investigation addressed the effect of occupation pattern on air temperature and contaminants concentration in the lecture hall. It was deduced that position of occupants with respect to diffusers is critical to both factors. It was also noted that dispersed occupants' patterns outperforms closely seated occupants cases in terms of heat and air quality. Although the CFD analysis differed in conditions and cases settings, the same conclusion was reached

Experiment

Generally speaking, from the concentration distribution results, it can be concluded that emitting CO_2 alone was non-indicative of how human generated contaminants would diffuse due to its high density and large volume. Heating the gas was found ineffective as well. Another point that is thought tot have affected the validity of the contaminant distribution results is the use of black lamps. Black lamps were used to simulate the heat generated by humans. Despite matching the wattage, the thermal plume of the lamps are of different shape and much smaller surface area. These differences in the thermal plume was visualized in the CFD analyses and can be observed by comparing the validation case to the pre-construction exploratory simulations. Hence, it can be deduced that in the field measurement, the aforementioned points have caused the contaminant concentration readings to be misrepresentative to the actual system performance in clearing the occupied zone from contaminants.

Diffusers settings

Exploring the effect of 2, 3, and 4-sides supply Diffusers on temperature and contaminant distribution for different occupants seating pattern cases, the following can be concluded. (1) Asymmetric 3-sides air supply causes horizontal flows and in some cases down mixing flows as noticed in the front-half seating pattern especially. (2) 2-sides and 4-sides supply sustained a more stable upward flow achieving a cleaner occupied zone in various seating cases. (3) For the fully-occupied case, the 4-sides supply gave the best results in terms of flow velocity for edge seats, as well as temperature and contaminant distribution.

2.7. Research limitations

The limitations can be summarized by the following points. The fact that the DV system installed in the case-study is nontypical restrains the observations to be generalized. Thus, similar studies on typical DV system design could support the findings presented. Another limitation is the human model simplification specially the seated model. Although adding details significantly affect the computation time following the sitting outline, even in simple cuboids, it may affect the plume velocity as the surface area would increase which may influence the airflow contours. In addition, using the k-ε model has limited accuracy compared to nonlinear eddy viscosity models, however with such a model size as of the case-study, models that require fine meshing require an extremely long processing time.

2.8. References

[1] P. Hansson, H. Stymne, A technique to improve the performance of displacement ventilation during cold climate conditions, in: 17th AIVC Conference, Gothenburg, Sweden, 1996: pp. 521–528.

[2] N. Choi, T. Yamanaka, T. Kobayashi, T. Ihama, M. Wakasa, Influence of vertical airflow along walls on temperature and contaminant concentration distributions in a displacement-ventilated four-bed hospital ward, Build Environ. 183 (2020) 107181. https://doi.org/10.1016/J.BUILDENV.2020.107181.

[3] R. Kosonen, A. Melikov, E. Mundt, P. Mustakallio, Displacement Ventilation, 2017. https://biblioteka.ktu.edu/wp-content/uploads/sites/38/2017/06/23_Displacement_Ventilation.pdf (accessed August 19, 2021).

[4] R. Yang, C.S. Ng, K.L. Chong, R. Verzicco, D. Lohse, Optimal ventilation rate for effective displacement ventilation, (2021). https://arxiv.org/abs/2104.03363v1 (accessed August 12, 2021).

[5] S. Gilani, H. Montazeri, B. Blocken, CFD simulation of stratified indoor environment in displacement ventilation: Validation and sensitivity analysis, Build Environ. 95 (2016) 299–313. https://doi.org/10.1016/J.BUILDENV.2015.09.010.

[6] M. Cehlin, B. Moshfegh, Numerical modeling of a complex diffuser in a room with displacement ventilation, Build Environ. 45 (2010) 2240–2252. https://doi.org/10.1016/J.BUILDENV.2010.04.008.

[7] H. Xing, A. Hatton, H.B. Awbi, A study of the air quality in the breathing zone in a room with displacement ventilation, Build Environ. 36 (2001) 809–820. https://doi.org/10.1016/S0360-1323(01)00006-3.

[8] P. Rohdin, B. Moshfegh, Numerical predictions of indoor climate in large industrial premises. A comparison between different k–ε models supported by field measurements, Build Environ. 42 (2007) 3872–3882. https://doi.org/10.1016/J.BUILDENV.2006.11.005.

[9] J. Srebric, W. Xu, Removal of contaminants released from room surfaces by displacement and mixing ventilation: modeling and validation, Indoor Air. (2005). https://doi.org/10.1111/j.1600-0668.2005.00383.x.

[10] A.Q. Ahmed, S. Gao, A.K. Kareem, A numerical study on the effects of exhaust locations on energy consumption and thermal environment in an office room served by displacement ventilation, (2016). https://doi.org/10.1016/j.enconman.2016.03.004.

[11] Q. Chen, N.-T. Chao, Comparing Turbulence Models for Buoyant Plume and Displacement Ventilation Simulation, Indoor and Built Environment . (1997). https://doi.org/10.1177/1420326X9700600304.

[12] J. Niu, J. van der Kooi, Grid-optimization for k–e turbulence model simulation of natural convection in rooms, in: ROOMVENT-92, 1992. https://www.aivc.org/resource/grid-optimization-k-e-turbulence-model-simulation-natural-convection-rooms (accessed August 19, 2021).

[13] H. Stymne, M. Sandberg, M. Mattsson, Dispersion pattern of contaminants in a displacement ventilated room-implications for demand control, in: 12th AIVC Conference, 1991: pp. 173–189.

[14] N.M. Mateus, G. Carrilho da Graça, A validated three-node model for displacement ventilation, Build Environ. 84 (2015) 50–59. https://doi.org/10.1016/J.BUILDENV.2014.10.029.

[15] ANSI/ASHRAE, Standard 140–2017—Standard Method of Test for the Evaluation of Building Energy Analysis Computer Programs, (2017).

[16] B. E, N. PV, Dispersal of exhaled air and personal exposure in displacement ventilated rooms., Indoor Air. 12 (2002) 147–164. https://doi.org/10.1034/J.1600-0668.2002.08126.X.

[17] Y. Yin, J.K. Gupta, X. Zhang, J. Liu, Q. Chen, Distributions of respiratory contaminants from a patient with different postures and exhaling modes in a single-bed inpatient room, Build Environ. 46 (2011) 75–81. https://doi.org/10.1016/J.BUILDENV.2010.07.003.

[18] R. Zhang, T. Yamanaka, T. Kobayashi, N. Kobayashi, J. Yoshihara, Performance of Local Exhaust System as Prevention Measure of Infection in Consulting Room (Part 1) Behavior of Droplet Nuclei from Human and Removal Performance of Exhaust System by Means of CFD Analysis , in: The Society of Heating, Air-Conditioning and Sanitary Engineers of Japan Kinki Branch, Proceedings of

Academic Research Presentation, 2022: pp. 61–64.
[19] N. Lastovets, R. Kosonen, J. Jokisalo, Calculation of airflow rate with displacement ventilation in dynamic conditions, 13-147. (2020) 13–14. https://sintef.brage.unit.no/sintef-xmlui/handle/11250/2683223 (accessed August 12, 2021).
[20] ASHRAE Standard Committee, ANSI/ASHRAE Addendum b to ANSI/ASHRAE Standard 55-2013, (2013).
[21] Q. Chen, L.R. Glicksman, System Performance Evaluation and Design Guidelines for Displacement Ventilation, n.d. https://scholar.google.com/scholar?hl=en&as_sdt=0%2C5&q=System+Performance+Evaluation+and+Design+Guideline+for+Displacement+Ventilation&btnG= (accessed August 12, 2021).
[22] R. Kosonen, A. Melikov, E. Mundt, P. Mustakallio, Displacement Ventilation, 2017. https://biblioteka.ktu.edu/wp-content/uploads/sites/38/2017/06/23_Displacement_Ventilation.pdf (accessed August 19, 2021).
[23] F. Causone, B.W. Olesen, S.P. Corgnati, Floor heating with displacement ventilation: An experimental and numerical analysis, HVAC and R Research. 16 (2010) 139–160. https://doi.org/10.1080/10789669.2010.10390898.
[24] Ventilation Effectiveness: Rehva Guidebooks — Aalborg University's Research Portal, (n.d.). https://vbn.aau.dk/en/publications/ventilation-effectiveness-rehva-guidebooks (accessed August 19, 2021).
[25] S. Murakami, NEW SCALES FOR VENTILATION EFFICIENCY AND THEIR APPLICATION BASED ON NUMERICAL SIMULATION OF ROOM AIRFLOW, in: International Symposium on Room Air Convection and Ventilation Effectiveness , 1992.
[26] S. Zhu, P. Demokritou, J. Spengler, Experimental and numerical investigation of micro-environmental conditions in public transportation buses, Build Environ. 45 (2010) 2077–2088. https://doi.org/10.1016/J.BUILDENV.2010.03.004.
[27] S. Kato, J.H. Yang, Study on inhaled air quality in a personal air-conditioning environment using new scales of ventilation efficiency, Build Environ. 43 (2008) 494–507. https://doi.org/10.1016/J.BUILDENV.2006.08.019.
[28] P. Stankov, J. Denev, M. Bartak, J. Schwarzer, V. Zmrha L, Experimental and Numerical Investigation of Temperature Distribution in Room with Displacement Ventilation, Clima. (2000) 15–18.
[29] Y. Suwa, J.C. Park, Y.-S. Kim, Optimal Airflow Performance for FOUP Systems in Cleanrooms Using SVE Quantification Method, Journal of Asian Architecture and Building Engineering. 10 (2011) 257–261. https://doi.org/10.3130/JAABE.10.257.
[30] S. Chen, S. Kato, Y. Kang, K. Nakao, CFD Analysis about Influence of Human Movements on Diffusion of Indoor Air Pollutants, ISEE Conference Abstracts. 2013 (2013) 4245. https://doi.org/10.1289/ISEE.2013.P-2-01-01.

Chapter 3 Displacement Ventilation Performance Enhancement using a Novel Portable Cooling Unit with Air Purification Function

3.1. Introduction and Research Purpose

To enhance the performance of DV system, this chapter addresses three points: 1- Diffusers positioning, to overcome unbalanced supply due to room shape, size or occupants seating pattern. 2- Strengthening the temperature stratification to improve the air quality and comfort of the occupied zone. These points were discussed in previous chapters. In addition, thirdly, integrating portable air purifiers is considered.

3.1.1. Air purifiers

Integrating air purifiers with the ventilation system is one technique to reduce the contaminant spread and cross-infection risk as concluded from the experimental measurements and CFD analysis by Zhang et al. [1]

The reason why air purifiers are seen as efficient is because they address the mode of infection transfer. Although human exhalation contains a wide range of droplets sizes, 0.01–1000μm [2]. The transmission of infection was found to be caused by droplet nuclei or smaller droplets referred to as aerosols [3,4]. Being of smaller size, <5μm and less water content, they can stay suspended for longer than larger droplets which tend to fall quickly[5,6].

Droplets are considered to fall quickly to the floor close to the source, whereas aerosols are expected to remain airborne for long times [7]. However, by time the particle size decreases with a rate dependent on the initial size, relative humidity, temperature, air flow amongst other factors [8]

Given the infection spread mechanism, and especially with the recent pandemic situation, the importance integrating air filtration in the ventilation systems or add portable air cleaners has been highlighted in recent research [9]. The advantages of using portable air purifiers have been explored by Novoselac et al. in their 2009 study. They investigated three factors: particles size, flowrate, and position of the air purifier. It was found that the position of the air purifier has a major effect on overall particle removal and thus on the air quality in different parts of space. [10]

The effectiveness of air purifiers using MERV or High Efficiency Particulate Air filters (HEPA) and operating with mechanical ventilation has been proved in multiple research work [11–13]. A reduction in the particulate matter (PM) as high as 50% was measured in the investigated classrooms [11]. HEPA filters particularly have been studied in numerous research, either using air cleaner effectiveness, ultrafine particle removal, or sensory testing [14–16]. The results of these studies have shown positive results on the effectiveness of using HEPA filters for air purification.

To tackle the potential enhancement points, a novel air purifier unit that functions as a portable DV system is proposed. Although close ideas of merging portable air-conditioning units and air purifiers have investigated in some studies [1], no similar one unit has been proposed so far, especially in DV system. The proposed machine should function as a mobile DV diffuser. It consists of a heat pump with no ducts to be connected to outdoor. Being ductless, the exhaust heat is discharged in the room to act as an additional heat source to enhance the temperature vertical stratification. Mimicking a typical DV system, supply diffuser is in the lower section of the unit while the suction port in the top section as shown in Figure 3.1a. The suction port provides air for both function, air cooling and heat exhaust. Moreover, to function as standalone DV system, air filters such HEPA filters function should be added to purify the return air. Placement and functioning method of the portable DV unit (PDV unit) are illustrated in Figure 3.1b.

The concept of the PDV unit is examined using zonal model calculations and experimental measurements. In the following sections both methods' details and results are discussed.

3.1.2. Methodology

In this study, the effectivity of the novel PDV unit was assessed in terms of temperature and PM distribution. Zonal model calculation and experimental measurements were carried out for this purpose. First, in the zonal model, only the thermal effect of the PDV unit was formulated. A parametric study exploring the effect of multiple variables was carried out. Secondly, field measurement was performed in which a prototype model of the PDV unit was built and operated. In the experimental measurements, the effect of various parameters was assessed by monitoring both temperature and particulate matter concentration distribution.

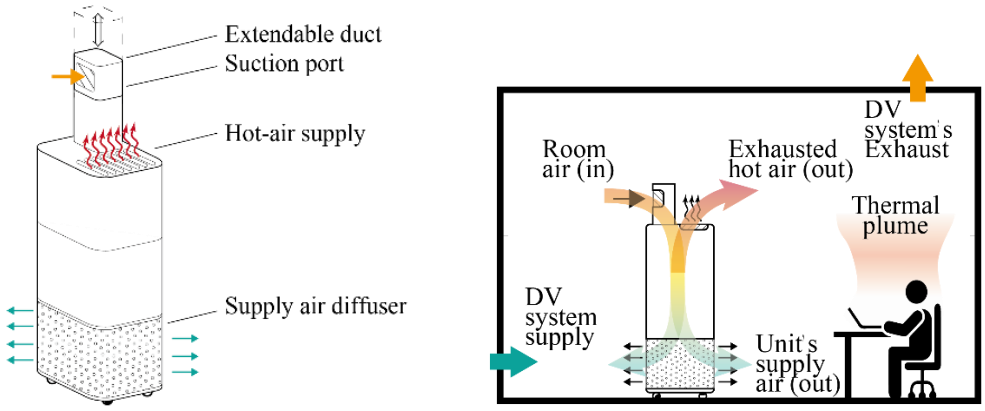

a. PDV unit conceptual design *b. PDV unit placement and functioning*

Figure 3.1 PDV unit proposed design

3.2. Zonal model calculations

It has been attempted in multiple research to formalize predictive models of DV temperature distribution. Varying degrees of simplification and different factors considered [17,18]. One example is Xu and Yamanaka

(2001) who focused on modeling heat loss through the room envelop [19]. In this calculation, the basic model illustrated in Figure 3.2, was adopted and the PDV unit effect was formulated in the adapted zonal model. The model assumes stratification in two layers and neglects radiation from the different surfaces. The thermal balance for the upper and lower zones is given by equations (3-1 to 3-2).

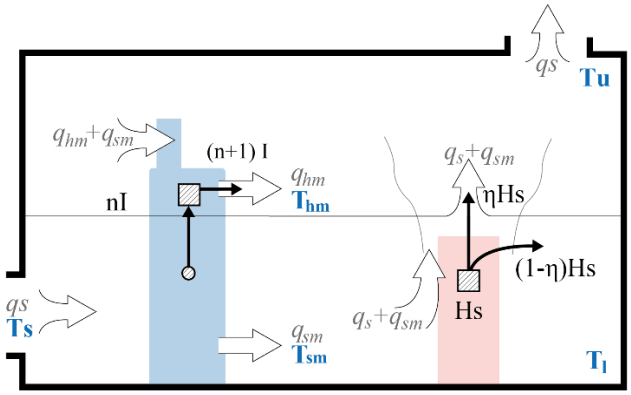

Figure 3.2 Zonal model

$$(n+1)\,I + \eta H_s + Cp\rho\,(q_s+q_{sm})\,T_l - Cp\rho q_s T_u - Cp\rho q_{sm} T_u = 0 \qquad (3\text{-}1)$$

$$-nI + (1-\eta)\,H_s + Cp\rho q_s T_s + Cp\rho q_{sm} T_u - Cp\rho\,(q_s+q_{sm})\,T_l = 0 \qquad (3\text{-}2)$$

PDV unit's cooling and heating capacities are shown in equations (3-3) and (3-4) respectively.

$$Q_{sm} = nI \;=\; Cp\rho q_{sm}\,(T_u - T_{sm}) \qquad (3\text{-}3)$$

$$Q_{hm} = (n+1)\,I \;= Cp\rho q_{hm}\,(T_{hm} - T_u) \qquad (3\text{-}4)$$

where for the DV system, q_s is the supply flowrate and T_s is the supply temperature. For the room, T_u and T_l are the air temperature of upper and lower sections respectively. C_p stands for specific heat of air (1.2 kg/m^3) while ρ is the air density (1004 J/K.kg). Representing heat sources in the room, human and computer devices, H_s is the heat load generated and η is the ratio of the heat that ascends to the upper part of the room assumed to be 1. Regarding the PDV unit, n is the unit's coefficient of performance, COP, I is the input power (W), q_{sm} and q_{hm} are the machine's supply flowrate and hot air flow rate respectively. T_{sm} and T_{hm} are the supply temperature and hot-air temperature respectively. Q_{sm} is the cooling capacity of the PDV unit and Q_{hm} is its heating capacity.

3.2.1. Parametric analysis

In this calculation, some of the DV system and PDV unit specifications were changed to study the effect of each variable on the unit's performance and the room temperatures. Table 3-1 summarizes the set of values used in the study. The factors studied in this section are: 1- PDV unit's COP, 2- PDV unit supply flowrate at fixed DV flowrate, 3- DV supply flowrate at a fixed PDV unit flowrate, and 4- PDV unit hot air flowrate. Equations (3-1 to 3-3) were solved simultaneously, then the resultants were used to calculate the hot air temperature using equation (3-4).

Table 3-1 Parametric study cases

		Cases-A	Cases-B	Cases-C	Cases-D
DV	q_s (m^3/h)	200	200	300 -100	200
	T_s (℃)	20			
PDVU	COP, n	3.0 – 4.0	3.5	3.5	3.5
	I (W)	Dependant			
	q_{sm} (m^3/h)	200	100 – 300	200	200
	q_{hm}(m^3/h)	$=Q_{sm}$	$=Q_{sm}$	$=Q_{sm}$	100 – 300
	T_{sm} (℃)	20			
	T_{hm} (℃)	Dependant			

3.2.2. Results

The results of the zonal model calculation of Cases A-D are plotted in this section. It should be noted that in all cases, since the idea situation of equals 1is assumed, the occupied zone temperature, T_l, is constant at 20 ℃, equal to the supply temperature.

3.2.2.1. PDV unit Coefficient of performance

Calculations of increasing the unit's COP from 3 to 4 at constant supply flowrate and temperature were carried out, Cases-A. From Figure 3.3a, the increase in COP is seen to enhance the performance by decreasing the exhausted heat as can be. Increasing the COP from 3 to 4 reduces the required input power by a third to provide a fixed flow rate at a fixed supply temperature, as shown in Figure 3.3b.

3.2.2.2. PDV unit supply flowrate at fixed DV flowrate

As shown in Figure 3.3c and Figure 3.3d, calculations with q_{sm} varying from 100 m^3/h to 300 m^3/h were performed, Cases-B. The 100 m^3/h case requires a relatively small wattage of around 20 W. It can be observed as well that increasing the flow volume requires a steep increase in the input power of the machine. Increasing I, thus, results in exhausting air at higher temperature (T_{hm}).

3.2.2.3. DV flowrate at fixed PDV unit supply flowrate

Decreasing the DV supply flowrate is intended to investigate the PDVU input power needed to compensate. As shown in Figure 3.3e, the relation is exponential. At q_s 100 m^3/h where the DV supply flowrate was lowest, the input power required for the PDV unit to compensate was more than 3 times that of q_s 200 m^3/h. This increase in I was reflected in the hot air temperature and upper zone temperature as shown in Figure 3.3f. Since T_u increased to 40 ℃ making the difference between the upper and lower zone temperatures 20 ℃, this shows that the PDV unit compensation capacity is bound by the temperature difference comfort between head and feet height. However, the PDV unit location, although not represented in the zonal model, might be a major factor in this aspect.

3.2.2.4. PDV unit hot air exhaust flow rate

The relation between hot air flow rate and temperature is given by equation (3-4). For a fixed case-D, Q_{hm} varying were used to calculate the hot air temperature. Figure 3.3g shows that increasing the flow rate from 100 to 300 m^3/h can decrease the temperature by 10 °C. However, the effect of this variable especially, needs to be investigated using CFD analysis or experiment measurements as the flowrate of hot air can highly affect the temperature horizontal distribution and generally the DV induced stratification.

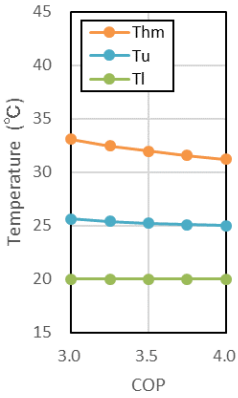

a. Cases-A: COP vs temperatures

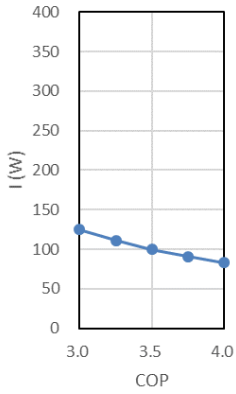

b. Cases-A: COP vs required input power

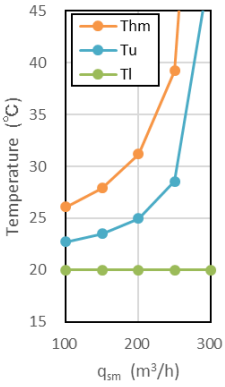

c. Cases-B: PDV unit supply flowrate vs temperatures

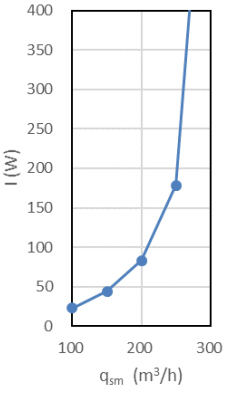

d. Cases-B: PDV unit supply flowrate vs required input power

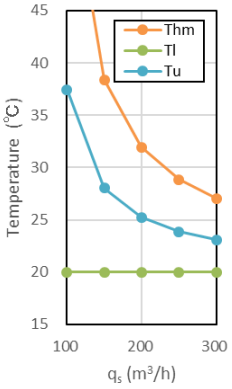

e. Cases-C: DV supply flowrate vs temperature

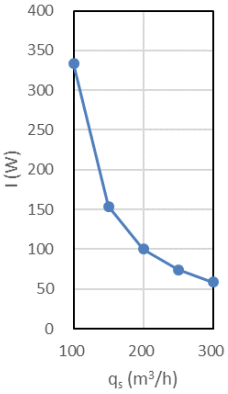

f. Cases-C: DV supply flowrate vs PDV unit required input power

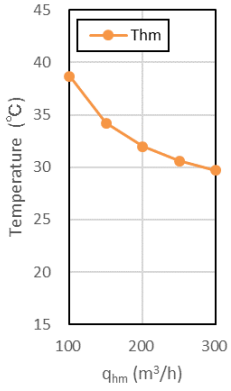

g. Cases-D: PDV unit hot air flowrate vs hot air temperature

Figure 3.3 PDV unit parametric study results

3.3. Experimental Measurements in Environmental Chamber

The field measurements were carried out in the period of January 26 – February 7, 2023 in an environmental chamber in Osaka University, Japan. The experiment room was built of insulated wooden boards. The inner walls were painted in matt black to minimized radiation reflection. As annotated in Figure 3.4a, the room dimensions are 2.84 mm × 2.34 m × 3.00 m, which is relatively small but was decided upon due to space limitation in the experiment building. However, in several research papers, experiments were carried out in similar sized rooms with similar supply flowrate [20].

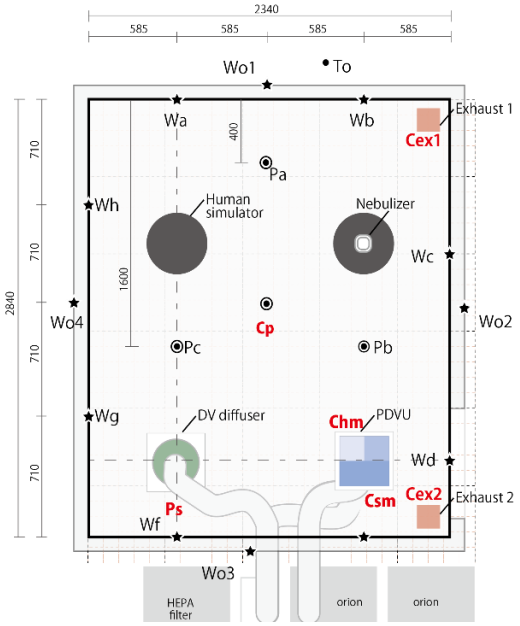

a. Room plan with measurement points

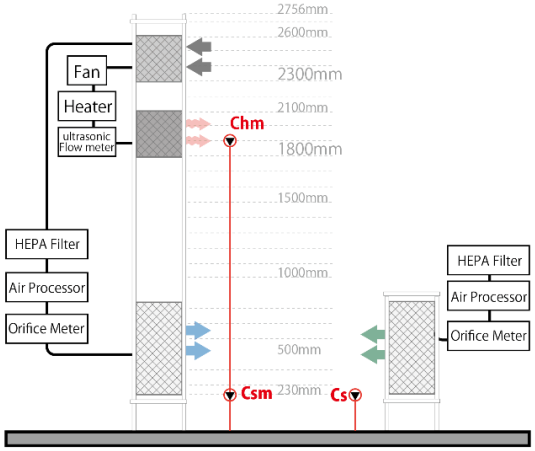

b. Ventilation system measurement points

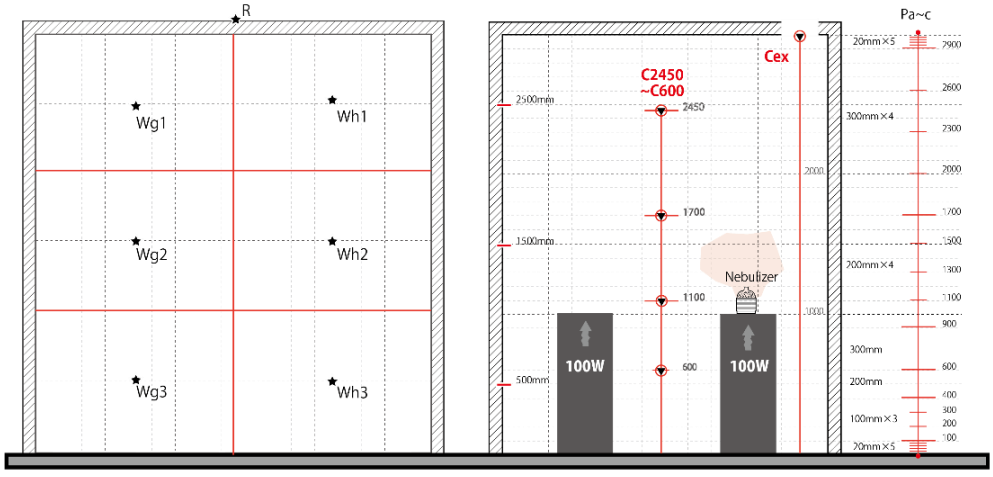

c.

c. Room sections with measurement points

Figure 3.4 Experiment room, measurement points, and system

3.3.1. Experiment Setup and Conditions

PDV unit

Due to limitations in the capabilities and equipment, the PDV unit was not built as an intact one unit as designed, but broken down into its basic components as illustrated in Figure 3.5 and shown in Figure 3.6a. All equipment was placed outside the room, only the diffusers, suction port, and hot-air inlet were placed inside the room.

The PDV unit components were fixed into a 2.7 m high metal frame. The suction port is 0.3 m size cube intaking air from three sides, top and bottom sides are solid while the remaining face is where the ducts were connected. The suction port is connected by 12.5 cm wide ducts to two paths; cooling and heating. The cooling and filtration function was achieved using air processor (AP-750M-C, ORION Machinery Co., Ltd.) connected to HEPA filter. Chilled filtered air flow through the inlet duct was connected to a fabric duct to act as a circular diffuser, 0.6 m high and 0.3 m in diameter. A similar arrangement was used for the room's DV system. As for the heating function, duct fan (FY-23DZ4, Panasonic) and duct heater (DM-11N, Nippon Heater Co., Ltd.) were used. The heated air flows through a 0.3 m× 0.3 m cylindrical fabric duct. The supply air flow from both DV and PDV unit are controlled by IRIS dampers and monitored by low differential pressure transducer (DP-45, Validyne Engineering). The hot-air flow was monitored by ultrasonic flow meter (TRZ150D-C, Aichi Tokei Denki) connected to current data logger (RTR-505, T&D Co., Ltd.). All ducts of the system were glass fiber insulated, and the openings in the walls were tightly sealed.

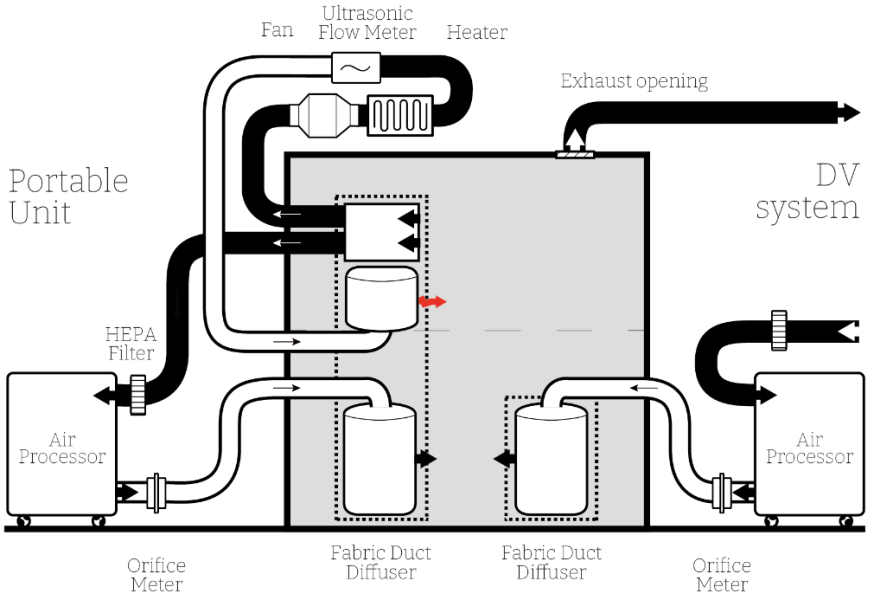

Figure 3.5 Experiment ventilation system design

a. PDV unit and DV diffuser

b. Person simulator

c. Particle emission by warmed plastic bottle covered nebulizer

Figure 3.6 Experiment room equipment

Person simulator

Representing seated occupants as heat source, two cylindrical heat simulators were operated at 100 W each, controlled by voltage regulators and monitored by watt meters. The heat simulators are 1.00 m high and of a diameter of 0.40 m. They were placed over an insulative-5 cm-foam disc in locations indicated in Figure 3.6b.

Temperature measurement

Temperature was measured using T-type thermal couple wires connected to CADAC-3 data logger (Eto Electric Co.). The measurement points are indicated in Figure 3.4a and Figure 3.4c. For surface temperature, Wa1~Wh3 stand for walls inner surface points, Wo1~4 stand for the outer surface points, and R stands for the roof surface point. To measure the vertical temperature distribution in the experiment room, 22 points at each pole, Pa-c were measured. The floor and ceiling surface temperature was measured at the same poles. The surface temperature of one heat simulator was measured as well. In addition, the air temperature of the PDV unit's supply diffuser, hot air diffuser, and suction port were measured as well as the DV supply and the exhaust temperatures. The temperature outside the room, inside the experiment building, was monitored at point To.

Particle counter

The contaminant simulated in this experiment was cough droplets. Given that the density of natural saliva varies between 1.0 – 1.1 g/mL [21], artificial saliva was prepared with 12 g salt (NaCl) and 76 g glycerin for

1 litre of distilled water to have a density of 1.088 g/mL. The droplets were produced by nebulizer (NE-C801, OMRON Healthcare, Inc.) and the emission rate was controlled by setting the gas flow to 2 NL/min. N_2 gas was chosen as its density is slightly less than that of air. In order to have a distributed emission, rather than a stream of droplets, the nebulizer was covered by a plastic bottle that has holes of 0.5 mm diameter in its upper part. The bottle was heated by a bottle warmer (12.3 W) wrapped around it in order to prevent condensation and to raise the temperature of the droplet emission as shown in Figure 3.6c.

The droplets were measured using handheld particle counters (RION and Kanomax) fixed at Pd at heights 900 mm (C900), 1100 mm (C1100), and 1700 mm (C1700). In addition to 2450 mm (C2450) which matches the suction port height. Measurements of the exhaust opening (Cex) were taken as well. In addition, to confirm the supply air filters, particles count at both supply diffusers (Cs, Csm) and hot-air supply (Chm) was monitored.

3.3.1.1. Cases and parameters

The parameters investigated in this study were: 1) Exhaust location, 2) DV flow rate, 3) PDV unit flow rate. Regarding the exhaust location, placing the exhaust outlet over the PDV unit was compared to having the opening on the opposite side of the room. The supply flowrate of both DV and PDV unit was tried with three variations 200 m^3/h, which is the recommended 100 m^3/h /person, and one lower and one higher flowrate, 100 m^3/h and 300 m^3/h. The hot air flowrate was set constant to 200 m^3/h regardless of the supply flowrate.

A total of 12 cases carried out are summarized in Table 3-2. The cases can be divided into 5 groups according to the comparative parameter. Group-1 shows the effect of changing the DV supply flowrate in the DV-only cases and the DV-PDV unit combination cases. Group-2 is a comparison between different PDV unit supply flowrate at a constant DV supply of both 200 m^3/h and 300 m^3/h. Viewing the PDV unit as a complementary ventilation system, Group-3 compares all cases with a total supply flow rate of 200 m^3/h as well as 300 m^3/h. Group-4 is set to evaluate the effect of changing the exhaust location, Ex1 or Ex2.

It should be noted that despite the fact that 300m^3/h can be seen has relatively high flow rate, it has been recommended by recent research work to increase the air change rate in an effort to achieve a better indoor quality and reduce the cross-infection risk [9,22].

As shown in Table 3-2, the case naming includes the system running, DV for the displacement ventilation supply, and PU is used as a shorted abbreviation for the PDV unit. Each system abbreviation is followed by the supply flowrate value. Finally, the exhaust opening number, either Ex1 or Ex2 is written.

Table 3-2 Summary of cases' parameters

Exhaust location	Flow rate (m^3/h) q_{sm}	q_s	Case no.	Case name
Ex1: Far	0	200	1	DV200_Ex1
	0	300	2	DV300_Ex1
	100	200	3	DV200_PU100_ Ex1
	200	200	4	DV200_PU200_ Ex1
	300	200	5	DV200_PU300_ Ex1
	200	100	6	DV100_PU200_ Ex1
	100	100	7	DV100_PU100_ Ex1
	300	300	8	DV300_PU300_ Ex1
	200	0	9	PU200_Ex1
Ex2: Near	200	0	10	PU200_Ex2
	300	300	11	DV300_PU300_ Ex2
	200	200	12	DV200_PU200_ Ex2

3.3.1.2. Measurement

Readings were taken at a one-minute interval. The timeline of the measurement is illustrated in Figure 3.7. The ventilation system was switched on and the temperature readings were monitored until steady state was reached, which took about 2.5 hours. Afterwards, the particles emission was run for two rounds because the particle counter devices were not enough to cover the measurement points in one round. The count at Cex, Cs, Csm, and Chm were monitored non-stop all through the experiment. The count at the pole Pd, on the other hand, were measured two points per round the nebulizer was turned two rounds because on for one hour. After stopping the emission, the particles count at the exhaust was monitored until it decreased back to the background count. Finally, the ventilation system was switched off. A sample of 30 minutes in which both temperature and particles distribution were at steady state was taken for data analysis.

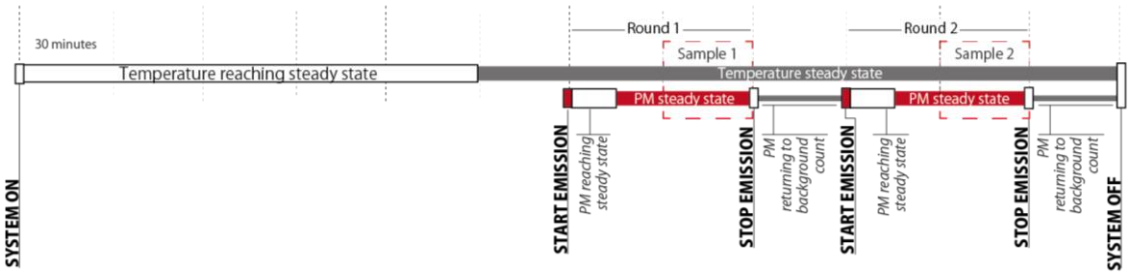

Figure 3.7 Experiment timeline

In this section, the experimental data is analyzed for both temperature and particle distribution. First, the temporal readings of one sample case is reviewed. Secondly, the detailed cases comparison is discussed. In addition to the heating and cooling capacity of the PDV unit.

A sample of the temperature readings through the experiment measurement time is analyzed. Figure 3.8 shows the temperature at different heights, on the ceiling and floors surfaces, and at the supply and exhaust ports. Having been carried out in winter, when operating the system at 6 ℃ the temperature increases compared to the room temperature cooled through the night. From Figure 3.8, the temperatures are seen to reach steady state after about 2.5 hours of turning the system on. The sample data taking for analysis from this case was 12:30~13:00 for round-1 and 14:30~15:00 for round-2 at which the temperature had minimal fluctuations thus the sample can be considered representative to the steady state.

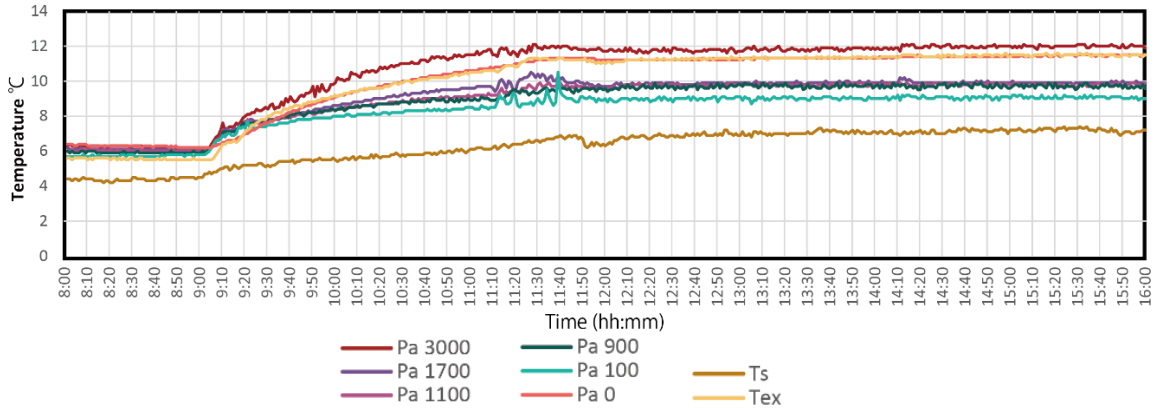

Figure 3.8 Sample of temperature readings for case DV100_PU200_Ex1

The particle count over the whole measurement period for one sample case is hereafter discussed followed by a detailed comparison between the cases. First, for the particle count timeline, the case DV100_PU200_Ex1 was chosen as a sample case. Figure 3.9. a~d shows the particles count per size on the experiment timeline. The graphs have two vertical axes showing particle count since the count at exhaust, hot-air supply, and top two heights, 1700 mm and 2450 mm, is much higher than that at supply ports and lower heights. Thus, Cex, Chm, C2450, and C1700 are plotted on the left axis while the Csm, Cs, C1100, and C900 follow the right-side one.

In the case at hand, the emission for round-1 was from 12:30 to 13:30, and round-2, from 14:30 to 15:30. In round-1, C1100 and C900 were measure while in round-2, C2450 and C1700. The count at all openings is relatively steady with a general trend of slight decrease. It can also be observed that the round-2 has an overall lower count than round-1. The difference in particles distribution by size can be seen by comparing the graphs a~d. For smaller particles, the exhaust has the highest count, however, the larger the particles get, the lower their count at the exhaust becomes. At the larger particles size, the count at Pd, (C900~C2450), particularly C1700, and C2450 become higher than Cex and Chm. This observation can be explained by the fact that larger particles tend to evaporate or settle on the surfaces. As for the count at the supply diffusers, only the smallest particles seem to be able to pass the HEPA filter (0.3 um ~ 0.5 um), however, the highest count is around 10,000 which can be seen as negligible.

In the following sections, the results of the particle count and volume for all cases are displayed. The graphs have the readings from Pd plotted along with the exhaust point. The hot air supply port readings are

plotted as an isolated point at the height of 1900 mm in all PDV unit cases. Measurements of the DV and PDV unit diffusers were used as control values and since they were of negligible values, they were not plotted in the cases graphs. For each case, the total volume of particles, total count, and count by particle diameters are plotted separately in the respective figure.

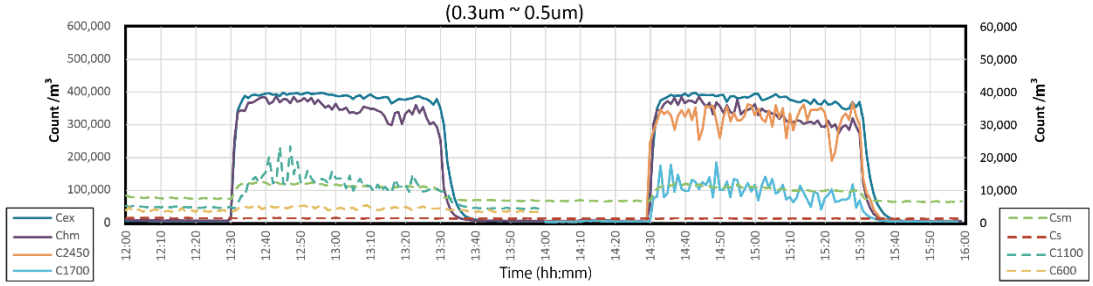

a. 0.3 um ~ 0.5 um

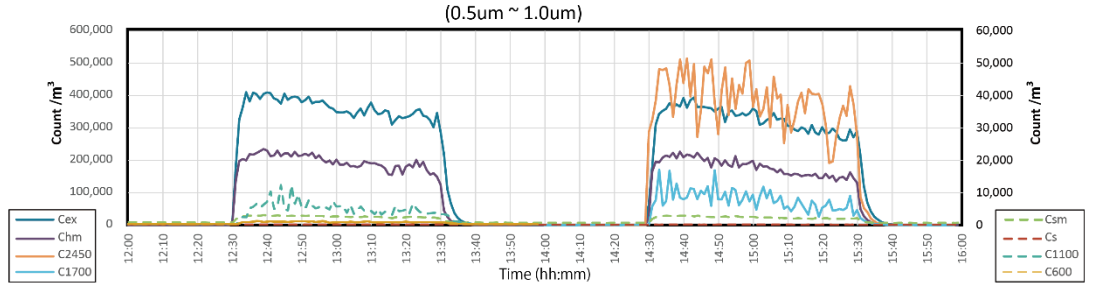

b. 0.5 um ~ 1.0 um

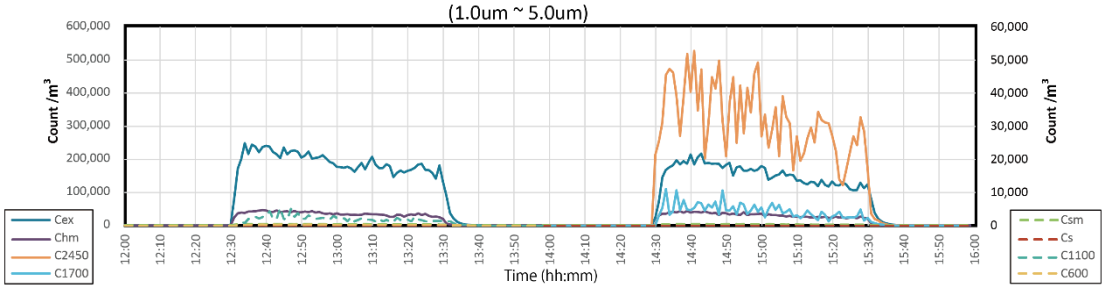

c. 1.0 um ~ 5.0 um

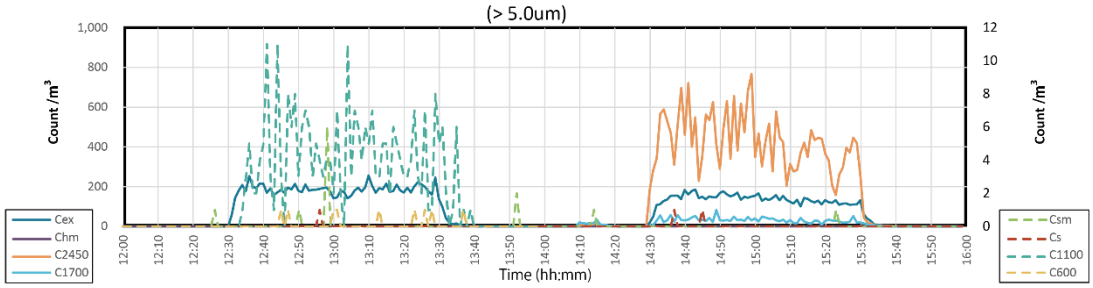

d. > 5.0 um

Figure 3.9 Particle count by size vs time for case DV100_PU200_Ex1

3.3.2. Measurement of particle size frequency distribution

Before carrying out the main experiment, further measurements were required to know the size distribution of the droplet emission by the system described earlier. To get accurate measurements of the particles' diameter and count, Particle Dynamics Analyzer (PDA) (Dantec Dynamics) was used. Measurements of one hole of the plastic bottle were taken at 1 cm distance. Readings for three 30 seconds intervals were recorded. The PDA components, i.e. Diode-Laser unit and Fiber PDA receiver probe were set as shown in Figure 3.10 and connected to the Burst Spectrum Analyzer processor unit (BSA) out of which the readings were acquired. The particles were grouped into fixed diameter intervals as shown in Figure 3.11. The frequency distribution shows that the larger particles 5.0um and larger take up around 40% of the emission followed by the 2.0~5.0 um. The smaller particles, on the other hand, range from around 10% to 15 % each. Compared to size distribution measured in a real human expiratory droplet investigation system, the peak is slightly higher [90]

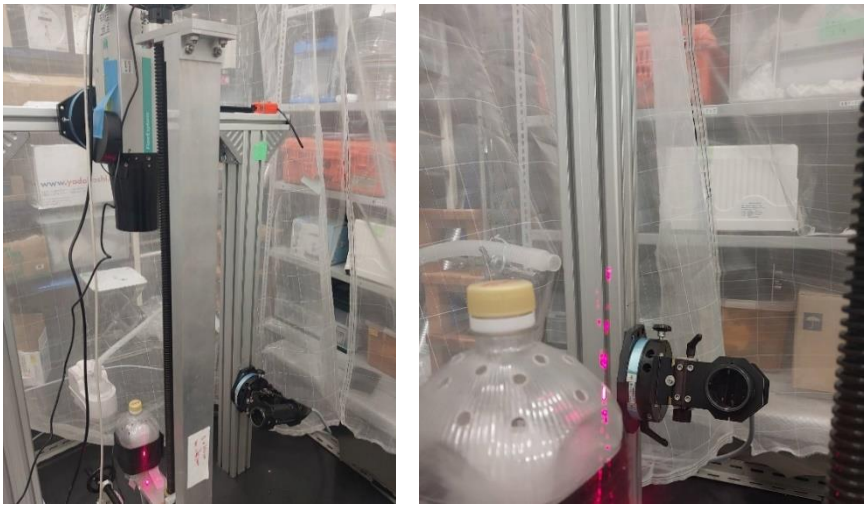

Figure 3.10 Settings of the particle size distribution measurement using PDA

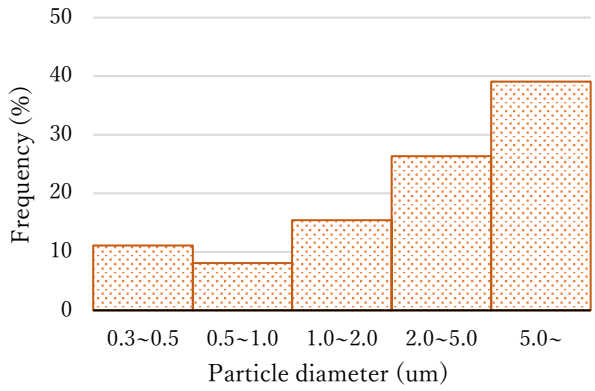

Figure 3.11 Particle size distribution frequency

3.3.3. Effect of Changing DV supply flow rate

In this section the effect of the DV system's supply flow rate is examined. A comparison of varying DV flowrates was carried out for both DV only cases and DV-PDV unit combination cases. In the combination cases' group, the PDV unit's flowrate was set constant to 200 m^3/h. The two cases of both groups are summarized in Table 3-3.

Table 3-3 Summary of cases' grouping

Group 1: q_s		
Group 1: q_s - DV		
DV200_Ex1	DV300_Ex1	
Group 1: q_s - PU+DV		
DV200_PU200_ Ex1	DV100_PU200_ Ex1	PU200_Ex1

3.3.3.1. Results and Discussions

The temperature vertical distribution of the DV only cases are shown in Figure 3.12a. The effect of increasing the supply flowrate can be seen as negligible. It can be deduced that the room's small size might be the reason behind the minimal effect. The exhaust temperature was not affected much as can be seen from Figure 3.12. Since the room volume is about 20 m^3, the 200 m^3/h means 10 ACH which made increasing it to 15 ACH with only two heat sources are present did not increase the ventilation efficiency. Similarly, in Figure 3.12b, decreasing the DV supply flowrate from 200 m^3/h to 100 m^3/h did not cause a major shift in the temperature curve. However, since these cases had the PDV unit in operation, it can be assumed that the PDV unit mitigated the decrease effect. Turning the DV off on the other hand, caused an increase in temperature ranging from 1 to 2°C depending on height.

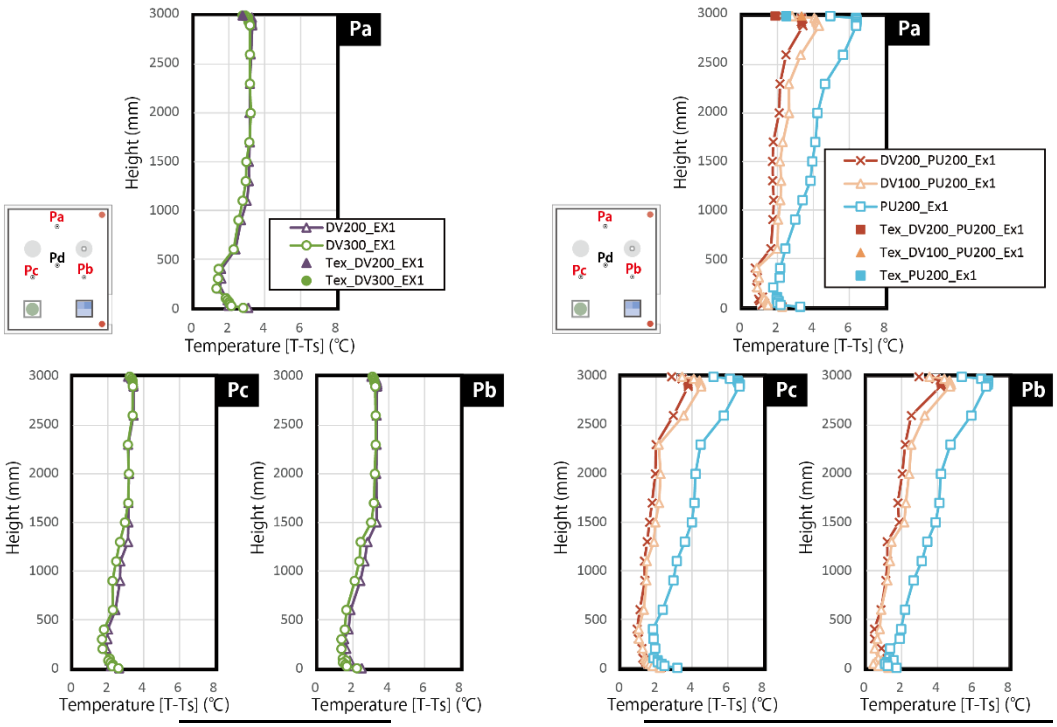

	DV200_ Ex1	DV300_ Ex1
T_{ex}	*2.77*	*2.77*

a. In DV only cases

	PU200_ DV200_Ex1	PU200_ DV100_Ex1	PU200_ Ex1
T_{ex}	*1.88*	*3.35*	*2.49*

b. In PDV unit + DV cases

Figure 3.12 Temperature vertical distribution of Group-1: Varied DV supply flowrate

Regarding the PM distribution, for the DV-only cases, despite showing no effect on the temperature distribution, increasing the DV flowrate to 300 m^3/h has notably increased the particle count at 2450 mm height, Figure 3.13a. However, looking at the total volume distribution, this increase shows to be not that significant but it can be an indication of turbulence causing particles to disperse instead of flowing upwards. In addition, the count at lower heights was slightly decreased. Secondly, the combination cases, Figure 3.13b, decreasing the DV flowrate had the foreseen effect of increasing the particle count and volume. The increase was not confined to the higher heights but extended to the 1700 mm height. Lower heights had almost no particles even with the DV turned off. Regarding the particles at the hot air supply port, the total volume in all cases is small which can be explained by the fact that the count is only high at the 0.3μm-0.5μm and 0.5μm-1.0μm categories.

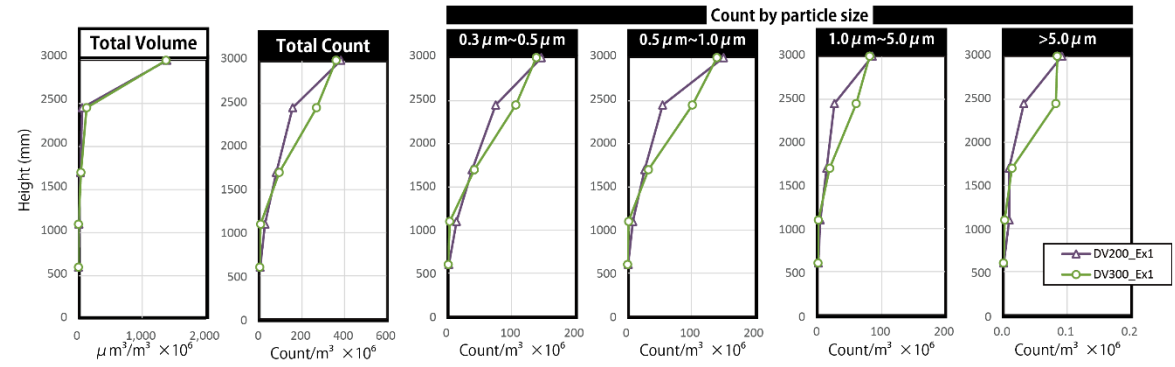

a. In DV only cases

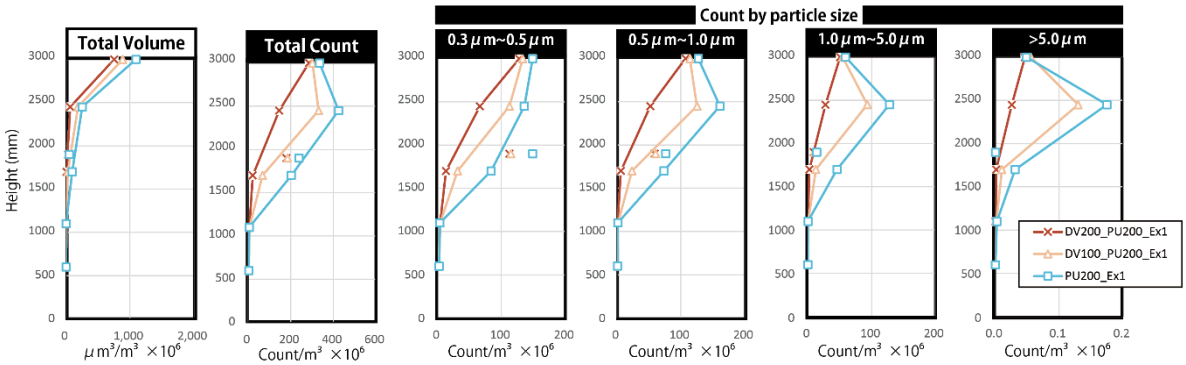

b. In PDV unit + DV cases

Figure 3.13 Particles vertical distribution of Group-1: Varied DV supply flowrate

3.3.4. Effect of Changing PDV unit's supply flow rate

The effect of changing the PDV unit's supply flowrate at constant DV supply is investigated. Hot air supply as well was set at a constant value. Table 3-4 is a summary of the cases used in this comparison.

Table 3-4 Summary of varient supply flow rate cases

Group 2: q_{sm}			
Group 2: q_{sm} - q_s200			
DV200_Ex1	DV200_PU100_ Ex1	DV200_PU200_ Ex1	DV200_PU300_ Ex1
Group 2: q_{sm} - q_s300			
DV300_Ex1	DV300_PU300_ Ex1		

3.3.4.1. Results and Discussions

To investigate the effect of operating the PDV unit in the room, cases of varying PDV unit supply flowrate 0 ~ 300 m^3/h at constant DV flowrate are compared in Figure 3.14 Comparing the DV-200 cases, Figure 3.14a, it can be observed that cases with PDV unit have a different vertical distribution. In the lower part of the room, the temperature has decreased while the top part, over 2300 mm, a significant raise in temperature is seen. Since the hot-air flowrate was set constant to 200 m^3/h in all cases, the PU_100 was the only case to have a larger exhaust temperature, and to have a exceeded the upper part temperature of the DV-only case. The larger PDV unit flowrate is the lower the overall temperature and especially the upper temperature peak becomes.

Regarding the DV-300 cases, Figure 3.14b, only two cases are compared, PDV unit 0 and 300 m^3/h. While in the DV-200 cases the horizonal distribution was almost uniform, the DV-300 case showed Pb, the pole nearer to the PDV unit, to have a stronger gradient than the other measurement poles.

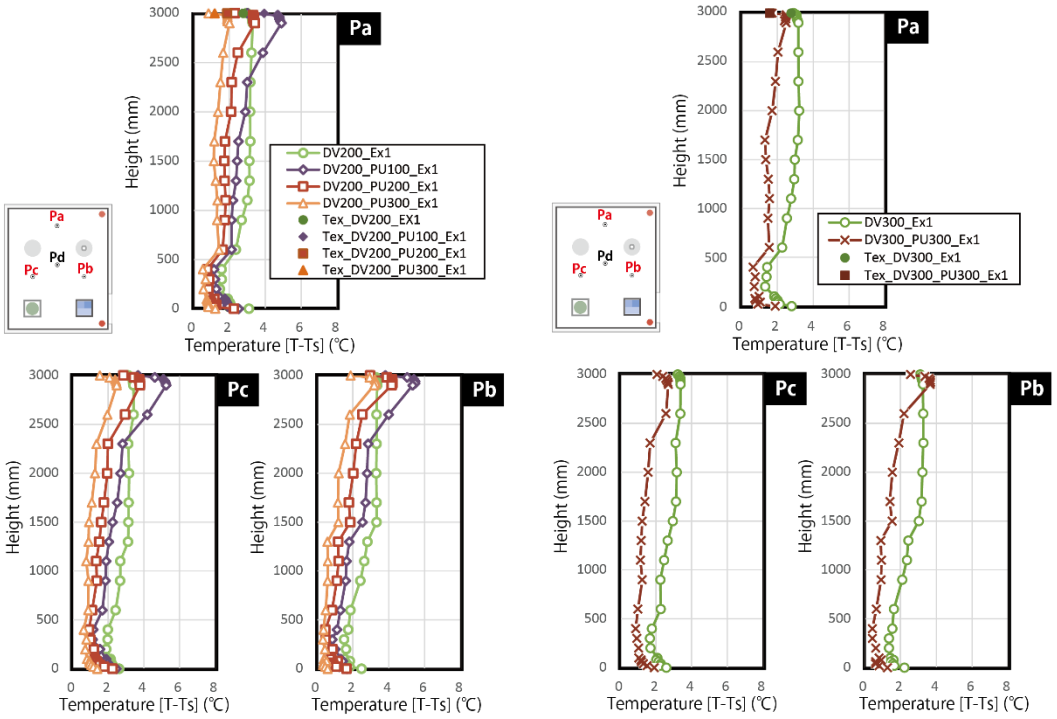

	DV200_ Ex1	DV200_ PU100_Ex1	DV200_ PU200_ Ex1	DV200_ PU300_Ex1
T_{ex}	2.77	3.94	1.88	1.18

a. 200 m^3/h DV supply cases

	DV300_ Ex1	DV300_ PU300_Ex1
T_{ex}	2.77	1.59

b. 300 m^3/h DV supply cases

Figure 3.14 Temperature vertical distribution of Group-2: Varied PDV unit supply flowrate

Regarding the PM distribution, for the DV200 cases, increasing the PDV unit supply flowrate caused an almost linear decrease in temperature. As for particles distribution, Figure 3.15, although increasing the unit's flowrate from 100-200 m^3/h caused a matching reduction of the particle count, two more observations can be noted. First, comparing the no-PDV unit case to the 100 m^3/h case shows that turning on the unit causes a surge in the upper zone particle count, however, in terms of volume, not much effect was found. As for the hot air supply, C_{hm}, as mentioned above the size distribution peaks at the 0.3µm-0.5µm diameter category. However, one observation that applies for all cases but is especially clear in this figure is that C_{hm} is higher than the vertical distribution curve interpolation at their height. Since the hot air is originally taken in from the higher suction port, it can be seen that the larger particles have evaporated resulting in a decrease in the larger particles count and a steep increase in the smaller ones.

Secondly, further increasing the flowrate from 200 m^3/h to 300 m^3/h breaks the inverse relation between flowrate and particle count as it caused particles especially the bigger sizes to increase at the height 2450 mm. Comparing with and without PDV unit in the DV300 case, operating the PDV unit reduced the particles count and volume following the temperature distribution. A general observation for both DV200 and DV300 cases

is that operating the PDV unit reduces the exhaust particle count, especially the larger particle sizes, and volume.

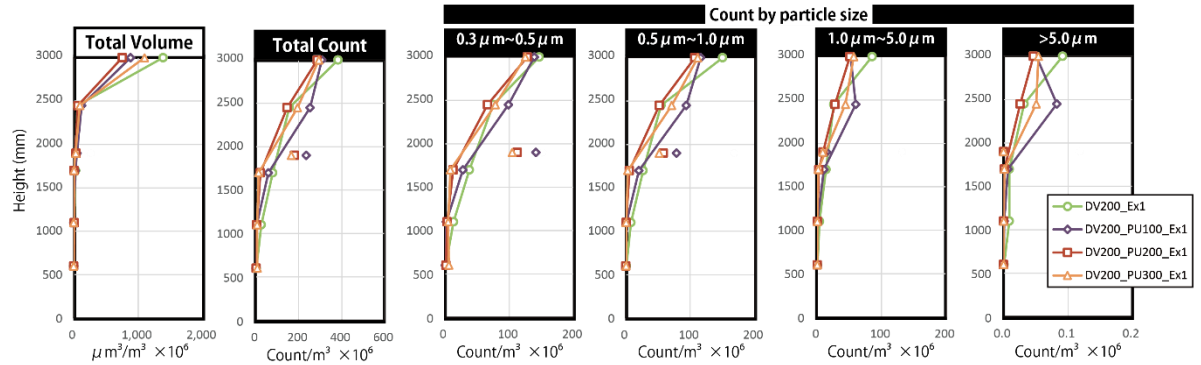

a. 200 m³/h DV supply cases

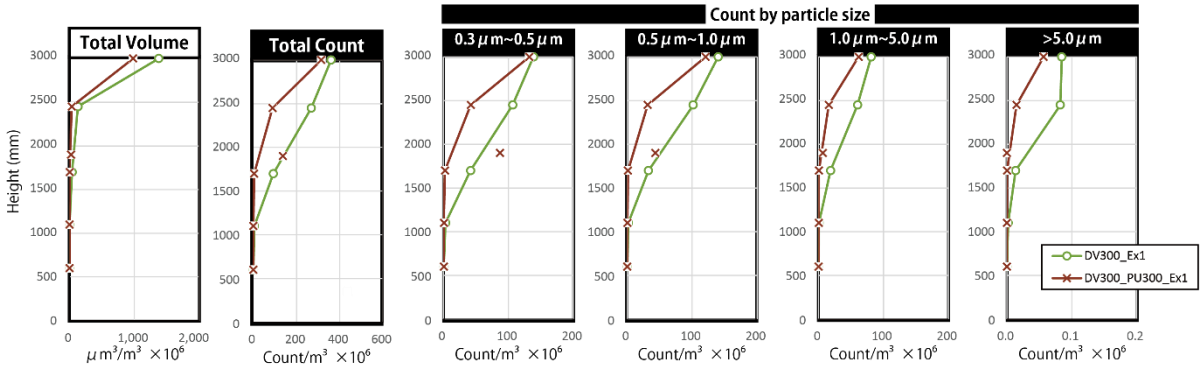

b. 300 m³/h DV supply cases

Figure 3.15 Particles vertical distribution of Group-2: Varied PDV unit supply flowrate

3.3.5. Effect of Changing Total flow rate

Cases of fixed total supply flowrate are compared in this section viewing the PDV unit as a complementary system. This comparison was carried out to test the unit's performance as a replacement system despite the fact that it does not affect the room's total inflow rate. Table 3-5 enlists the cases used in this investigation.

Table 3-5 Summary of varient Total flow rate cases

Group 3: q_s+q_{sm}		
Group 3: q_{total} 200		
DV200_Ex1	DV100_PU100_ Ex1	PU200_Ex1
Group 3: q_{total} 300		
DV300_Ex1	DV200_PU100_ Ex1	DV100_PU200_ Ex1

3.3.5.1. Results and Discussions

Cases of fixed total supply flowrate are compared in this section viewing the PDV unit as a complementary system. This comparison was carried out to test the unit's performance as a replacement system despite the fact that it does not affect the room's total inflow rate. Figure 3.16a shows the cases of q_{total}-200. At all measurement poles, the DV200 case displayed the lowest temperature in the upper zone. The PU200 case and DV100_PU100 case showed very close results, slightly lower temperature below 900mm and an increase in the upper part temperature that reaches 4℃. However, the exhaust temperature was only higher in the DV100_PU100 case. This high increase in temperature might be caused by the drop in the room inflow/outflow rate. With two occupants in the room, an inflow rate below 200m^3/h can be seen as not enough Therefore, the q_{total}-300 cases might be a better representative of the PDV unit capability to partially replace the DV system.

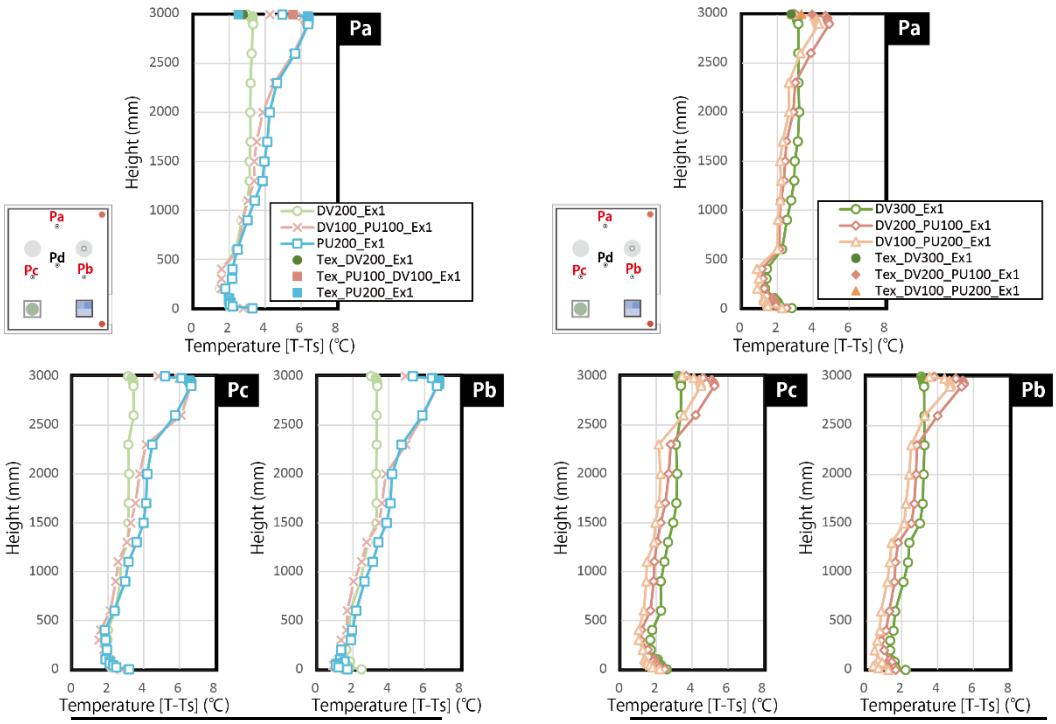

	DV200_ Ex1	DV100_ PU100_Ex1	PU200_ Ex1
T_{ex}	2.77	5.54	2.49

a. Total supply flowrate: 200 m^3/h

	DV300_ Ex1	DV200_ PU100_Ex1	DV100_ PU200_Ex1
T_{ex}	2.77	3.94	3.35

b. Total supply flowrate: 300 m^3/h

Figure 3.16 Temperature vertical distribution of Group-3: Varied total supply flowrate

Secondly, the PM distribution results are to be reviewed. Agreeing with the temperature profiles, the effect of compensating the reduction in DV flowrate by the PDV flowrate was dependent on the total flowrate value. As shown in Figure 3.17, reducing DV flowrate at the q_{total}=200 m^3/h causes an increase in the top zone particle count and volume. However, the reduction in the q_{total}=300m^3/h cases showed a reduction in the particles count at all heights in the DV200_PU100 case. This can be an indication of the limit of the PDV unit to act as a complementary ventilation system.

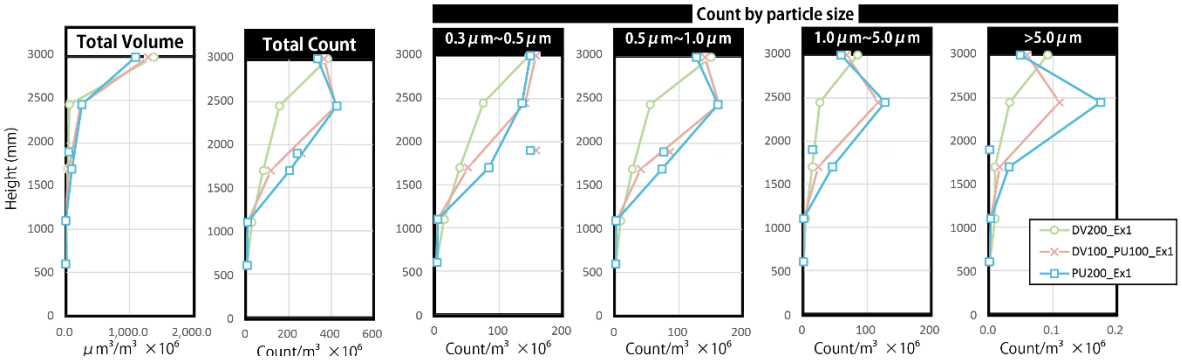

a. 200 m³/h

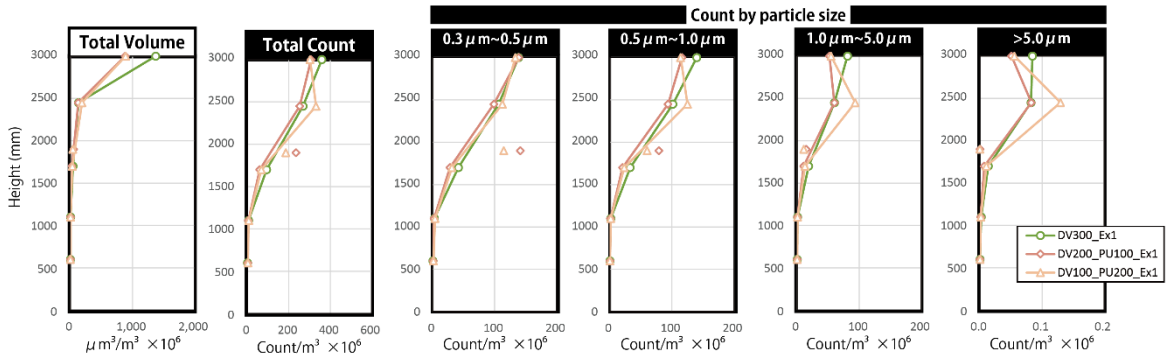

b. 300 m³/h

Figure 3.17 Particles vertical distribution Group-3: Varied total supply flowrate

3.3.6. Effect of Changing Exhaust location with respect to PDV unit

The effect of changing the exhaust location, Ex1: far and Ex2: near, with respect to the PDV unit. The cases are enlisted in Table 3-6.

Table 3-6 Summary of varient Exhaust location cases

Group 4: Ex			
Group 4: Ex-PU+DV			
DV300_PU300_ Ex1	DV300_PU300_ Ex2	DV200_PU200_ Ex1	DV200_PU200_Ex2

3.3.6.1. Results and Discussions

Observing the temperature profiles in Figure 3.18, it can be concluded that the exhaust location as almost no effect on the temperature distribution in both cases DV200_PU200 and DV300_PU300. However, in the high flowrate case, DV300_PU300, a limited increase in the upper zone temperature can be seen especially in Pb, the pole closest to the PDV unit. In both comparisons, the nearer exhaust cases, Ex2, had a higher exhaust temperature as shown in Figure 3.18

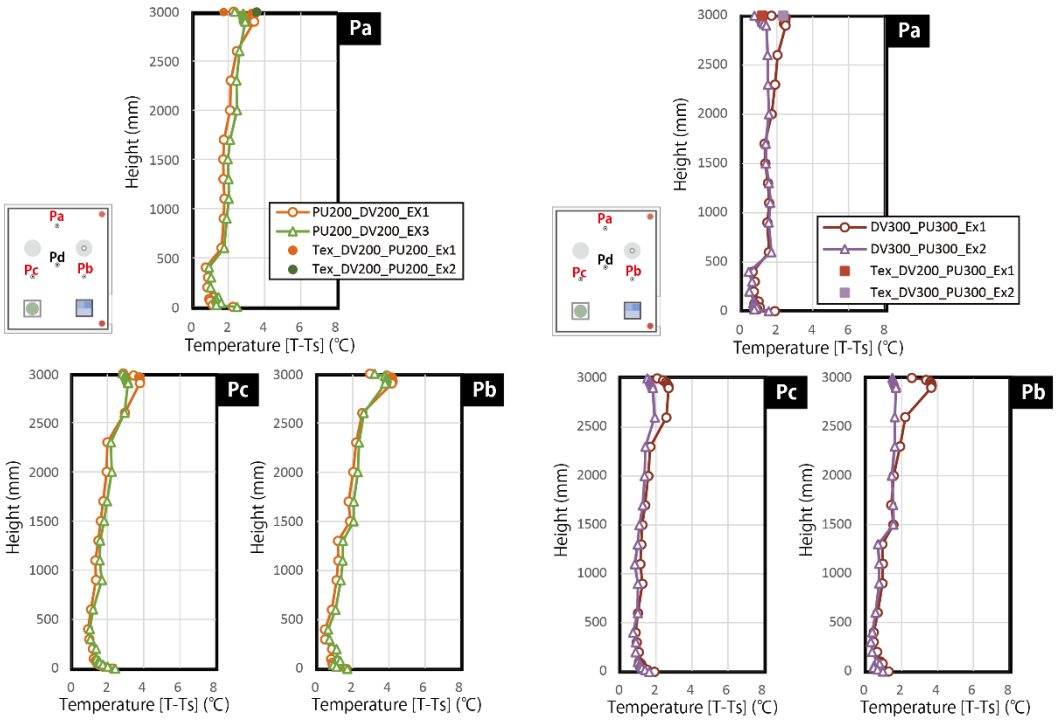

	DV200_ PU200_Ex1	DV200_ PU200_Ex2
T_{ex}	1.88	3.60

a. In PDV unit only cases

	DV300_ PU300_Ex1	DV300_ PU300_Ex2
T_{ex}	1.59	2.36

b. In DV+ PDV unit cases

Figure 3.18 Temperature vertical distribution of Group-4: Varied exhaust location

Figure 3.19 shows the PM distribution plots for all cases. Regarding the effect of changing the exhaust location with respect to the PDV unit, for temperature, negligible change was seen. As for the particles' distribution, as shown in Figure 3.19, it can be seen that it depends mainly on the flowrate. For the smaller flowrates DV200_PU200, the effect was minimal. However, for the 300 m^3/h cases, having the near exhaust caused the count to increase significantly at the top zone although the exhaust count and lower zone count was not affected. This observation might as well be caused by turbulence caused by opposing flows, flowing out of the PDV unit and towards it to be exhausted in Ex2 positioned just above the unit.

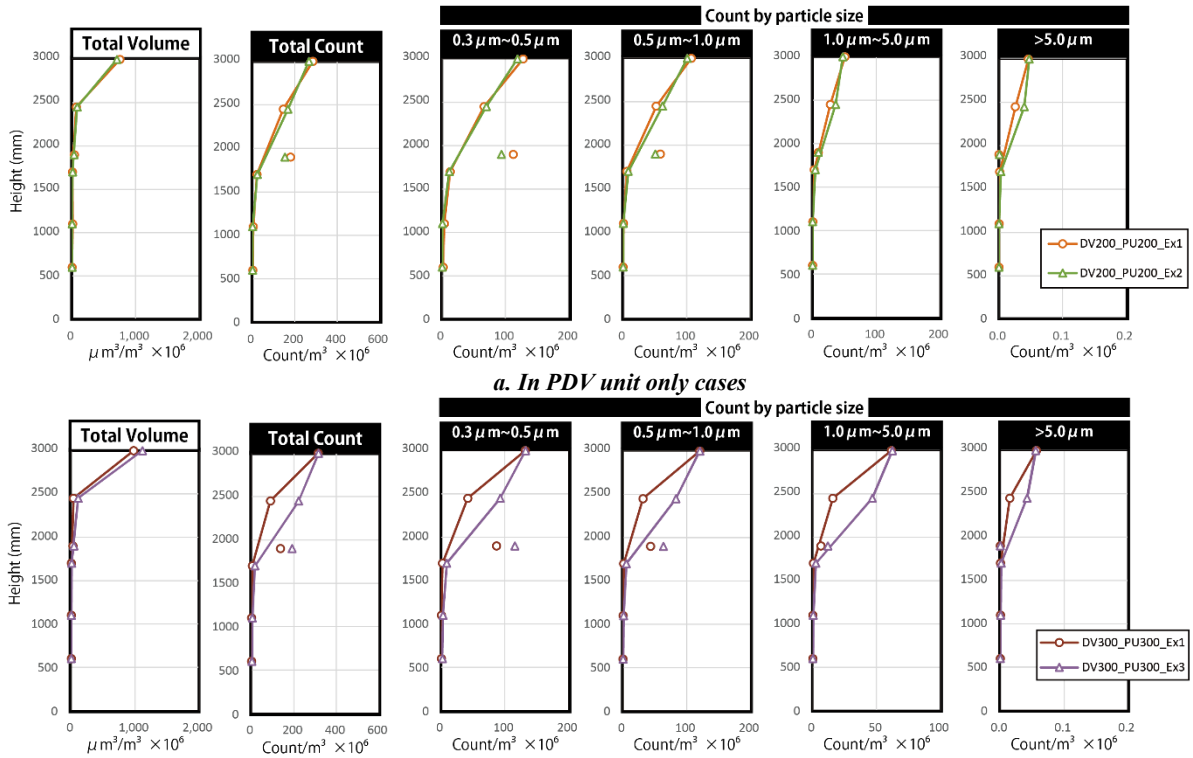

a. In PDV unit only cases

b. In DV+ PDV unit cases

Figure 3.19 Particles vertical distribution of Group-4: Varied exhaust location

3.3.7. Heat Balance Calculation

Since the PDV unit operated using separate systems, the heating and cooling capacities at each case were calculated using equations (3-5) and (3-6).

$$Q_{sm} = Cp\rho q_{sm}(T_u - T_{sm}) = 0 \qquad (3\text{-}5)$$

$$Q_{hm} = Cp\rho q_{hm}(T_{hm} - T_u) = 0 \qquad (3\text{-}6)$$

where Q_{sm} is the cooling capacity and Q_{hm} is the heating capacity of the PDV unit.

3.3.7.1. Results and Discussions

The temperature readings used in this calculation are summed up in in Table 3-7 and the calculation results are shown in Table 3-8. The calculation shows that despite setting the heater's power to 450W and monitoring it using the watt meter, the actual heat gain was not constant in all cases. Most of the cases had a lower heating capacity. Reviewing the temperature readings in Table 3-7, although the supply temperature was calculated to be lower than the outdoor temperature, it can be noticed that the outside temperature To was below the supply air temperature. The low To temperature can be the result of the experiments building envelope's thermal capacity. The colder To means that given the long ducts connections, that include the uninsulated ultrasonic anemometer, heat seems to have been lost before arriving at the hot air supply port.

Table 3-7 Temperature readings with respect to DV supply temperature (T - Ts)

			T_o	T_s	T_{sm}	T_{hm}	T_u	T_{ex}	T_{Hs}	q_s	q_{sm}	q_{hm}
Ex1	DV only	DV200_ Ex1	-1.05	**0**	-	-	2.89	**2.77**	9.66	198	0	0
		DV300_ Ex1	0.34	**0**	-	-	2.89	**2.77**	9.3	309	0	0
		DV200_PU100_Ex1	-1.08	**0**	-0.21	12.19	6.03	**3.94**	9.37	194	104	200
		DV200_PU200_Ex1	-3.37	**0**	-0.46	10.3	5.4	**1.88**	8.95	193	193	201
		DV200_PU300_Ex1	-1.97	**0**	-0.54	10.07	3.9	**1.18**	8.35	189	288	197
		DV100_PU200_Ex1	-0.76	**0**	-0.56	11.05	4.15	**3.35**	9.13	119	200	196
		DV100_PU100_Ex1	-1.43	**0**	-0.35	12.83	6.62	**5.54**	9.38	108	98	201
		DV300_PU300_Ex1	-1.54	**0**	-0.49	9.91	3.19	**1.59**	8.84	299	282	198
	PU only	PU200_ Ex1	2.02	-	**0**	13.36	7.63	**2.49**	9.86	0	199	201
Ex2		DV300_PU300_Ex2	-2.32	**0**	-0.7	9.5	3.27	**2.36**	8.35	292	284	196
		DV200_PU200_Ex2	0.35	**0**	-0.28	10.91	4.94	**3.6**	9.23	188	198	199

Table 3-8 PDV unit cooling and heating capacity

					Q_{sm}	Q_{hm}
	DV only	DV200_		Ex1	-	-
		DV300_		Ex1	-	-
	Far Exhaust	DV200_	PU100_	Ex1	217	411
		DV200_	PU200_	Ex1	379	329
		DV200_	PU300_	Ex1	428	407
		DV100_	PU200_	Ex1	316	454
		DV100_	PU100_	Ex1	228	417
		DV300_	PU300_	Ex1	348	445
	PU only		PU200_	Ex1	507	385
Near Exhaust		DV300_	PU300_	Ex2	377	410
		DV200_	PU200_	Ex2	345	397

3.4. CFD Validation

3.4.1. CFD Modeling Method

As a first step, CFD validation for the thermal performance of the PDV unit was carried out. One experiment case was chosen for this analysis, DV200_PU200_Ex1. The room was modelled in Stream software as shown in Figure 3.20. The analysis model included the person simulators, DV diffuser, and PDV unit components. The connecting ducts were modeled as well since there relatively big size can affect the air flow in the room. Another reason for modelling the ducts is to test their thermal effect on the surrounding air. The experiment room materials and field measurement readings were input as fixed conditions including all supply temperatures, flowrates, surface temperatures, and heat generation power. Analysis conditions and boundary conditions are summarized in Table 3-9 and Table 3-10.

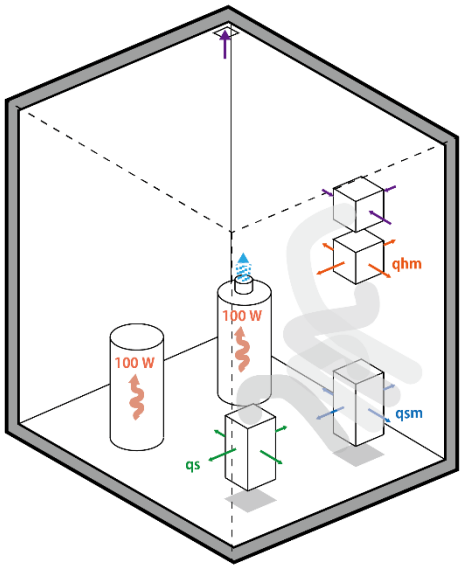

Figure 3.20 Experiment room CFD model

Table 3-9 Analysis conditions

Analysis software	Stream v.22
Turbulence model	RNG k-ε model
Analysis type	Steady state
Calculations	Heat, radiation, and diffusion
Mesh settings	
Default size	20 mm
Growth rate	1.15
Cells count	~ 1M

Table 3-10 Boundary conditions

Thermal Boundaries	
Heat transfer condition	
Solid- Fluid	Case-1: log law transfer
	Case-2: Coefficient of heat
External surfaces	Adiabatic
Internal surfaces	Fixed temperature
Construction	
Walls, floor, ceiling	Wooden board: λ=0.18W/(m.K)
Emissivity	0.9
Heat Generation	
Heat load	100 W /person simulator

3.4.2. Results and Discussion

The CFD results were evaluated by comparing the temperature vertical distribution at the three poles, Pa~c,, Figure 3.21 The wall surface temperatures were also plotted to compare the CFD results and experimental measurement as a check that the inputs are correctly processed. Three cases were analysis in which conditions were slightly changed in order to achieve best results. In case-1, the heat transfer from inner surfaces, i.e. walls, floor, and ceiling, was set to logarithmic law. Viewing the results in it can be seen that the air temperature was much lower than the actual measurements. The difference reached 2 ℃ at Pa.

Since the boundary surfaces temperature is higher than the air temperature, it was deduced that the heat transfer, especially from floor and ceiling, was not calculated correctly. Therefore, in Case-2, the floor and ceiling heat transfer condition was changed to coefficient of heat transfer of a relatively high value, 20 $W/m^2.K$. As shown in the temperature distribution have to come to match the experiment readings with small differences at the lower part of Pc and near the ceiling at Pa and Pc.

Finally, in Case-3, the simulation was carried out without the connecting ducts. This step was needed validate the simulation of the ductless PDV unit and thus make its placement in different spaces at different conditions possible. Minimal difference was found comparing cases 2 and 3. Hence, in the application section, the ductless model of the PDV unit will be used.

The temperature contours of Case-2 vs Case-3 are shown in Figure 3.22. Despite the fact that air currents in the room are affected by the presence of ducts, the difference in temperature distribution is minimal as heat exchange from the insulated ducts is negligible. One major observation can be made from the contours of both cases is that the hot air supply is short-circuiting to the suction port directly.

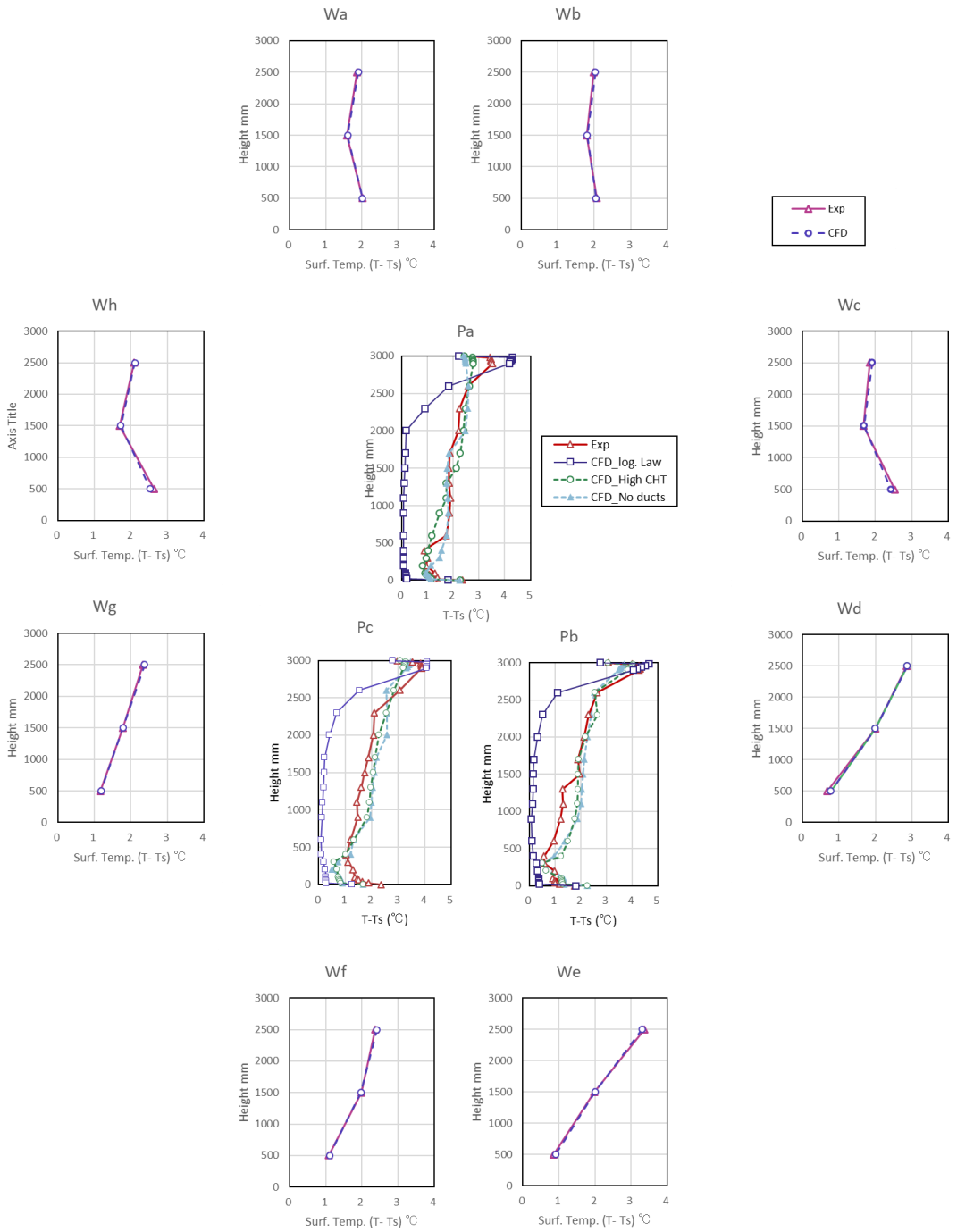

Figure 3.21 Temperature vertical disitribution experiment measurements vs CFD analysis results for Pa~c and Wa~h

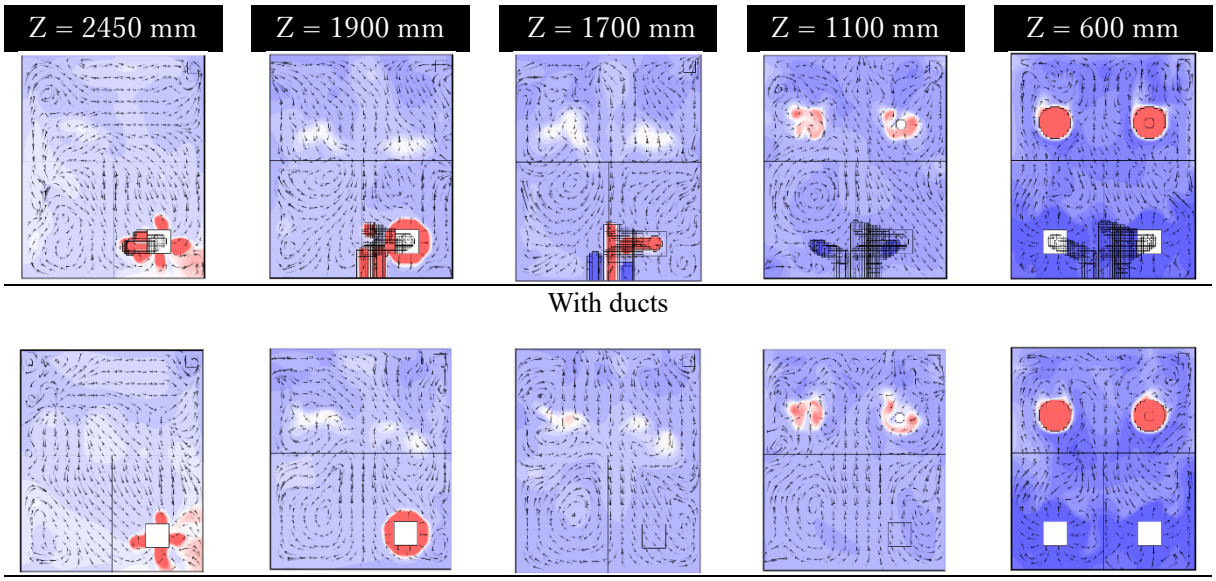

a. Plan view

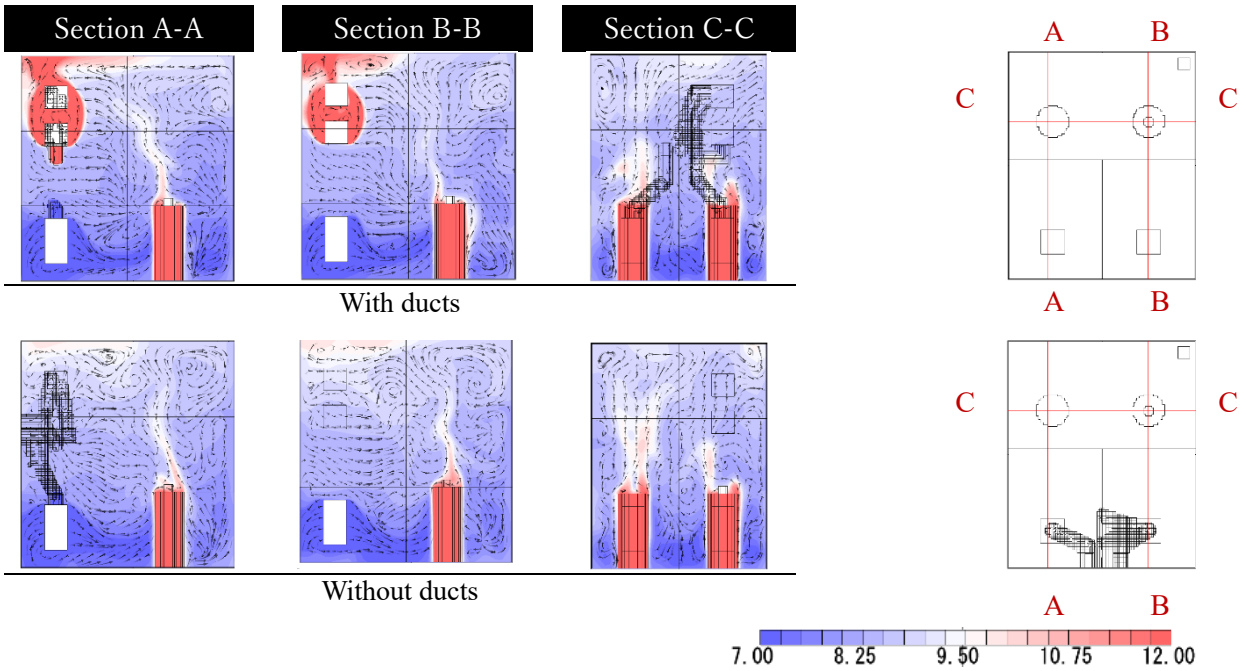

b. Longitudinal and cross-sections

Figure 3.22 Tempearture contours for with vs without ducts cases

3.5. Chapter Discussion and Limitations

Zonal model

In this study a novel portable DV unit with air purifying feature was proposed supported by zonal model calculation. Exploring the PDV unit specification and operation settings, the effect of key variables, i.e. DV supply flowrate, PDV unit flowrate, COP, and input wattage were investigated for two-occupants case. The calculations showed that increasing the supply flowrate of the PDV unit exponentially increases the upper zone temperature as it requires higher input power. Increasing the hot air flowrate was found to decrease the exhausted air temperature, thus this relation can be studied further as it can have a great effect on the temperature gradient and the turbulence.

Since the zonal model does not cover some important variables, such as the PDV unit filtration capacity, and to verify the effect of the studied factors, further investigation using full-scale experiment was carried out.

Experiment

From the experiment results, it was found the proposed PDV unit can efficiently enhance the temperature stratification and reduce the particle count in the occupied zone. However, higher particle count accumulated at higher levels. The flowrates of both DV and PDV unit were found to cause significant effect changing between 100 and 200 m^3/h. On the other hand, increasing the flowrate further caused turbulence, undesirably mixing the particles at lower heights.

One major finding from this experiment was that without operating the ventilation system, the novel PDV unit can work as a replacement. However, the efficiency and the application limitations need further study.

Although it was expected for the nearer exhaust opening to reduce the accumulated heat load from the PDV unit, the results showed increased temperature at the exhaust, especially, in the high flowrate case, 300 m^3/h. One explanation for this increase is that turbulence caused by the opposing horizontal flow from hot air supply and exhaust air. A similar conclusion was reached by Yang et al., they found that increasing the flow rate higher than 180m^3/h.person does not increase the efficiency of the contaminant removal but rather, the supply air was found to exit the room without aiding in the room temperature stratification [24].

Regarding the particle emission and distribution, the following observations were found. Using a nebulizer for particles emission, the decrease in the fluid by time caused the decrease in generation rate which was especially visible after 30 minutes of emission. However, except for this slight drop, the emission rate was relatively steady.

Comparing all the particle count measured at the experiment to the PDA measurement, it can be seen that the particles had already evaporated and or settled even before reaching the closest point of measurement at Pd. As for the particles' distribution, since larger particles tend to evaporate or settle on the surfaces, their count was found to be higher at Pd than at the exhaust and than the return air at the hot-air port. Finally, given

the current setting of hot air supply post and suction ports, the particles re-emitted from the hot air supply were higher than the interpolated value at the same height. This is caused by the fact that the suction port, being higher, takes in air that contains more particles. Not passing through filtration, the particles evaporate so the size distribution is shifted to the smaller diameter ranges. Although the current settings made it possible to recognize the effect of heating on the return air particle count and volume, filtration of the return air might have been a more efficient option to further investigate in future work.

For design development, two main changes are suggested to the current design. First, the position of the hot air supply relative to the suction port should be reconsidered. Placing the suction port above the hot air supply might have reduced the heat dispersion in the room through the short-circuiting, however, extra load was put on the PDV unit. For better performance of the machine, especially in rooms with high ceiling, the suction port is recommended to be placed lower than the hot air supply. Secondly, the current arrangement with the HEPA filter installed for the cool air supply alone was decided to minimize the energy consumption of the machine. However, the unfiltered hot air supply has shown to have a considerable effect on the air quality. Therefore, it is recommended for the filter to be installed for both cool and hot supply air diffusers.

3.6. Limitations:

1) The particle count's vertical distribution was only measured at one point in the space which does not reflect the horizontal distribution.
2) Ducts connecting the PDV unit components although limited to the wall side, their existence in the room must have affected the air flow. Being insulated their thermal effect might have been small, but still must have influenced the surround air temperature.
3) The experiment room, due to space limitation, is rather small which might limit the generalization of the findings
4) The effect of changing PDV unit and exhaust port relative location cannot be generalized due to the room size.
5) Validation of the PM distribution was not carried out which limits the reliability of the CFD simulations in terms of air quality. It is planned in the further study plan.

3.7. Nomenclature

I: PDVU Input power (W)
n: COP (-)
q_{sm}: PDVU supply flow rate (m^3/h)
T_{sm}: PDVU supply temperature (°C)
q_{hm}: PDVU hot air flow rate (m^3/h)
T_{hm}: PDVU hot air temperature (°C)
qs: DV supply flow rate (m^3/h)

Ts: DV supply temperature (℃)

Tu: Upper zone temperature (℃)

Tl: Lower zone temperature (℃)

T_{ex}: Exhaust air temperature (℃)

Hs: Heat from different sources (W)

η: ratio of heat ascending to upper zone

Q_{sm}: PDVU cooling capacity

Q_{hm}: PDVU heating capacity

3.8. References

[1] T. (Tim) Zhang, S. Wang, G. Sun, L. Xu, D. Takaoka, Flow impact of an air conditioner to portable air cleaning, Build Environ. 45 (2010) 2047–2056. https://doi.org/10.1016/J.BUILDENV.2009.11.006.

[2] B. Bake, P. Larsson, G. Ljungkvist, E. Ljungström, A.-C. Olin, Exhaled particles and small airways, Respir Res. 20 (2019) 8. https://doi.org/10.1186/s12931-019-0970-9.

[3] W.F. Wells, On air-borne infection. Study II. Droplets and droplet nuclei., Am J Hyg. 20 (1934) 611–618.

[4] World Health Organization, Infection prevention and control of epidemic-and pandemic-prone acute respiratory infections in health care WHO Guidelines, (2014).

[5] D.K. Milton, A Rosetta Stone for Understanding Infectious Drops and Aerosols, J Pediatric Infect Dis Soc. 9 (2020) 413–415. https://doi.org/10.1093/jpids/piaa079.

[6] L. Liu, J. Wei, Y. Li, A. Ooi, Evaporation and dispersion of respiratory droplets from coughing, (2016). https://doi.org/10.1111/ina.12297.

[7] X. Xie, Y. Li, A.T.Y. Chwang, P.L. Ho, W.H. Seto, How far droplets can move in indoor environments--revisiting the Wells evaporation-falling curve., Indoor Air. 17 (2007) 211–225. https://doi.org/10.1111/J.1600-0668.2007.00469.X.

[8] R.K. Bhagat, M.S. Davies Wykes, S.B. Dalziel, P.F. Linden, Effects of ventilation on the indoor spread of COVID-19, (n.d.). https://doi.org/10.1017/jfm.2020.720.

[9] L. Morawska, J. Allen, W. Bahnfleth, P.M. Bluyssen, A. Boerstra, G. Buonanno, J. Cao, S.J. Dancer, A. Floto, F. Franchimon, T. Greenhalgh, C. Haworth, J. Hogeling, C. Isaxon, J.L. Jimenez, J. Kurnitski, Y. Li, M. Loomans, G. Marks, L.C. Marr, L. Mazzarella, A.K. Melikov, S. Miller, D.K. Milton, W. Nazaroff, P. V. Nielsen, C. Noakes, J. Peccia, K. Prather, X. Querol, C. Sekhar, O. Seppänen, S. Tanabe, J.W. Tang, R. Tellier, K.W. Tham, P. Wargocki, A. Wierzbicka, M. Yao, A paradigm shift to combat indoor respiratory infection, Science (1979). 372 (2021) 689–691.

[10] A. Novoselac, J.A. Siegel, Impact of placement of portable air cleaning devices in multizone residential environments, Build Environ. 44 (2009) 2348–2356. https://doi.org/10.1016/J.BUILDENV.2009.03.023.

[11] M. Aldekheel, A. Altuwayjiri, R. Tohidi, V. Jalali Farahani, C. Sioutas, The Role of Portable Air Purifiers and Effective Ventilation in Improving Indoor Air Quality in University Classrooms, Int J Environ Res Public Health. 19 (2022) 14558. https://doi.org/10.3390/IJERPH192114558/S1.

[12] A. Staszowska, Assessment of the air purifier effectiveness under model conditions, J Phys Conf Ser. 1736 (2021) 012043. https://doi.org/10.1088/1742-6596/1736/1/012043.

[13] E. Cooper, Y. Wang, S. Stamp, E. Burman, D. Mumovic, Use of portable air purifiers in homes: Operating behaviour, effect on indoor PM2.5 and perceived indoor air quality, Build Environ. 191 (2021). https://doi.org/10.1016/J.BUILDENV.2021.107621.

[14] R.J. Shaughnessy, E. Levetin, J. Blocker, K.L. Sublette, Effectiveness of Portable Indoor Air Cleaners: Sensory Testing Results, Indoor Air. 4 (1994) 179–188. https://doi.org/10.1111/J.1600-

0668.1994.T01-1-00006.X.

[15] P. Barn, T. Larson, M. Noullett, S. Kennedy, R. Copes, M. Brauer, Infiltration of forest fire and residential wood smoke: an evaluation of air cleaner effectiveness, Journal of Exposure Science & Environmental Epidemiology 2008 18:5. 18 (2007) 503–511. https://doi.org/10.1038/sj.jes.7500640.

[16] Z.M. Sultan, G.J. Nilsson, R.J. Magee, Removal of ultrafine particles in indoor air: Performance of various portable air cleaner technologies, HVAC and R Research. 17 (2011) 513–525. https://doi.org/10.1080/10789669.2011.579219.

[17] P.V. Nielsen, Temperature and air velocity distribution in rooms ventilated by displacement ventilation, in: Temperature and Air Velocity Distribution in Rooms Ventilated by Displacement Ventilation, 2003: pp. 691–696.

[18] E. MUNDT, The performance of displacement ventilation systems, Dissertation, Dept. of Building Service Engineering, the Royal Institute of Technology. 67 (1996). https://cir.nii.ac.jp/crid/1571980074646693888.bib?lang=en (accessed April 11, 2023).

[19] M. Xu, T. Yamanaka*, H. Kotani, Vertical Profiles of Temperature and Contaminant Concentration in Rooms Ventilated by Displacement with Heat Loss through Room Envelopes, Indoor Air. 11 (2001) 111–119. https://doi.org/10.1034/J.1600-0668.2001.110205.X.

[20] C. Habchi, K. Ghali, N. Ghaddar, Displacement ventilation zonal model for particle distribution resulting from high momentum respiratory activities, Build Environ. 90 (2015) 1–14. https://doi.org/https://doi.org/10.1016/j.buildenv.2015.03.007.

[21] J. PYTKO-POLONCZYK, A. JAKUBIK, A. PRZEKLASA-BIEROWIEC, B. MUSZYNSKA, ARTIFICIAL SALIVA AND ITS USE IN BIOLOGICAL EXPERIMENTS, JOURNAL OF PHYSIOLOGY AND PHARMACOLOGY. 68 (2017) 807–813.

[22] J. Hang, Y. Li, R. Jin, The influence of human walking on the flow and airborne transmission in a six-bed isolation room: Tracer gas simulation, Build Environ. 77 (2014) 119–134. https://doi.org/https://doi.org/10.1016/j.buildenv.2014.03.029.

[23] L. Morawska, G.R. Johnson, Z.D. Ristovski, M. Hargreaves, K. Mengersen, S. Corbett, C.Y.H. Chao, Y. Li, D. Katoshevski, Size distribution and sites of origin of droplets expelled from the human respiratory tract during expiratory activities, J Aerosol Sci. 40 (2009) 256–269. https://doi.org/https://doi.org/10.1016/j.jaerosci.2008.11.002.

[24] R. Yang, C.S. Ng, K.L. Chong, R. Verzicco, D. Lohse, Do increased flow rates in displacement ventilation always lead to better results?, J Fluid Mech. 932 (2022) A3. https://doi.org/10.1017/JFM.2021.949.

Chapter 4 CFD Application: Operating the Portable Displacement Ventilation Unit in the Large Lecture Hall

4.1. Introduction and Research Purpose

Throughout this study, weaknesses of the case-study's DV system has been observed using CFD analyses and field measurements. Findings were supported by literature evaluating the DV performance in large spaces [1–5]. With the DV disadvantages in mind, a novel portable DV unit was proposed, designed and with the help of field measurements, the PDV unit potential was revealed. Similar to multiple research work, this is aimed at stimulating the installation of the portable unit in targeted large space. In terms of air filtration effectiveness, Qian et al., for one, simulated portable air purifier to assess its performance in a hospital ward [6]. Zhai et al. carried out a similar study focusing on reducing the COVID cross-infection risk [7]. They adopted RNG k-ε turbulence model. However, in those studies, the filtration analysis was not simulated using particles as the application space is too big, the calculation requires massive computational power. Instead of particles, tracer gas was used as a more feasible option. As previously mentioned, tracer gas is widely used as representative for droplet nuclei and small droplets [8–10]. In their 2022 study, Karam et al opted to used tracer gas to assess the air cleaner's efficiency. RNG k-ε turbulence model was adopted as well [11].

In this chapter, the effectiveness of the novel PDV unit in large spaces is tested. Tracer gas was chosen to represent the small particles supported by the aforementioned literature. The unit's efficiency at balancing the flow in the 3-sides diffuser lecture hall is assessed as well as its effect on the temperature and contaminant concentration in the occupied zone.

4.2. CFD Modeling of the Portable Displacement Ventilation Unit in the Large Lecture Hall

4.2.1. Analysis Conditions

It has been deduced from the field measurements and visualized by CFD that the 3-sided diffusers installation cause an asymmetric air distribution lowering the air quality at the back section of the hall especially. Hence, the effect of balancing the air supply using the PDV units is examined in this chapter. To simulate the actual PDV unit function, the hot air supply temperature was calculated using user defined function, dependent on the cooling power required for the machine to provide the supply air at 20 °C. Thus, equation (4-1) was used to get the input power, I, in terms of T_u, which is measured at the suction port during the analysis. Afterwards, T_{hm} was calculated using equation (4-2) in terms of I and T_u as formulated in equation (4-3). The COP, n, was assumed 3.5, q_{sm} and q_{sm} were set equal.

$$Q_{sm} = nI = Cp\ \rho\ q_{sm}\ (T_u - T_{sm}) \qquad (4\text{-}1)$$

$$Q_{hm} = (n + 1)\ I = Cp\ \rho\ q_{hm}\ (T_{hm} - T_u) \qquad (4\text{-}2)$$

$$T_{hm} = T_u + ((n + 1)\ I\ /\ Cp\ \rho\ q_{hm}) \qquad (4\text{-}3)$$

In the fully occupied room, two scenarios of DV operation mode were analyzed. First Cases-A, the regular full capacity mode, measured and validated in chapter 2. Two PDV unit arrangements were compared to the base-case to assess the effect of operating PDV units in a large lecture hall. Secondly Cases-B, the effectiveness of using PDV units as complementary ventilation system was investigated. The DV supply flowrate was reduced to the minimum, 30 m^3/h.person and the supply flowrate of the PDV units was set to complement the flowrate per person to 103 m^3/h.person provided by the DV system in the base-case. The analysis and boundary conditions are summarized in Table 4-1 and Table 4-2

Due to the hall's size and limited computational capacity, tracer gas generation was simulated to represent the contaminant particles. The Sources position in the field measurement was copied in this simulation, Figure 4.1.

Table 4-1 Analysis conditions

Analysis software	Stream v.22
Turbulence model	RNG k-ε model
Analysis type	Steady state
Calculations	Heat, radiation, and diffusion
Mesh settings	
Default size	50 mm
Growth rate	1.15
Cells count	~ 5M

Table 4-2 Boundary conditions

Thermal Boundaries	
Heat transfer condition	
External surfaces	Adiabatic
Floor and ceiling	Coefficient of heat transfer 30 W/m^2K
Other internal	Fixed temperature
Emissivity	0.9
Heat Generation	
Heat load	100 W /person simulator

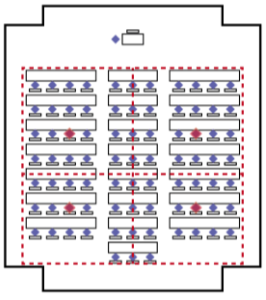

Figure 4.1 Lecture hall plan with source occupants highlighted

Based on Chapter 3 conclusion, two changes were made in the PDV unit's settings. The position of hot air supply and suction port was reversed having the hot air diffuser on top as shown in Figure 4.2. The second change was the filtration of the hot air. The suction port was set to take out the contaminants, however, both supply diffuser and hot air diffuser were set to supply no contaminants.

For cases set-A, the base-case, with no PDV units, is compared to using 4 units and 8 units cases. The units were placed in order to balance the horizontal flows observed in the lecture hall simulation in Chapter 2. Cases details are shown in Table 4-3. Regarding cases set-B, the DV supply flowrate and the total flowrate of the PDV units were set constant. Individual units flowrate changed based on the number of units per case. One extra case of 16 PDV units was added with the settings shown in Table 4-4.

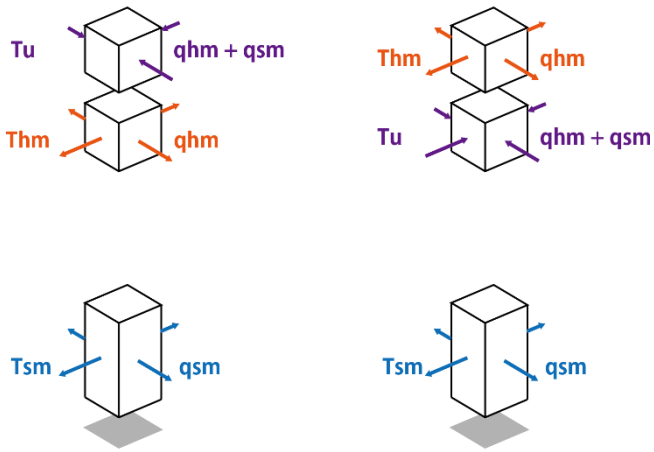

a. Experiment settings **b. Altered settings for application**

Figure 4.2 PDV unit settings

. Table 4-3 Cases set-A attributes

	Case-A-0PU	**Case-A-4PU**	**Case-A-8PU**
	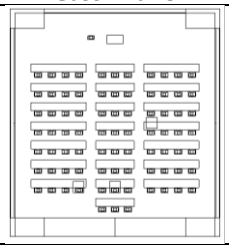	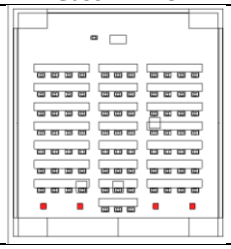	
Number of PDV units	0 units	4 units	8 units
PDV units location	-	Back side, center	Back side, center
DV flowrate q_s (m^3/h)	8400 m^3/h		
PDV unit supply temperature T_s (℃)	20 ℃	20 ℃	
PDV unit flowrate/ unit q_{sm}, q_{hm} (m^3/h)	-	200 m^3/h	
Total PDV units flowrate q_{sm}, q_{hm} (m^3/h)		800 m^3/h	1600 m^3/h
PDV unit supply temperature T_{sm} (℃)	-	20	
PDV unit hot air temperature T_{hm} (℃)	-	Dependent (UDF using eq. 4-3)	

Table 4-4 Cases set-B atributes

	Case-B-0PU	**Case-B-4PU**	**Case-B-8PU**	**Case-B-16PU**
	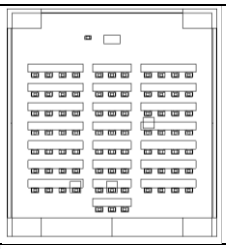	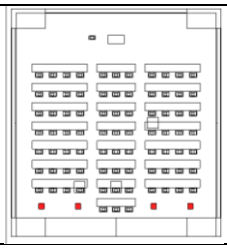	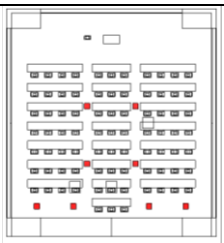	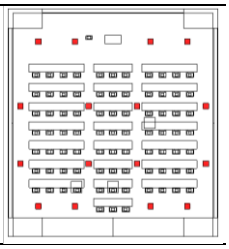
Number of PDV units	0 units	4 units	8 units	16 units
PDV units location	-	Back side, center	Back side, center	Front, back, sides, center
DV flowrate q_s (m^3/h)	2430 m^3/h			
PDV unit supply temperature T_s (℃)	20 ℃			
PDV unit flowrate/ unit q_{sm}, q_{hm} (m^3/h)	-	1493 m^3/h	746 m^3/h	372 m^3/h
Total PDV units flowrate q_{sm}, q_{hm} (m^3/h)	5970 m^3/h			
PDV unit supply temperature T_{sm} (℃)	-	20 ℃		
PDV unit hot air temperature T_{hm} (℃)	-	Dependent (UDF using eq. 4-3)		

4.2.2. Results and Discussion

For all cases, the temperature and contaminant concentration vertical distributions are assessed. To compare to the lecture hall simulations, the same pole positions were used to plot the temperature and contaminant vertical distribution. In addition, the cooling and heating power of the individual PDV units is calculated, and accordingly, the total heat load exerted by the PDV units is determined.

4.2.2.1. Effect of Operating the PDV unit

To start with, the PDV unit output temperatures and cooling/heating capacities for each unit are shown in Table 4-5. Hot air temperature, T_{hm}, is measured at the surface of the diffuser and T_u, is not the upper zone temperature but the PDV unit's local, measured at the surface of the suction port. From the results, it can be observed that for both cases, the temperature at the suction port was only 1℃ over the supply temperature. Therefore, not much cooling power was needed, and accordingly, little heat was generated. Viewing the temperature vertical distribution at poles a~j, shown in Figure 4.3, small local effect can be detected at poles b, c , d, f, g, and h. Particularly at pole g and h, a decrease in the lower zone temperature and an increase in that of the upper part can be seen. The temperature contours at z= 1100 mm, 1700 mm, and 2500 mm are shown in Figure 4.4 and at longitudinal and cross-sections in Figure 4.5. The effect observed is overall minimal except for the hot air plume from the PDV units.

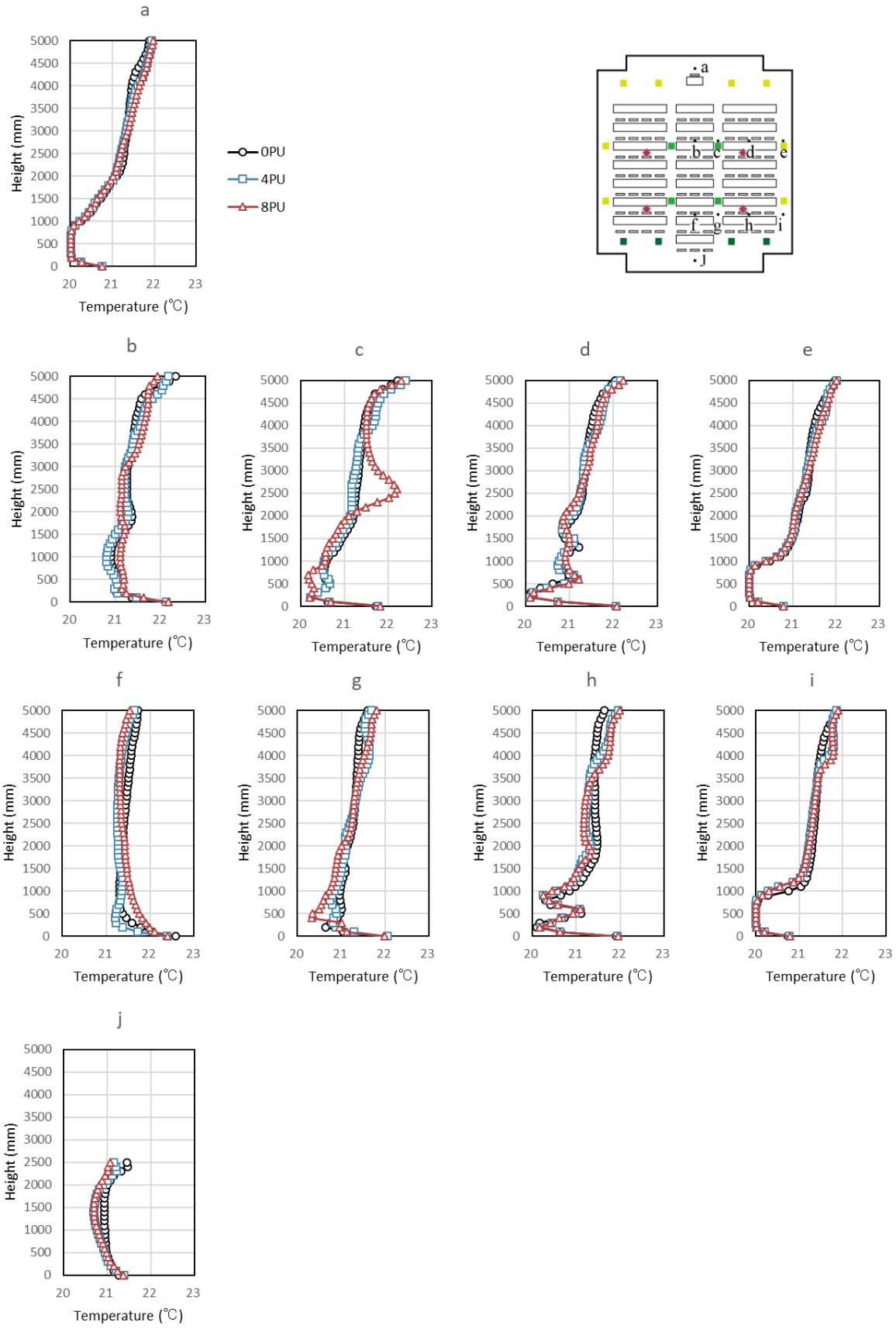

Figure 4.3 Temperature vertical distribution for cases set-A

Table 4-5 PDV units temperatures and power for cases set-A

		T_{hm} (°C)	T_u (°C)	I (W)	COP	Q_{sm} (W)	Q_{hm} (W)
Case-A-4PU	PDV unit _1	22.7	21.2	19.5	3.9	77	97
	PDV unit _2	22.9	21.2	20.7	4.0	82	107
	PDV unit _3	22.7	21.2	19.9	3.9	78	100
	PDV unit _4	22.8	21.2	20.5	4.0	82	106
						Total heat	**411 W**
Case-A-8PU	PDV unit _1	22.6	21.2	18.9	4.0	75	96
	PDV unit _2	22.6	21.1	18.5	3.8	71	97
	PDV unit _3	22.6	21.1	18.2	3.8	69	99
	PDV unit _4	22.3	21.0	16.7	4.1	68	82
	PDV unit _5	22.3	21.0	16.7	4.1	68	85
	PDV unit _6	22.9	21.2	20.6	4.0	82	107
	PDV unit _7	22.6	21.1	18.8	4.0	74	95
	PDV unit _8	22.8	21.2	20.2	4.0	80	107
						Total heat	**769 W**

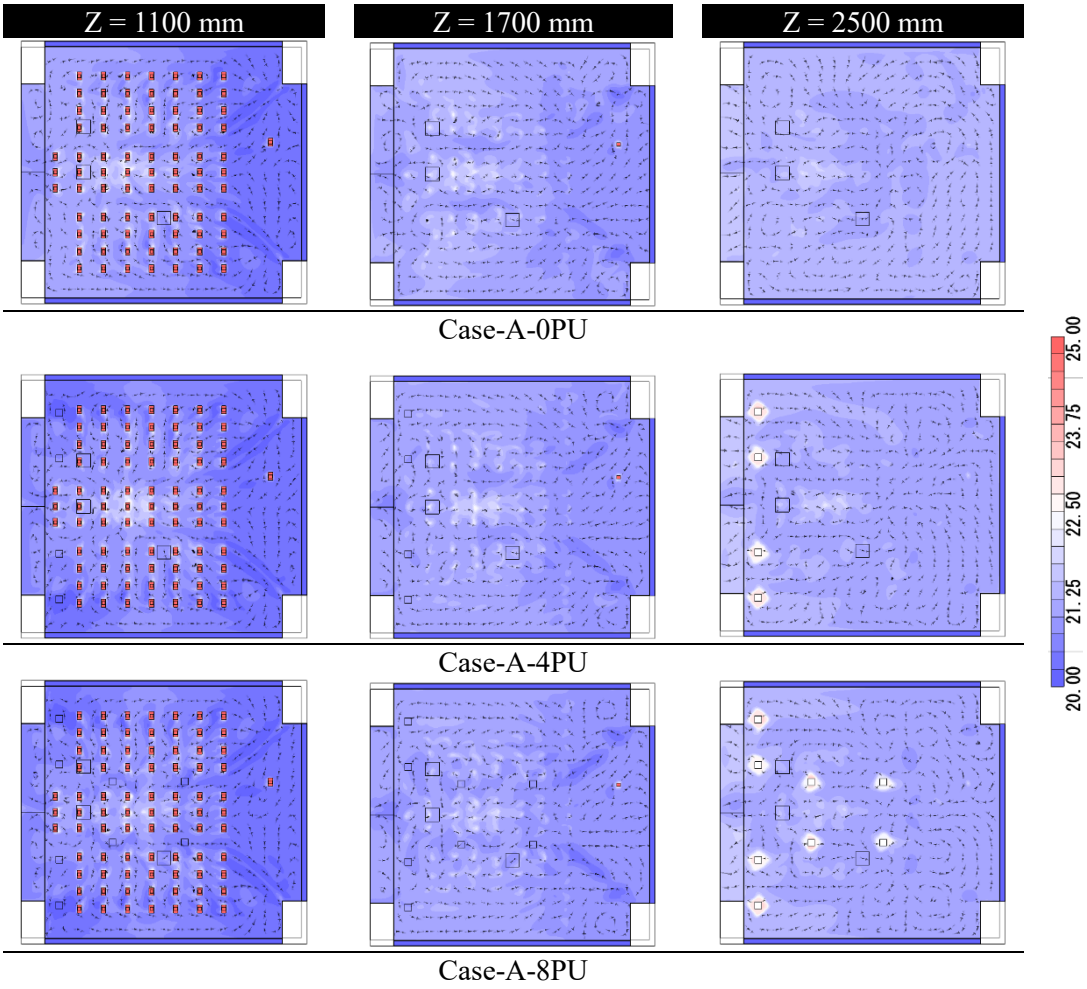

Figure 4.4 Tempearture contours for cases set-A, Plan view

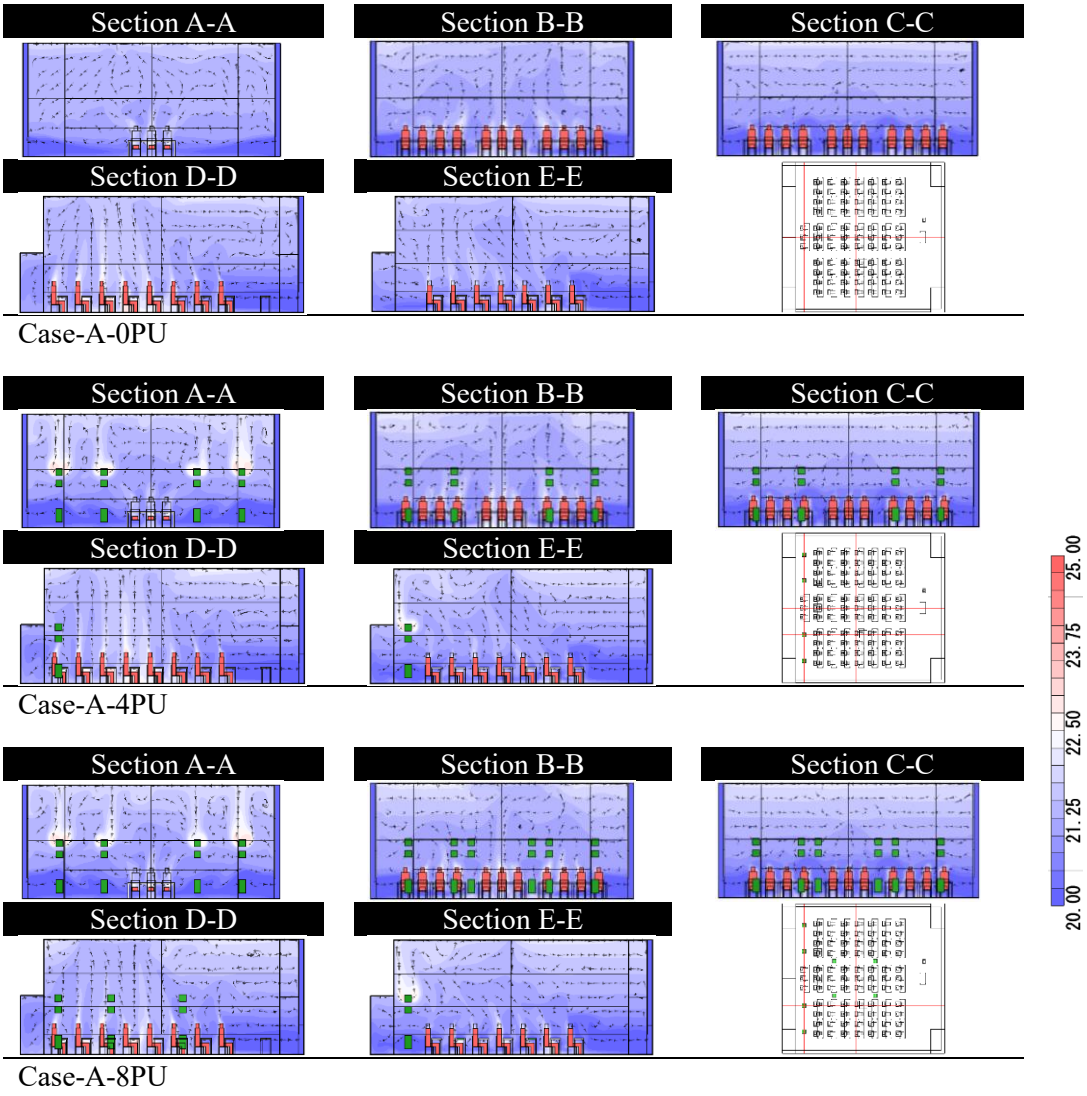

Figure 4.5 Tempearture contours for cases set-A, Longitudinal and cross-sections

Secondly, the effect on contaminant distribution is assessed through graphs of vertical distribution at the poles and concentration contours. All concentration values are normalized by the exhaust concentration of the base-case, Case-A-0PU. From the plots in Figure 4.6, a large difference in distribution between the three cases can be noticed. The 4PU case seems to have almost no effect on the occupied zone concentrations, however, the 8PU case was found to have lowered the interface level especially at the poles near the contaminant sources, i.e. poles d, e, h, and i. Figure 4.12 and Figure 4.13 show the concentration contours in plan and section views respectively. Visualizing the whole plan, it can be observed that the PDV unit cases have reduced the concentration at 1100 mm in the back section of the room. It can also be noticed that in the upper zone, high concertation clouds have formed in both 4PU and 8PU cases while in the base-case the concentration was almost uniform.

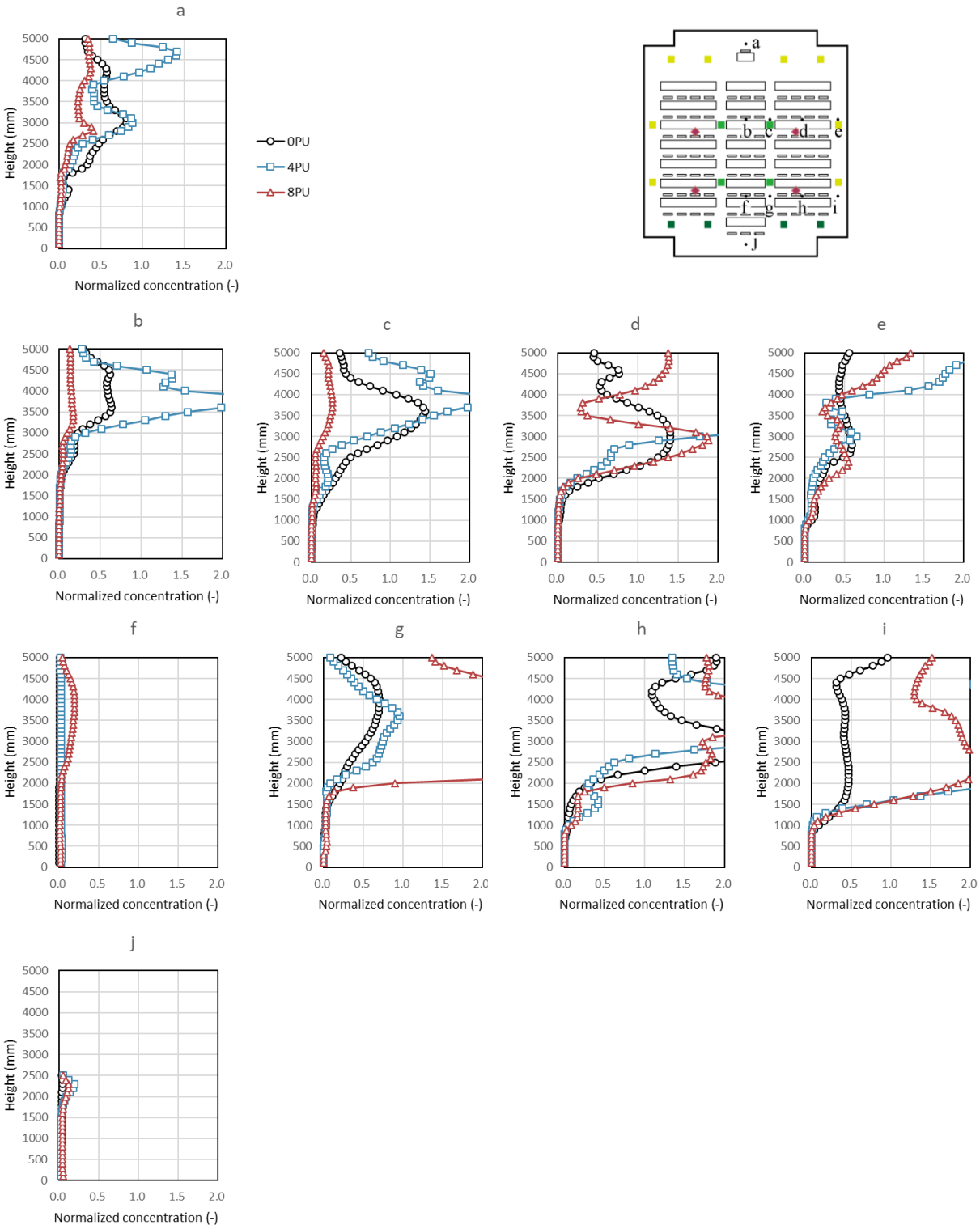

Figure 4.6 Contaminants concentration vertical distribution for cases set-A

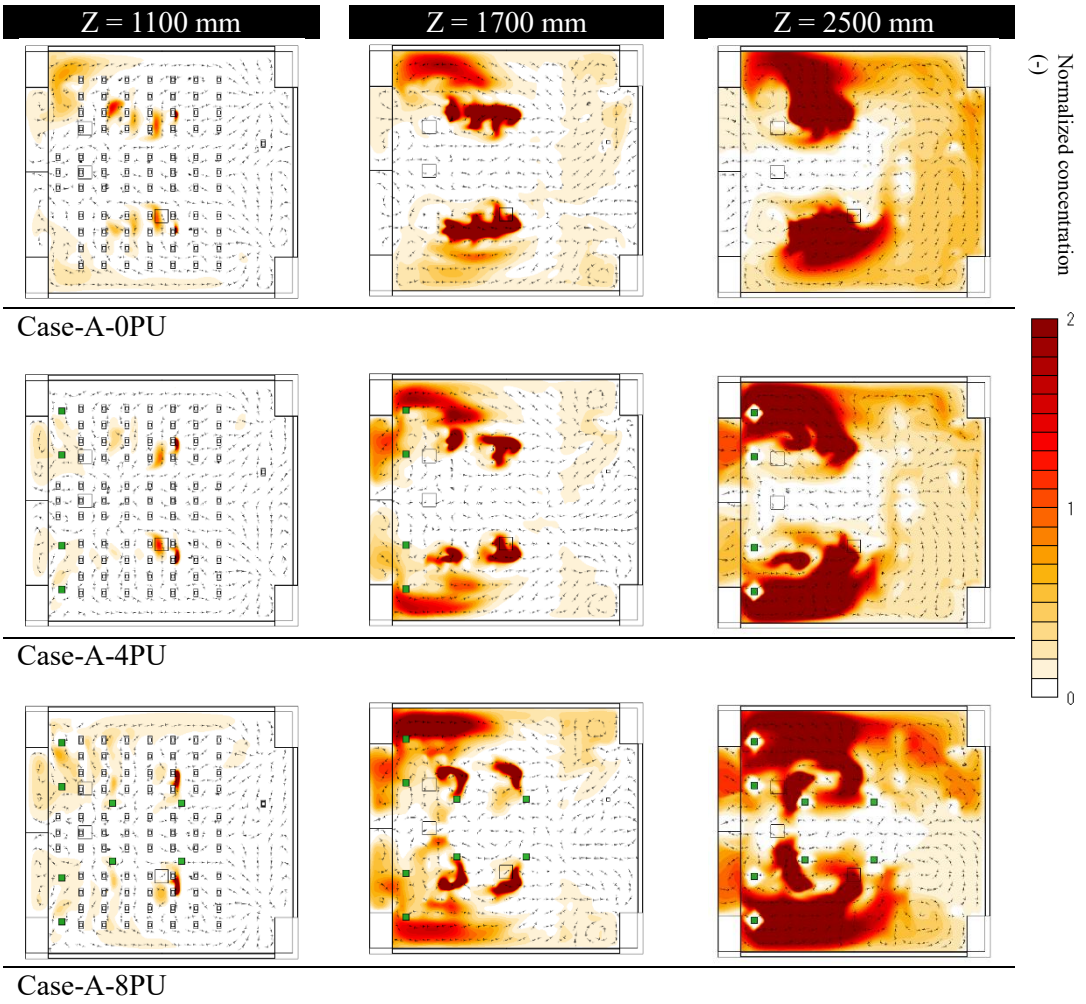

Figure 4.7 Contaminant concentration contours for cases set-A, Plan view

Observing the contaminants diffusion pattern in sections in *Figure 4.8* together with the velocity contours in Figure 4.10, the reduction in the backwards air flow can be seen. A slight opposing forward flow was generated by the PDV units in the 4PU case and a stronger flow in the 8PU case.

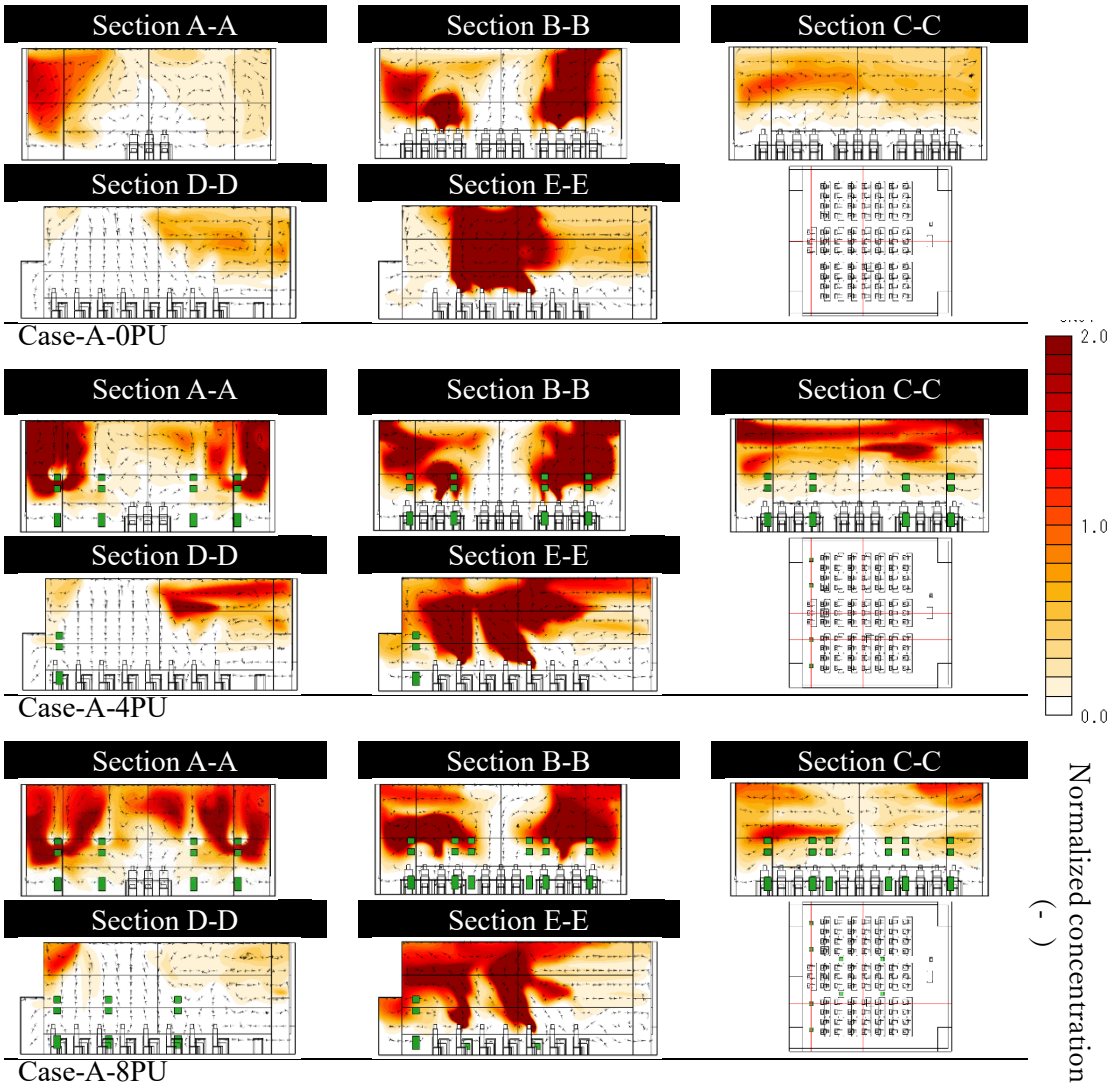

Figure 4.8 Contaminant contours for cases set-A, Longitudinal and cross-*section*

Assessing the effect on breathing zone air quality, the normalized contaminant concentration at mouths the all non-source occupants are plotted in Figure 4.9. A significant reduction in the concentration of the middle row occupants can be noticed comparing both PDV unit cases to the base-case. Case-4PU shows a forward shift of the high concentration which implies its effectiveness in balancing the pre-existing backwards flow. This reduction can be seen in the velocity contours, Figure 4.10

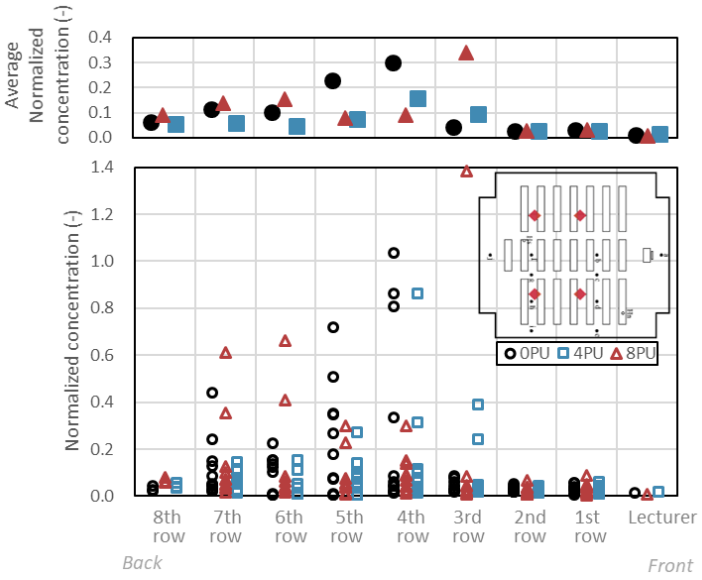

Figure 4.9 Normalized conataminant concentration at individual breathing zone by row

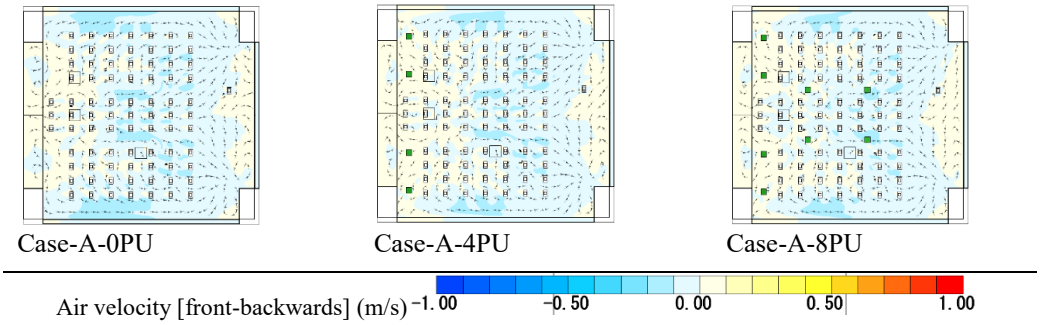

Figure 4.10 Velocity contours for cases set-A

4.2.2.2. Effectiveness as a replacement ventilation system

In cases set-B, since the DV supply is lowered to minimum, the PDV units flowrate and thus heat load increased compared to set-A. As shown in Table 4-6, the hot air temperature reaches 30 in some units and the average heat load per unit is around 300 W. The effect of the increase heat load can be assessed by its effect on the vertical distribution of temperature shown in Figure 4.11. The hot air causes in the adjacent poles only and have no effect on farther points. However, a general uniform increase in the upper zone can be observed at all poles in all PDV cases especially in 16PU case.

Table 4-6 PDV units temperatures and power for cases set-B

		T_{hm} (℃)	T_u (℃)	I (W)	COP	Q_{sm} (W)	Q_{hm} (W)
Case-B-4PU	PDV unit _1	31.0	25.1	94.2	3.5	329	388
	PDV unit _2	27.4	23.8	68.9	3.6	247	241
	PDV unit _3	31.0	25.1	94.8	3.4	326	386
	PDV unit _4	29.6	24.4	80.4	3.6	287	345
						Total heat	**1360 W**
Case-B-8PU	PDV unit _1	29.2	24.1	74.6	3.3	248	337
	PDV unit _2	27.0	23.1	56.7	3.4	191	255
	PDV unit _3	29.3	23.8	68.6	3.2	219	365
	PDV unit _4	26.8	23.4	61.3	3.2	199	228
	PDV unit _5	28.2	23.8	69.1	3.5	245	290
	PDV unit _6	27.9	23.8	68.6	3.6	244	274
	PDV unit _7	28.1	23.9	71.0	3.6	253	277
	PDV unit _8	28.1	23.8	70.0	3.6	249	278
						Total heat	**2304 W**
Case-B-16PU	PDV unit _1	30.6	25.0	91.8	2.7	252	373
	PDV unit _2	29.4	24.5	83.1	2.7	222	324
	PDV unit _3	30.8	25.1	94.6	2.3	221	376
	PDV unit _4	29.8	24.2	76.2	3.6	274	369
	PDV unit _5	30.3	24.6	83.9	3.6	301	378
	PDV unit _6	29.1	24.5	82.1	2.5	207	302
	PDV unit _7	30.3	24.3	78.5	3.6	283	400
	PDV unit _8	30.0	24.4	81.0	3.6	290	365
	PDV unit _9	28.8	24.1	74.9	3.6	266	313
	PDV unit _10	29.8	24.3	79.2	3.6	282	360
	PDV unit _11	29.3	24.2	76.2	3.6	271	337
	PDV unit _12	30.2	24.5	83.4	3.6	298	372
	PDV unit _13	29.6	24.3	79.2	3.6	281	347
	PDV unit _14	29.2	24.1	75.5	3.6	270	337
	PDV unit _15	29.8	24.3	78.2	3.6	278	365
	PDV unit _16	30.0	24.3	78.0	3.6	280	376
						Total heat	**5695 W**

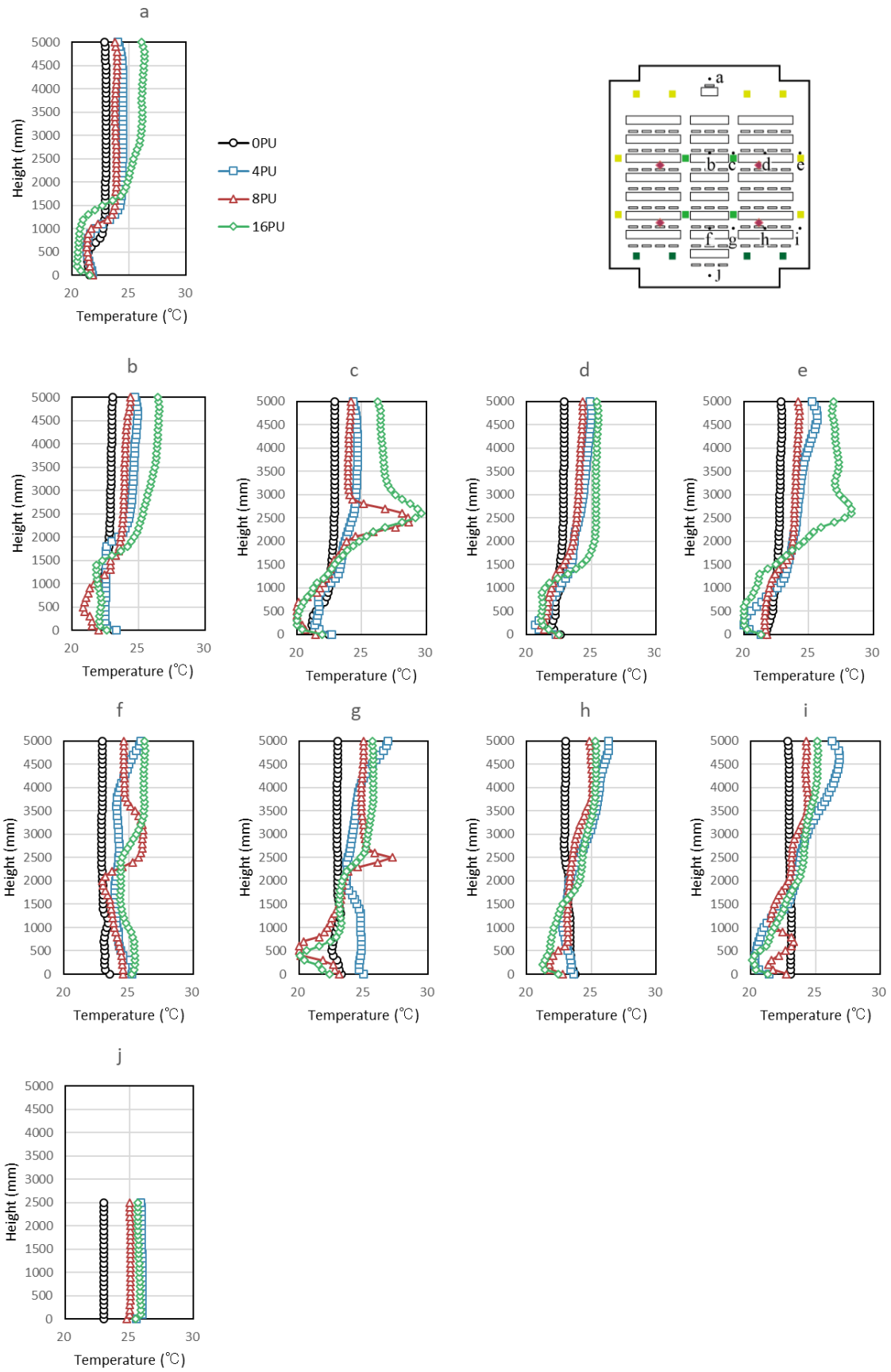

Figure 4.11 Temperature vertical distribution for cases set-B

The temperature contours in Figure 4.12 shows that supplying hot air strengthened the temperature gradient and effectively lowered the temperature at 1100 mm. Although the scarification height has risen compared to the 0PU case, it remains at sitting level, Figure 4.13.

The contaminant distribution, on the other hand, shows a distinct decrease at all heights as shown in the vertical distribution graph, Figure 4.14, and contours, Figure 4.15 and *Figure 4.16*. The local air filtration is found to be effective. The horizontal air flow problem was not entirely resolved as the back zone of the room collects heat and contaminants in all PDV cases. The extra heat load might have contributed as well. The velocity contours, Figure 4.18, shows the small backwards flow persisting in all cases

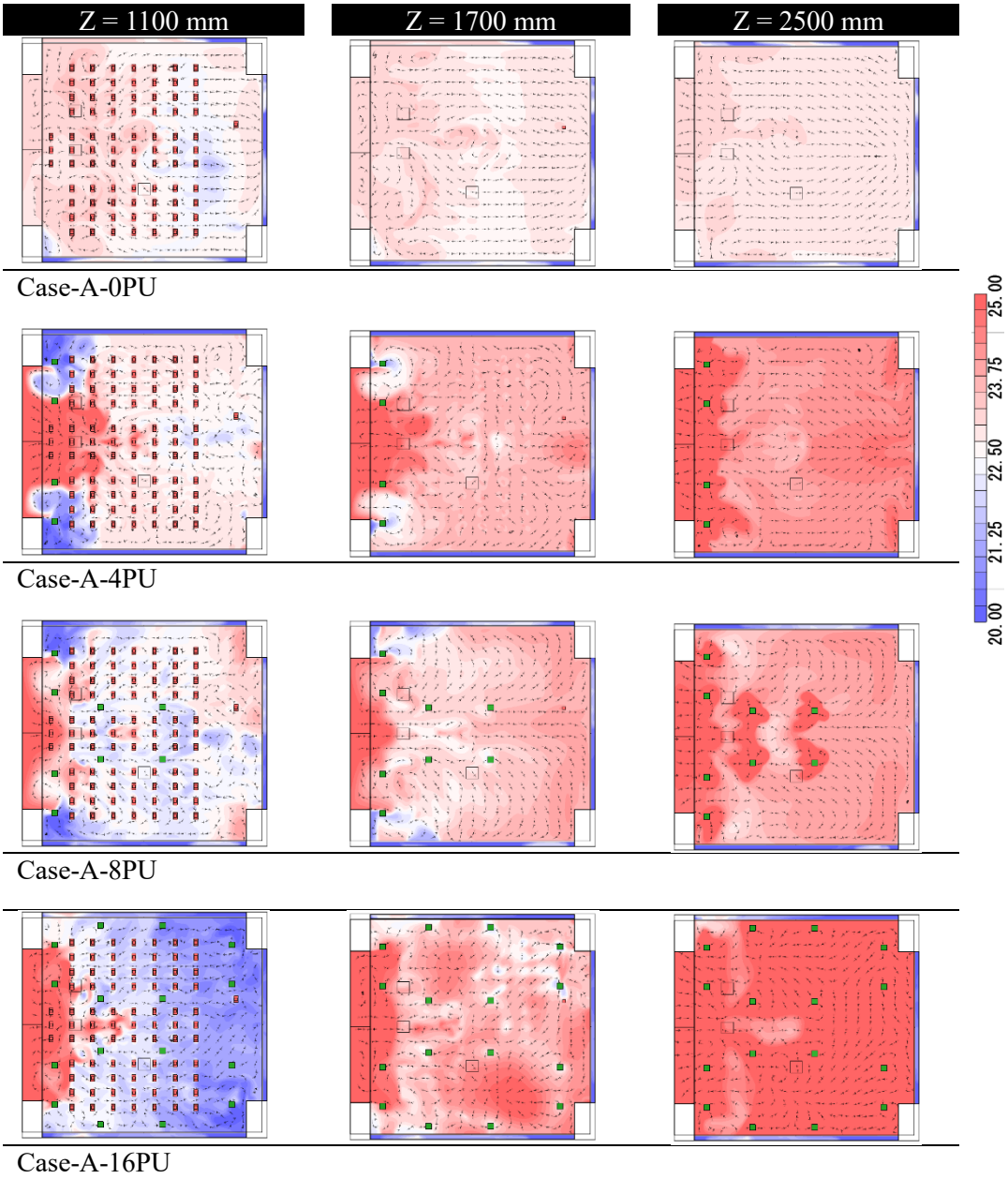

Figure 4.12 Tempearture contours for cases set-B, Plan view

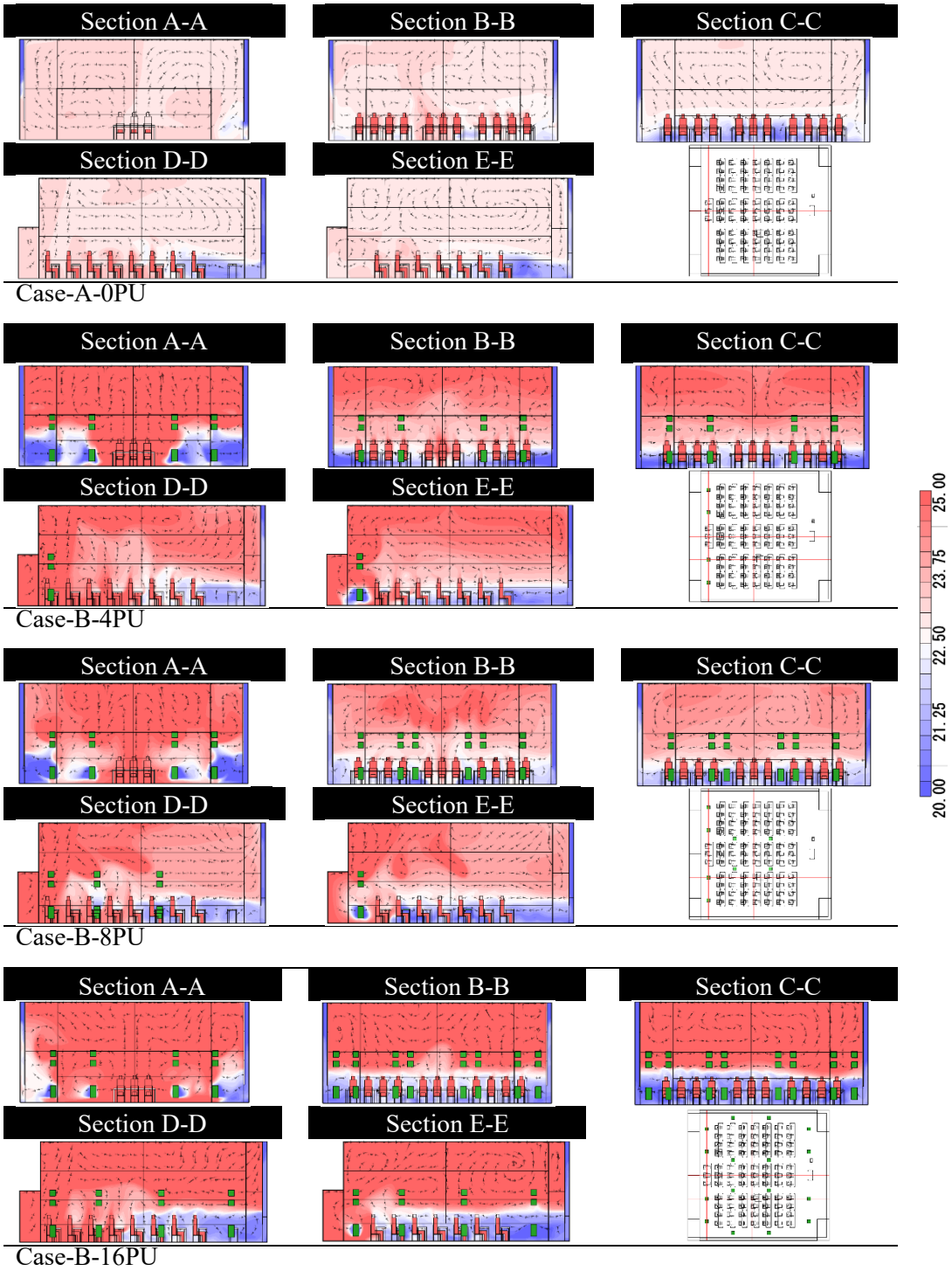

Figure 4.13 Temperature contours for cases set-B, Longitudinal and cross-sections

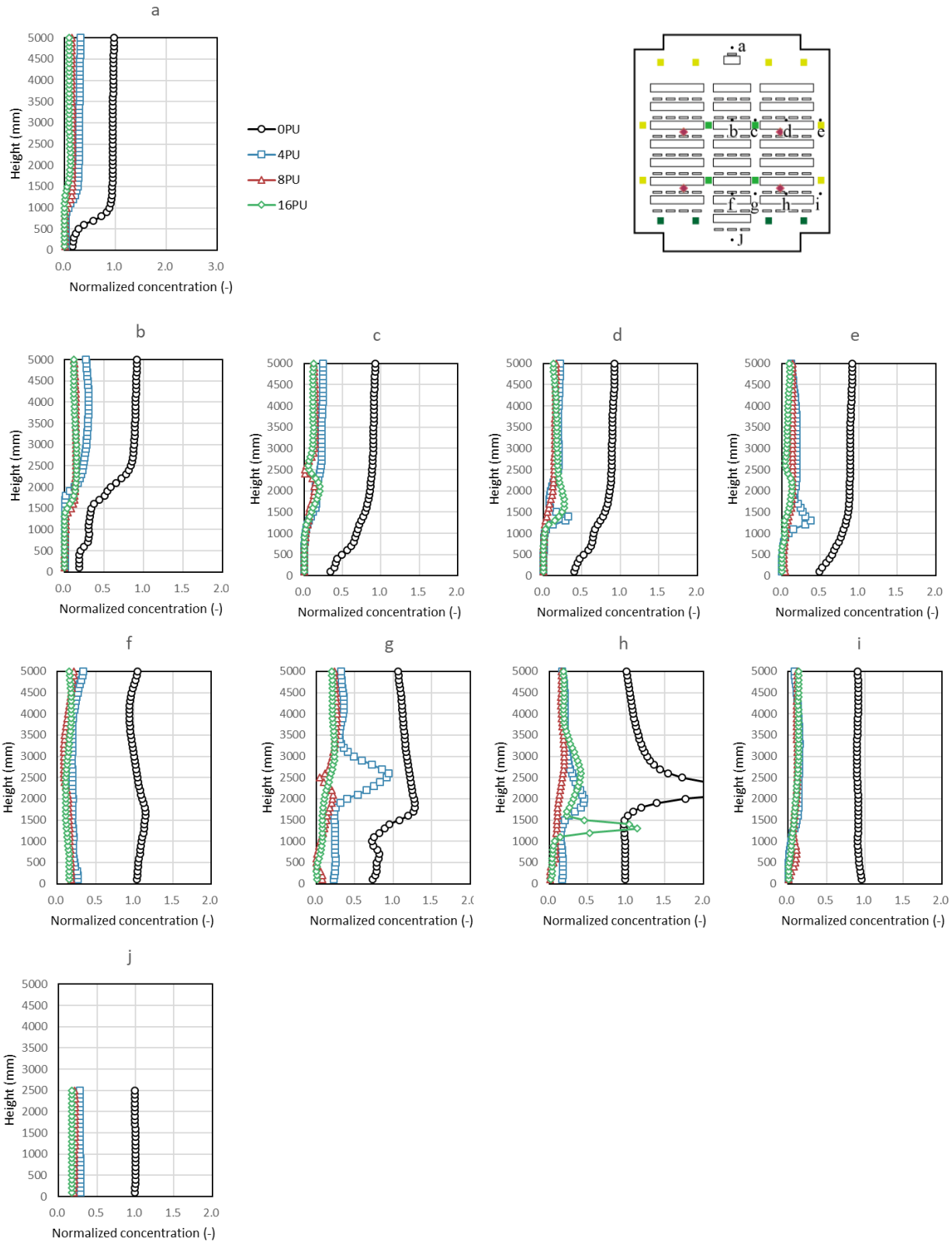

Figure 4.14 Contaminants concentration vertical distribution for cases set-B

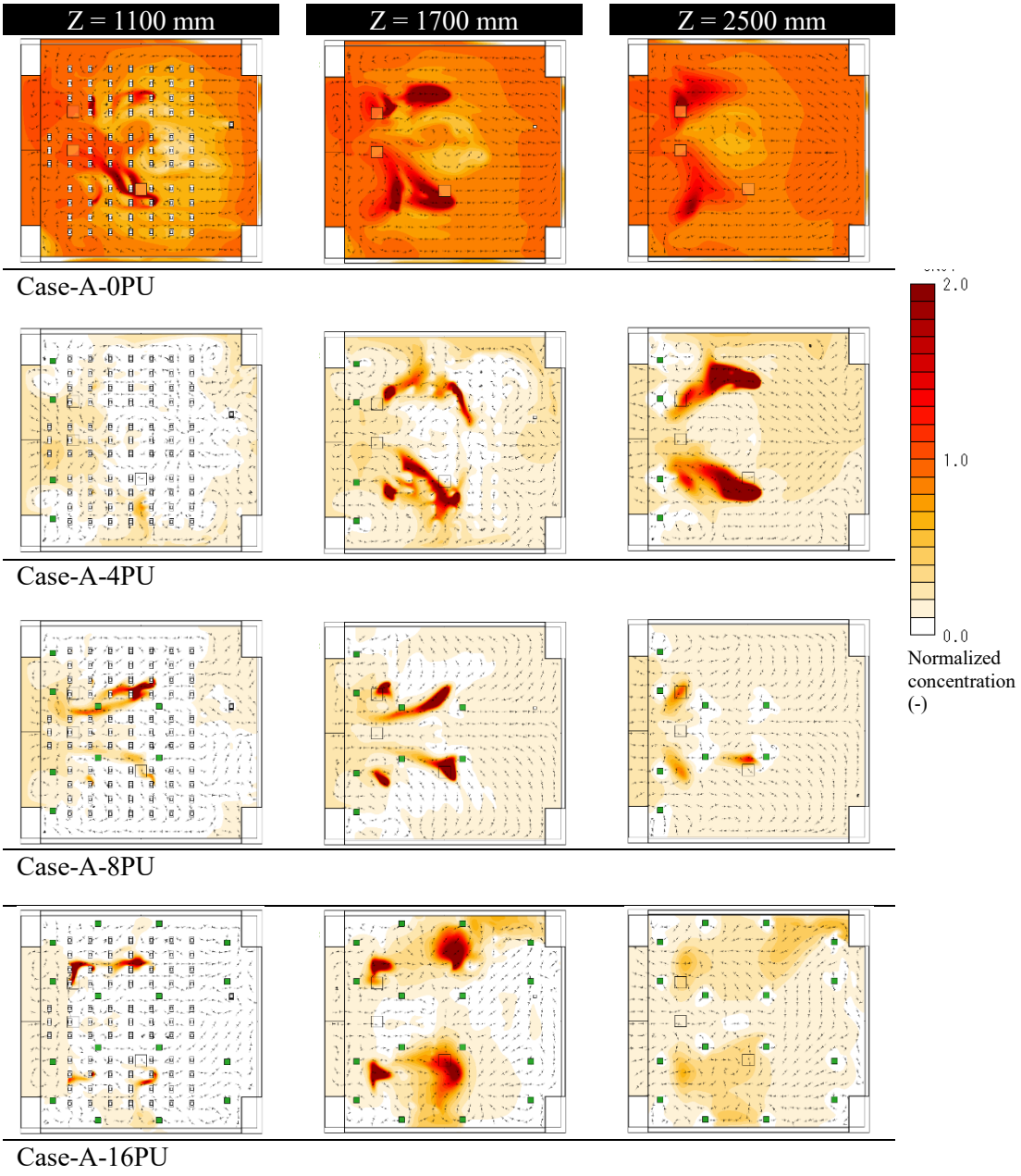

Figure 4.15 Contaminant concentration contours for cases set-B, Plan view

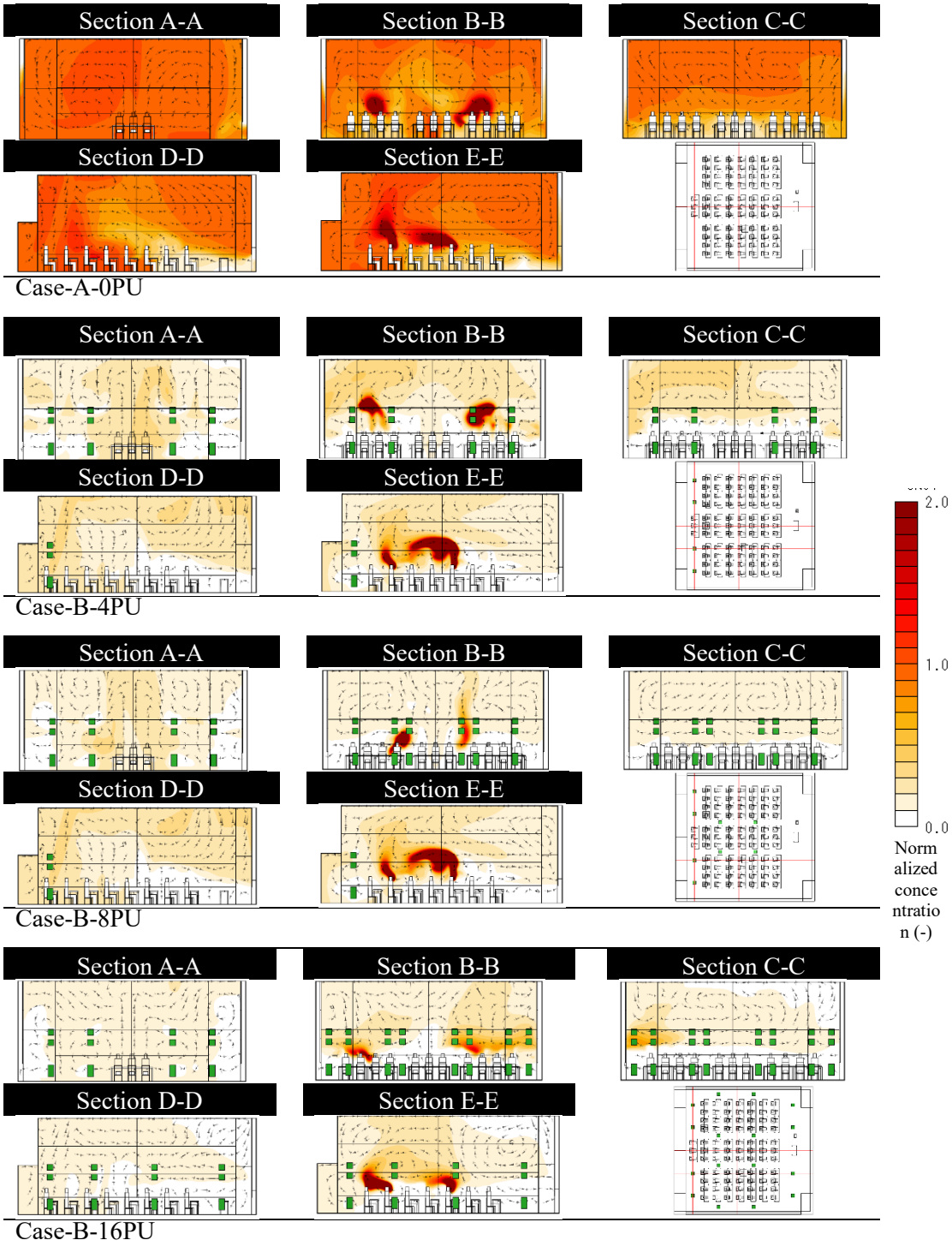

Figure 4.16 Contaminant contours for cases set-B, Longitudinal and cross-*section*

The breathing zone concentrations are plotted in Figure 4.17. Normalized by the lowest exhaust concentration, that of Case-16PU. It can be concluded that Case-4PU shows best results while Case-8PU and Case-16PU showed significant improvement compared to the base-case, Case-0PU. Finally, Figure 4.18 shows that the backwards flow is reduced in the 3 PDV unit cases especially the 8PU which calls for different placement options to neutralize the flow in future studies.

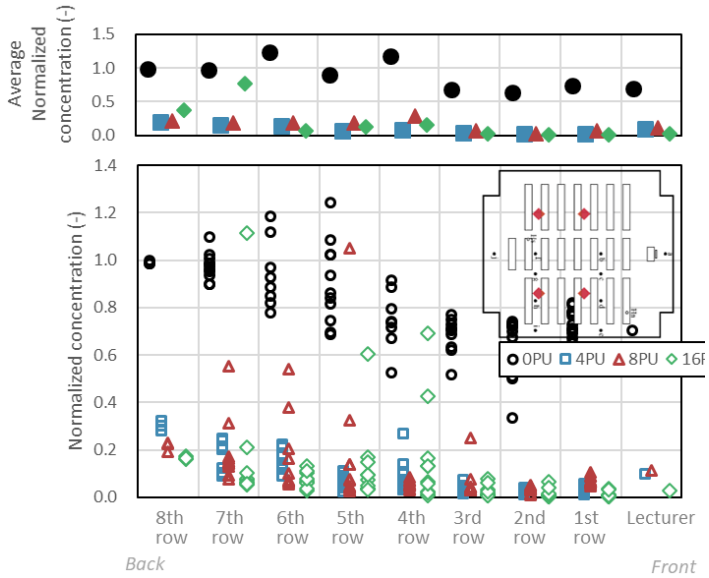

Figure 4.17 Normalized conataminant concentration at individual breathing zone by row

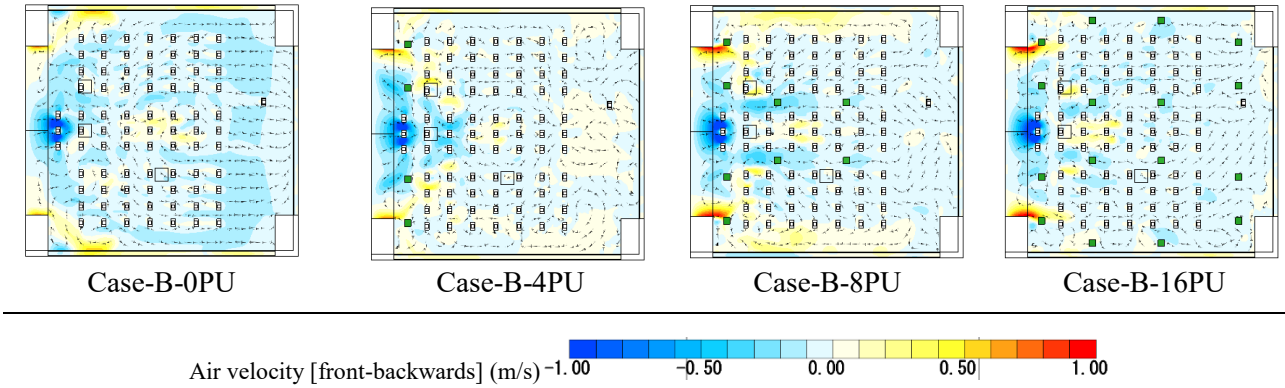

Figure 4.18 Velocity contours for cases set-B

4.3. Chapter Conclusion and Discussion

In this chapter, application of operating the PDV unit in the lecture hall was carried out. Two sets of simulations were carried out, once to evaluate the PDV unit performance in enhancing the DV system performance and another to assess the use of PDV units as a partial replacement to the ventilation system. Temperature distribution, contaminant concentration and horizontal air velocity results were analysed to understand how effective the unit is. As an enhancement, the PDV units were found to locally reduce the contaminant concentration in the occupied zone and raise the interface level as well as locally balancing the horizonal flows caused by the non-uniform system supply. On the other hand, operating the PDV unit at minimal DV flowrate renders it ineffective in enhancing the temperature gradient. Despite the fact that slight improvement can be observed comparing to the minimal DV flowrate case with no PDV unit, viewing the unit as a replacement system needs further investigations and optimization of the unit design and operation method..

4.4. References

[1] H. Stymne, M. Sandberg, M. Mattsson, Dispersion pattern of contaminants in a displacement ventilated room-implications for demand control, in: 12th AIVC Conference, 1991: pp. 173–189.

[2] N.M. Mateus, G. Carrilho da Graça, Simulated and measured performance of displacement ventilation systems in large rooms, Build Environ. 114 (2017) 470–482. https://doi.org/10.1016/J.BUILDENV.2017.01.002.

[3] Z. Bakó-Biró, D.J. Clements-Croome, N. Kochhar, H.B. Awbi, M.J. Williams, Ventilation rates in schools and pupils' performance, Build Environ. 48 (2012) 215–223. https://doi.org/10.1016/J.BUILDENV.2011.08.018.

[4] R. Kosonen, Panu Mustakallio, Ventilation in Classroom: a Case-Study of the Performanceof Different Air Distribution Methods, in: 10th REHVA World Congress-Clima, 2010.

[5] M.L. Fong, Z. Lin, K.F. Fong, T.T. Chow, T. Yao, Evaluation of thermal comfort conditions in a classroom with three ventilation methods, Indoor Air. 21 (2011) 231–239. https://doi.org/10.1111/J.1600-0668.2010.00693.X.

[6] H. Qian, Y. Li, H. Sun, P. V Nielsen, X. Huang, X. Zheng, Particle removal efficiency of the portable HEPA air cleaner in a simulated hospital ward, Build Simul. 3 (2010) 215–224. https://doi.org/10.1007/s12273-010-0005-4.

[7] Z. (John) Zhai, H. Li, R. Bahl, K. Trace, Application of Portable Air Purifiers for Mitigating COVID-19 in Large Public Spaces, Buildings. 11 (2021). https://doi.org/10.3390/buildings11080329.

[8] N. Choi, T. Yamanaka, T. Kobayashi, T. Ihama, M. Wakasa, Influence of vertical airflow along walls on temperature and contaminant concentration distributions in a displacement-ventilated four-bed hospital ward, Build Environ. 183 (2020) 107181. https://doi.org/10.1016/J.BUILDENV.2020.107181.

[9] R. SN, M. DK, Risk of indoor airborne infection transmission estimated from carbon dioxide concentration., Indoor Air. 13 (2003) 237–245. https://doi.org/10.1034/J.1600-0668.2003.00189.X.

[10] R. Yang, C.S. Ng, K.L. Chong, R. Verzicco, D. Lohse, Optimal ventilation rate for effective displacement ventilation, (2021). https://arxiv.org/abs/2104.03363v1 (accessed August 12, 2021).

[11] J. Karam, E. Katramiz, K. Ghali, N. Ghaddar, Effective mitigation of cross-contamination in classroom conditioned by intermittent air jet cooling with use of portable air cleaners, Build Environ. 219 (2022). https://doi.org/10.1016/J.BUILDENV.2022.109220.

Chapter 5 Conclusions and Outlook

This study investigated DV system efficiency in large lecture hall. A special DV system installed in Osaka university was first evaluated. The double wall flat diffuser system was initially simulated using CFD before construction completion. Afterwards, experimental measurements were carried out. From the experiment readings, CFD validation was carried out. Temperature results were in good agreement with the experiment readings with the high coefficient of heat transfer settings. Logarithmic law condition and low coefficient showed little heat transfer from the floor and ceiling surfaces which can caused by the software calculation method. On the other hand, CO_2 distribution could not be adjusted to match the experiment readings. The reason is thought to be attributed to two points in the experiment setup. 1. Only CO_2 gas was emitted, not mixed with lighter gas such as helium, the emitted gas was to heavy to be entrained along the thermal plumes even though it was heated. 2. Simulating the human heat generation, black lamps which have a relatively small surface area were used. The narrow plumes, although strong, were less likely to entrain the contaminants upwards.

In both investigations, CFD and experiment, multiple variables were studied; occupants seating pattern including full-occupancy case and alternating-seats case which is similar to the social distancing seating arrangement, Through CFD and field measurements, it was found that thermal plumes were weakened by narrowing the interpersonal spaces. Alternating-seats case was found to achieve stronger temperature gradient and cleaner occupied zone. Secondly, the effect of changing the contaminant source position on occupied zone air quality and probability of cross-infection was investigated using steady-state and transient CFD analysis as well as field measurements. Aggravated by the non-symmetric supply of the system, changing the position of the source had a significant effect on the contaminant dispersion direction, range, and speed. Horizontal air flows, despite being of minimal speed, together with downward draft caused by the cold double wall surfaces played a major role in directing the contaminant spread. Based on these findings, the effect of changing the diffusers position was studied in a CFD analysis. It was found that symmetric supply, either 2-sides, or preferably 4-sides result in a more balanced flow and thus reduces the horizonal spread of the contaminants.

Concluding the DV system weaknesses, a proposal to enhance its performance in large spaces generally, and the case-study lecture hall specifically, was investigated. A novel portable DV unit with air purification feature was designed with the following attributes. Stand-alone heat pump with suction port above occupied zone and supply diffuser near the floor. Being completely ductless, the hot air is exhausted in the space at high level as not to affect the occupied zone. Hence, the unit is intended to boost the DV system performance on three levels; 1- strengthening the temperature gradient by adding a heat source in the upper zone of the space, 2- balancing the supply flow by adding an extra mobile diffuser, and 3- improving the air quality through its filtering feature. Parametric study using zonal model revealed the influence of the machine's COP, input power, flowrate and the DV system's flowrate. Nevertheless, to assess the actual effectiveness of the proposed design, a full-scale experiment was carried out in which a simplifies prototype of the PDV unit was built. In spite of the experiment limitations mainly in terms of space size, some general conclusions can be derived. First, operating the PDV unit in a DV space strengthens the temperature gradient, reduces the contaminant concentration in the occupied zone. Secondly, the PDV unit has the potential to replace the ventilation system,

In addition, placing the PDV unit under the exhaust outlet. It was found to cause conflicting air flows and the turbulence mixes the contaminants to the occupied zone lowering the air quality. Two main recommended design alterations were concluded when visualizing the experiment results using CFD simulation. One is placing the hot air supply diffuser above the suction port was recommended as hot air was found to be short-circuiting and directly sucked into the unit before diffusing into the room. In addition, adding filters for the hot-air supply similar to the cool air supply, as the contaminants returning into the space through the hot air was found to lower the air quality. The two recommendations along with the limitations of the unit's operation mode need further investigations. Optimizing the flowrate in order to maximize its effect and prevent the formation of lock-up layer that can be caused by excess heat from the unit accumulating in the top layer or by turbulence overpowering the buoyancy flow.

Finally, application of operating the PDV unit in the lecture hall was carried out. Two sets of simulations were carried out, once to evaluate the PDV unit performance in enhancing the DV system performance and another to assess the use of PDV units as a partial replacement to the ventilation system. As an enhancement, the PDV units were found to locally reduce the contaminant concentration in the occupied zone and raise the interface level as well as locally balancing the horizonal flows caused by the non-uniform system supply. On the other hand, in some areas, lock-up layer of contaminants were spotted. As a replacement system, the air purification function was found to effectively reduce the contaminant concentration in the occupied zone. Thermally, however, the output heat compromised the performance of the units opening the door to further optimization of the machine limits, specifications and design.

All in all, considering the double wall DV system, the weaknesses and strengths have been clarified through simulations and measurements despite the limitations of both investigation methods. Regarding the PDV unit on the other hand, the experiment and simulations revealed its potential, however, an optimum design and specification could not be firmly concluded. Deeper investigation is needed to explore the parameters thoroughly to optimize the design in terms of ports position, optimum supply flowrate, exhaust hot air flow rate, and heat pump wattage. Exploration in various spaces with different functions, sizes, and shapes is needed to give a better understanding of the machine's potential and limitations. Furthermore, experimenting the use of PDV unit in a non-DV space, e.g. mixed ventilation, could widen the use of the unit if positive effect on the air quality of the occupied zone was found.

List of the Published Papers

Published Journal paper (Time order)

1) Aya Essa, Toshio Yamanaka, Narae Choi, Tomohiro Kobayashi, Noriaki Kobayashi, Miharu Komori, Nobuki Matsui, Tetsuya Okamoto, Takeshi Arakawa, Yuki Yamoto, Shougo Otaka, "Effect of Source Location on Contaminant Dispersion Pattern and Occupants Inhaled Air Quality in Lecture Room Under Displacement Ventilation", *International Journal of Japan Architectural Review, 2022.10*
2) Aya Essa, Toshio Yamanaka, Narae Choi, Tomohiro Kobayashi, Noriaki Kobayashi, Miharu Komori, Nobuki Matsui, Tetsuya Okamoto, Takeshi Arakawa, Yuki Yamoto, Shougo Otaka, "A Novel Portable Cooling Unit with Air Purification for Displacement Ventilation: Parametric Study with Zonal Model and Field Experiment" *Building and Environment, 2023.07*

Published International Conference paper (Time order)

Aya Essa, Toshio Yamanaka, Narae Choi, Tomohiro Kobayashi, Noriaki Kobayashi, Miharu Komori, Nobuki Matsui, Tetsuya Okamoto, Takeshi Arakawa, Yuki Yamoto, Shougo Otaka, "Enhancing displacement ventilation performance: Proposal of a new portable air purifying displacement ventilation unit", *IAQVEC (Tokyo),* 2023.05

Published Conference paper (Time order)

1) Aya Essa, Toshio Yamanaka, Tomohiro Kobayashi, Narae Choi, "Performance of displacement ventilation in a university Lecture hall (Part 1) Effect of occupation pattern on distribution of temperature and contaminant concentration", *Technical Papers of Kinki Chapter of the Society of Heating, Air-conditioning and Sanitary Engineers of Japan*, 2021.03
2) Aya Essa, Toshio Yamanaka, Tomohiro Kobayashi, Narae Choi, "Assessing displacement ventilation performance in university lecture room (Part 1) Effect of occupants' seating pattern on temperature and contaminant concentration distribution", *Conference Paper of technical papers of meeting of the Kinki Branch of the Architectural Institute of Japan*, 2021.06
3) Aya Essa, Toshio Yamanaka, Tomohiro Kobayashi, Narae Choi, "Assessing Displacement Ventilation Performance in University Lecture Room (Part2) Effect of Infection Source Position on Contaminants Spread Pattern", *Conference paper of technical papers of meeting of the Architectural Institute of Japan, Touka*", 2021.09
4) Aya Essa, Toshio Yamanaka, Tomohiro Kobayashi, Narae Choi, "Performance of Displacement Ventilation in A University Lecture Hall (Part 2) Effect of Infected Individual Position on Infection Spread", *Technical Papers of Annual Meeting the Society of Heating, Air-conditioning and Sanitary Engineers of Japan (Fukishima)*, 2021.09
5) Aya Essa, Toshio Yamanaka, Tomohiro Kobayashi, Narae Choi, "Effect of infected occupant position on contaminant spread in a university lecture room with displacement ventilation", *Annual Meeting of the Society of Indoor Environment, Japan*, 2021.12
6) Aya Essa, Toshio Yamanaka, Tomohiro Kobayashi, Narae Choi, "Performance of displacement ventilation in a university Lecture hall (Part3) Effect of contaminant source position on transient spread of contaminant based on CFD analysis", *Technical Papers of Kinki Chapter of the Society of Heating, Air-conditioning and Sanitary Engineers of Japan*, 2022.03
7) Miharu Komori, Toshio Yamanaka, Tomohiro Kobayashi, Narae Choi, Aya Essa, Shinnosuke Ishikawa "Performance of displacement ventilation in a university Lecture hall (Part 4) Effect of Contaminant Source Position on Distribution of Contaminant Concentration", *Technical Papers of Kinki Chapter of the Society of Heating, Air-conditioning and Sanitary Engineers of Japan*,

2022.03
8) Shinnosuke Ishikawa, Toshio Yamanaka, Tomohiro Kobayashi, Narae Choi, Aya Essa, Miharu Komori "Performance of displacement ventilation in a university Lecture hall (Part5) Effect of distance between occupants on distribution of contaminant concentration and upward airflow from occupant", *Technical Papers of Kinki Chapter of the Society of Heating, Air-conditioning and Sanitary Engineers of Japan*, 2022.03
9) Aya Essa, Toshio Yamanaka, Tomohiro Kobayashi, Narae Choi, "Assessing displacement ventilation performance in university lecture room (Part 3) A Transient CFD Analysis of The Effect of Source Position on Contaminant Spread", *Conference paper of technical papers of meeting of the Kinki Branch of the Architectural Institute of Japan*, 2022.06
10) Miharu Komori, Toshio Yamanaka, Tomohiro Kobayashi, Narae Choi, Aya Essa, Shinnosuke Ishikawa, "Assessing displacement ventilation performance in university lecture room (Part4) Study on the Spread of Human-originated Contaminant in a Lecture Room", *Conference paper of technical papers of meeting of the Kinki Branch of the Architectural Institute of Japan*, 2022.06
11) Shinnosuke Ishikawa, Toshio Yamanaka, Tomohiro Kobayashi, Narae Choi, Aya Essa, Miharu Komori, "Assessing displacement ventilation performance in university lecture room (Part5) Effect of distance between occupants on upward airflow from occupant", *Conference paper of technical papers of meeting of the Kinki Branch of the Architectural Institute of Japan*, 2022.06
12) Shinnosuke Ishikawa, Toshio Yamanaka, Tomohiro Kobayashi, Narae Choi, Aya Essa, Miharu Komori, "Performance of Displacement Ventilation in A University Lecture Hall (Part6) Effect of handling of heat transfer and contaminant concentration distribution on CFD Analysis", *Annual Meeting the Society of Heating, Air-conditioning and Sanitary Engineers of Japan (Kobe)*, 2022.09
13) Miharu Komori, Toshio Yamanaka, Tomohiro Kobayashi, Narae Choi, Aya Essa, Shinnosuke Ishikawa, "Performance of Displacement Ventilation in A University Lecture Hall (Part7) Effect of Occupation Pattern on Distribution of Air Temperature and Contaminant Concentration on Field Measurement", *Annual Meeting the Society of Heating, Air-conditioning and Sanitary Engineers of Japan (Kobe)*, 2022.09
14) Aya Essa, Toshio Yamanaka, Tomohiro Kobayashi, Narae Choi, Miharu Komori, Shinnosuke Ishikawa, "Performance of Displacement Ventilation in A University Lecture Hall (Part 8) Effect of Supply Diffusers Position on Temperature and Contaminant Concentration Distribution in Different Occupants Seating Pattern Cases Using CFD", *Annual Meeting the Society of Heating, Air-conditioning and Sanitary Engineers of Japan (Kobe)*, 2022.09
15) Aya Essa, Toshio Yamanaka, Tomohiro Kobayashi, Narae Choi, Miharu Komori, Shinnosuke Ishikawa, "Assessing Displacement Ventilation Performance in University Lecture Room (Part 6) Investigation of Temperature Distribution in an Actual Lecture Room with Three Side Inlets", *Conference paper of technical papers of meeting of the Architectural Institute of Japan, Hokkaido*, 2022.09
16) Miharu Komori, Toshio Yamanaka, Tomohiro Kobayashi, Narae Choi, Aya Essa, Shinnosuke Ishikawa, "Assessing Displacement Ventilation Performance in University Lecture Room (Part7) Distribution of Human-originated Contaminant in a Lecture Room with Three Side Supply Inlet", *Conference paper of technical papers of meeting of the Architectural Institute of Japan, Hokkaido*, 2022.09
17) Shinnosuke Ishikawa, Toshio Yamanaka, Tomohiro Kobayashi, Narae Choi, Aya Essa, Miharu Komori, "Assessing Displacement Ventilation Performance in University Lecture Room (Part8) Effect of handling of heat transfer on temperature and contaminant concentration distribution in room on CFD Analysis", *Conference paper of technical papers of meeting of the Architectural Institute of Japan, Hokkaido*, 2022.09
18) Shinnosuke Ishikawa, Toshio Yamanaka, Tomohiro Kobayashi, Narae Choi, Aya Essa, Miharu Komori, "Effect of distance between occupants and insulation performance of window on ventilation efficiency in a room with displacement ventilation system", *Annual Meeting of the Society of Indoor Environment, Japan*, 2022.12
19) Miharu Komori, Toshio Yamanaka, Tomohiro Kobayashi, Narae Choi, Aya Essa, Shinnosuke

Ishikawa, “Evaluation of Ventilation Performance in a Lecture Room with Displacement Ventilation (Part1) Effect of Seating Position of Occupants on Distribution of Air Temperature and Contaminant Concentration on Field Measurement”, *Annual Meeting of the Society of Indoor Environment, Japan*, 2022.12

20) Aya Essa, Toshio Yamanaka, Tomohiro Kobayashi, Narae Choi, Miharu Komori, Shinnosuke Ishikawa, “Evaluation of Ventilation Performance in a Lecture Room with Displacement Ventilation (Part 2) Effect of Supply Diffusers Position on Temperature and Contaminant Concentration Distribution in Different Seating Pattern Cases”, *Annual Meeting of the Society of Indoor Environment, Japan*, 2022.12
21) Aya Essa, Toshio Yamanaka, Narae Choi, Tomohiro Kobayashi, Noriaki Kobayashi, Miharu Komori, Nobuki Matsui, Tetsuya Okamoto, Takeshi Arakawa, Yuki Yamoto, Shougo Otaka, “A Study on a Novel Portable Cooling Unit with Air Purification for Displacement Ventilation (Part 1) Parametric Study with Zonal Model and CFD Analysis for PM Concentration and Temperature Distribution”, *Technical Papers of Kinki Chapter of the Society of Heating, Air-conditioning and Sanitary Engineers of Japan*, 2023.03
22) Miharu Komori, Toshio Yamanaka, Narae Choi, Tomohiro Kobayashi, Noriaki Kobayashi, Aya Essa, Nobuki Matsui, Tetsuya Okamoto, Takeshi Arakawa, Yuki Yamoto, Shougo Otaka, “A Study on a Novel Portable Cooling Unit with Air Purification for Displacement Ventilation (Part 2) Experimental Investigation of Temperature Gradient and Droplet Nuclei Removal Effectiveness”, *Technical Papers of Kinki Chapter of the Society of Heating, Air-conditioning and Sanitary Engineers of Japan*, 2023.03